Introduction to PDR‘s

M.Röllig

I. Phys. Institut, Universität zu Köln

Introduction

- PDR stands for
  - Photo-Dissociation Region
  - Photon Dominated Region

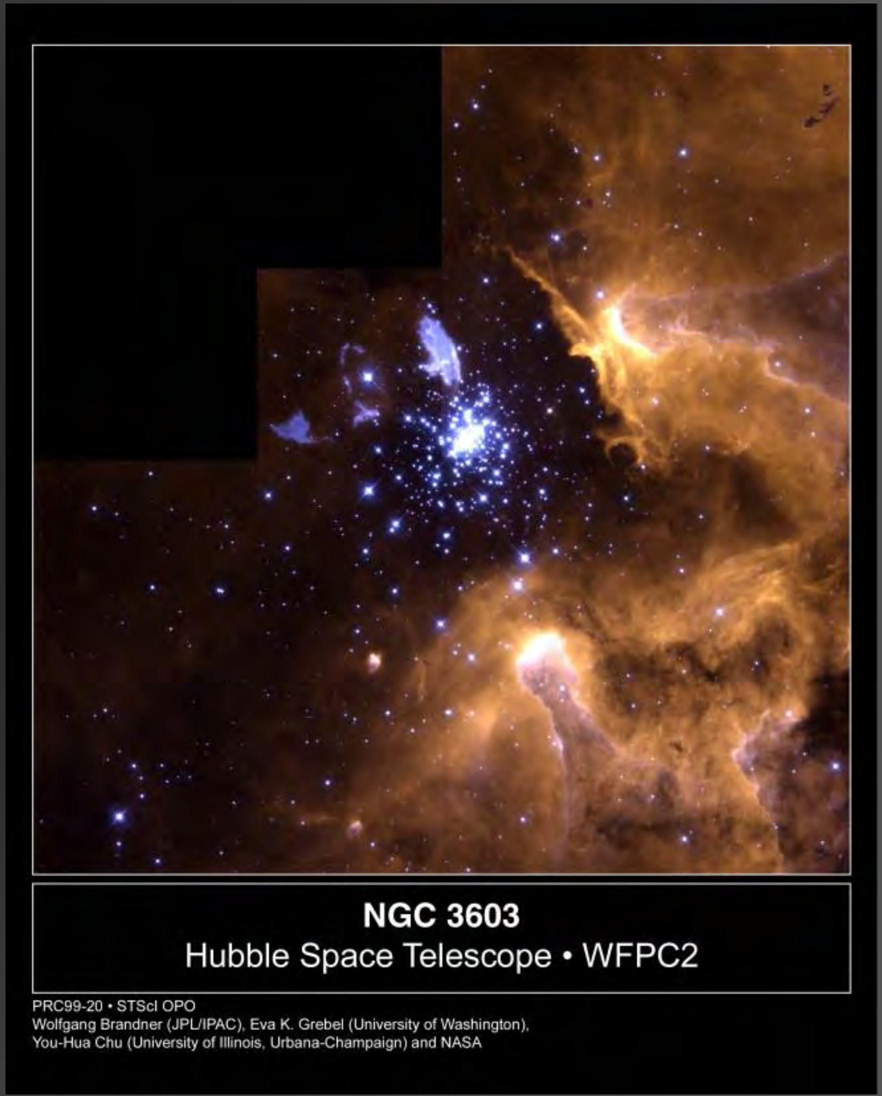

Introduction

- A region where far-ultraviolett (FUV: 6-13.6 eV) photons from young, massive stars dominate the physics and the chemistry of the interstellar medium.
  - **6 eV (2066 Å)** ~ionization potential of dust/PAHs
    11.1 eV (1117 Å) dissociation energy of CO
    11.3 eV (1097 Å) ionization potential of C
  - **13.6 eV (912 Å)** ionization potential of H
    ionization potential of O
    14.5 eV (855 Å ionization potential of N

Introduction

- A region where far-ultraviolett (FUV: 6-13.6 eV) photons from young, massive stars dominate the physics and the chemistry of the interstellar medium.

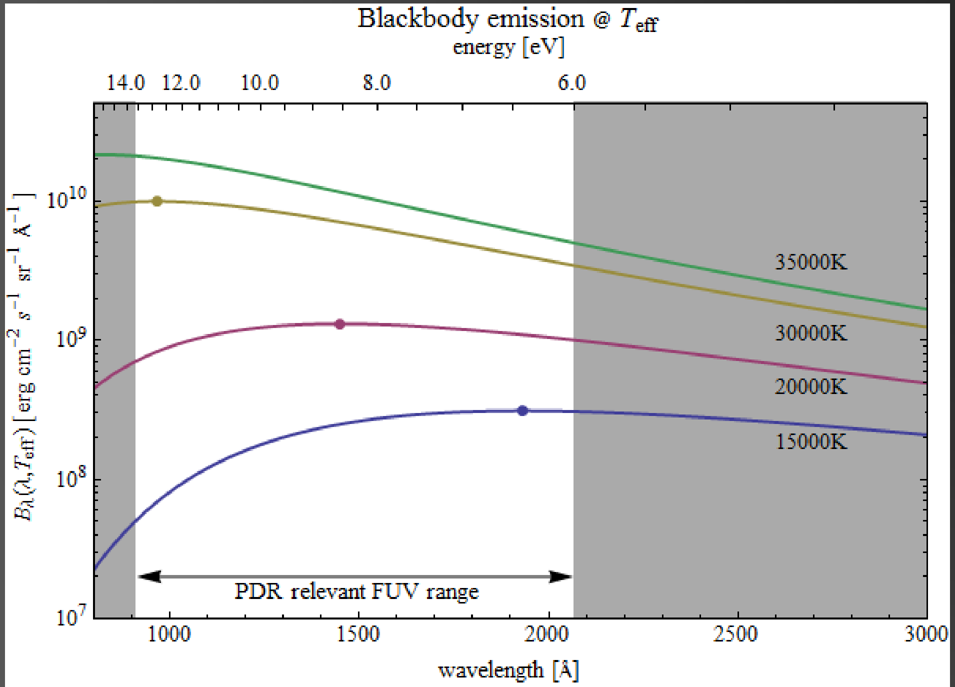

massive stars emit a significant fraction of their energy at $\lambda < 912$ Å

Introduction

- A region where far-ultraviolett (FUV: 6-13.6 eV) photons from young, massive stars dominate the physics and the chemistry of the interstellar medium.

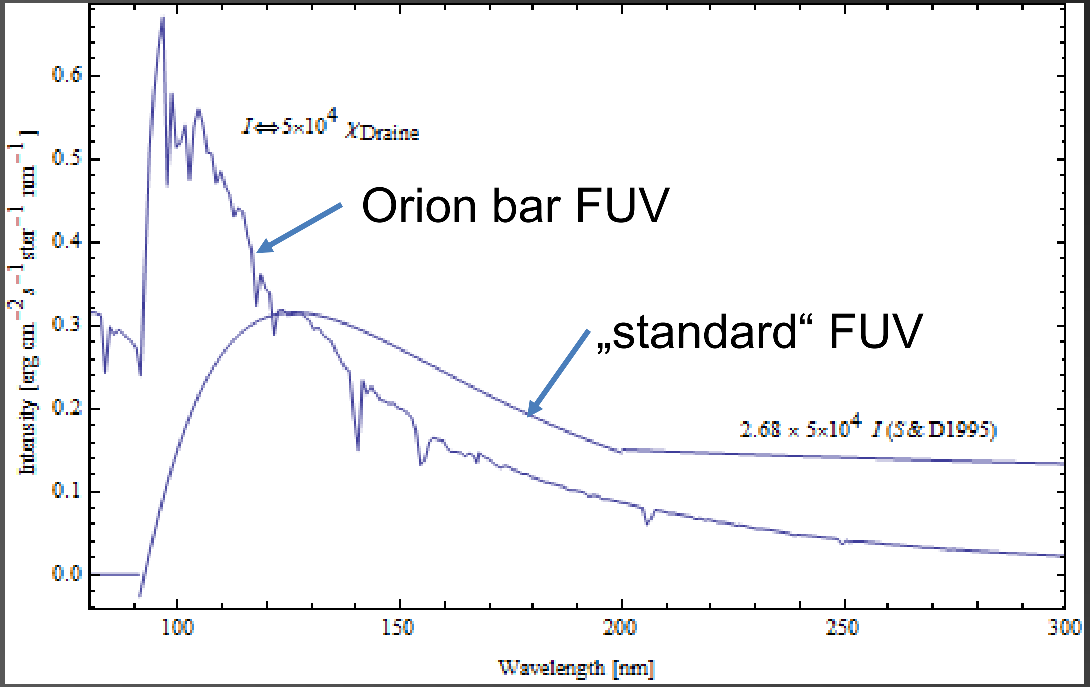

PDRs close to an OB star experience spectrally different UV radiation compared to the standard mean FUV field (Draine ‘78, Habing ‘68)

Introduction

Interstellar PDRs include:

- Diffuse WNM and CNM clouds.
- Translucent clouds: $A_V < 5$, $n_H < 1000$ cm^{-3},weak interstellar FUV fields.
- Dense molecular clouds: A_V up to ~10, $n_H > 1000$ cm^{-3} including intense FUV fields near OB stars

➡ ~90% of the Galactic molecular ISM may be “photon- dominated”.

Introduction

Ring nebula

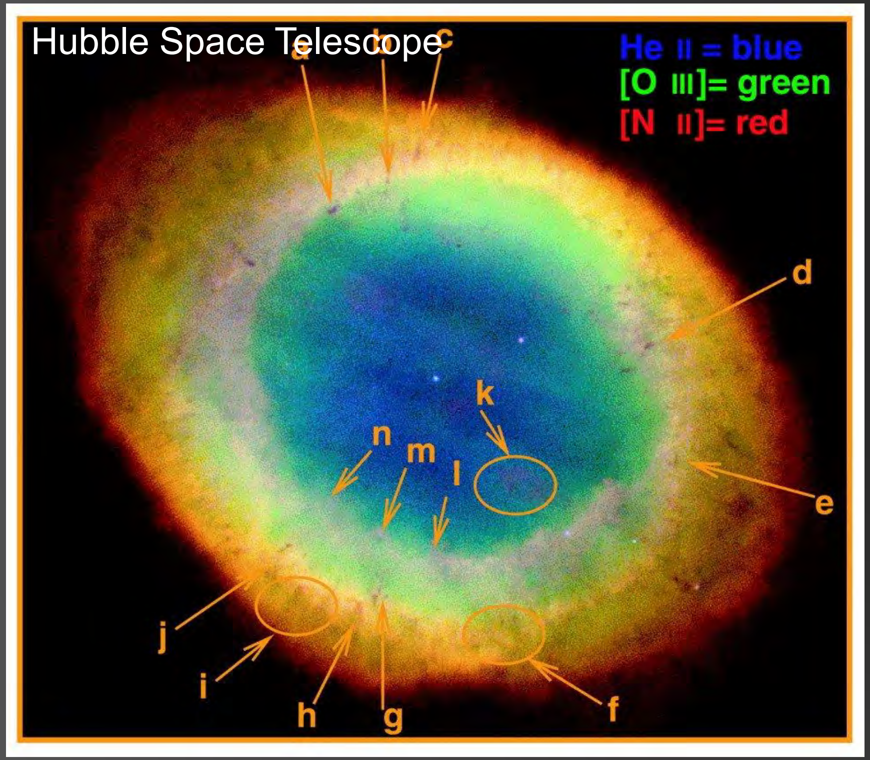

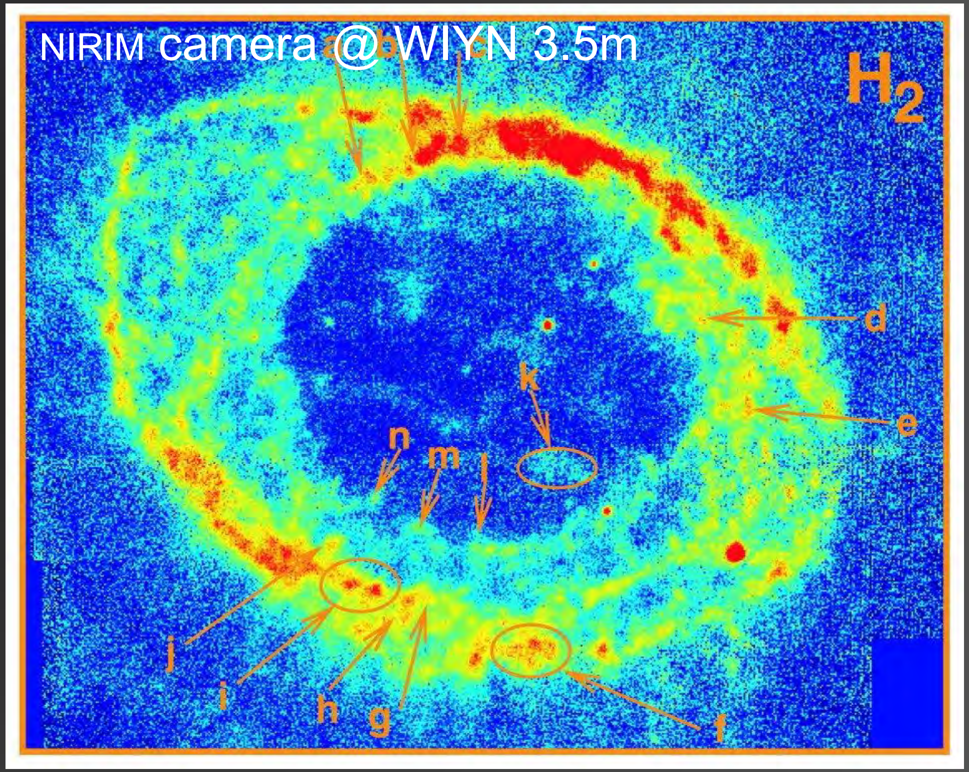

Speck et al. 2003 PASP 115, 170

Introduction

Credit: NASA, ESA, and F. Paresce and R. O'Connell

PDRs are also observed in extragalactic source

30 Doradus in the LMC

Introduction

Credit: ESA/Hubble & NASA

PDRs are also observed in extragalactic source

Antennea galaxies (NGC 4038/39)

Introduction

Thilker et al. 2005

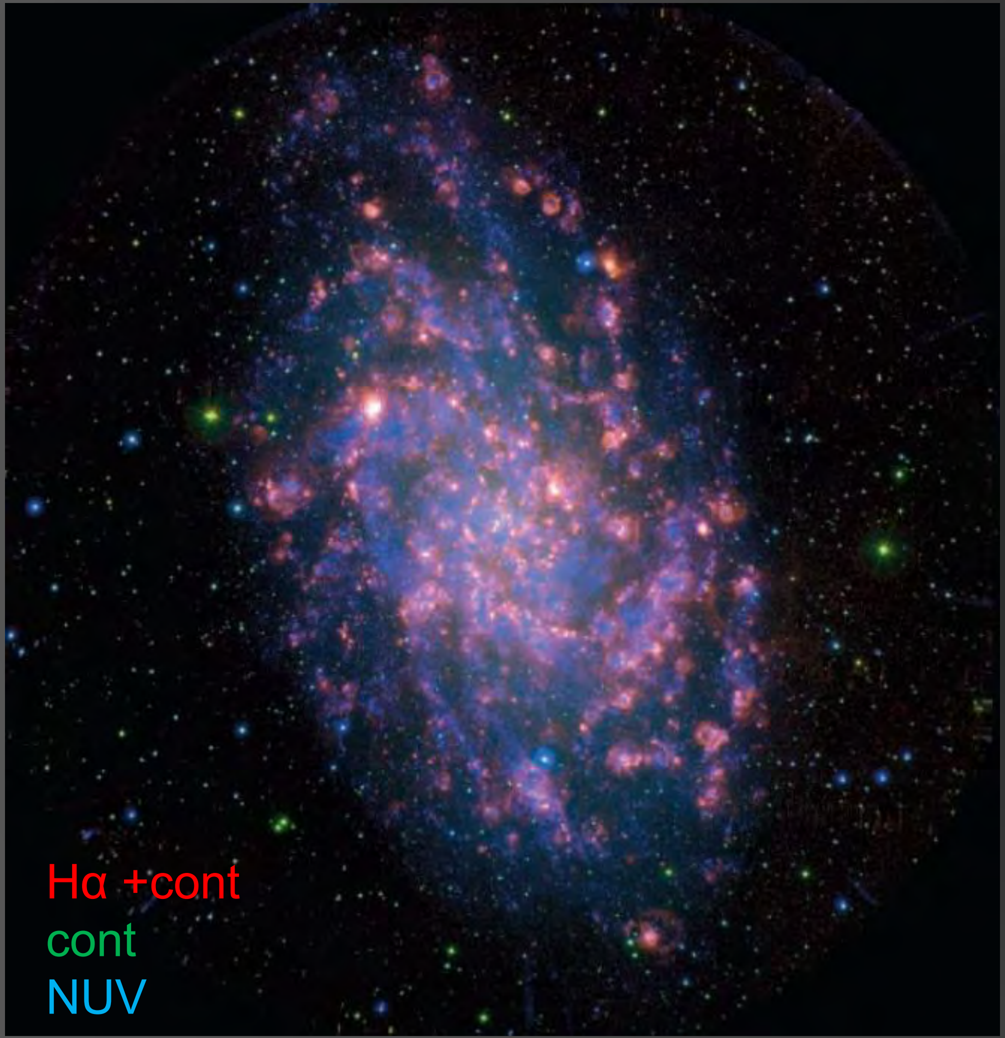

PDRs are also observed in extragalactic source

M33

Introduction

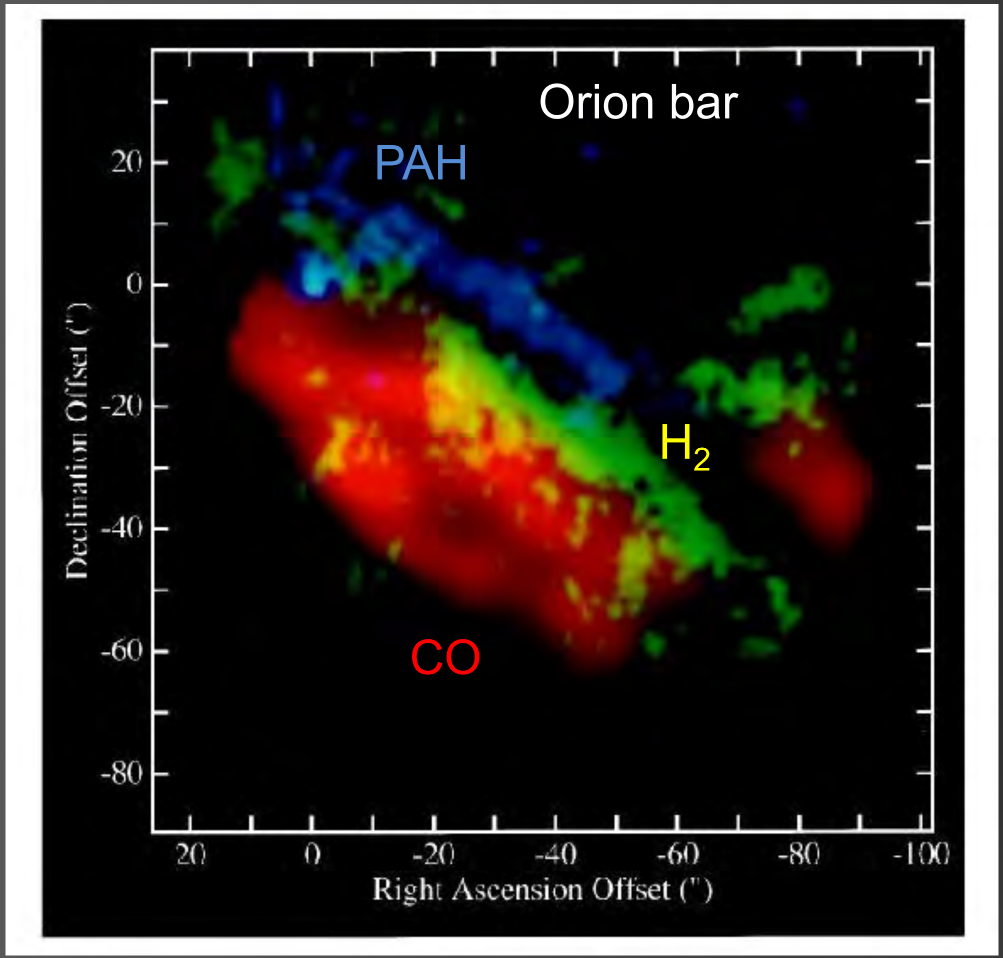

Tielens & Hollenbach 1998

Motte et al. 2010

Introduction

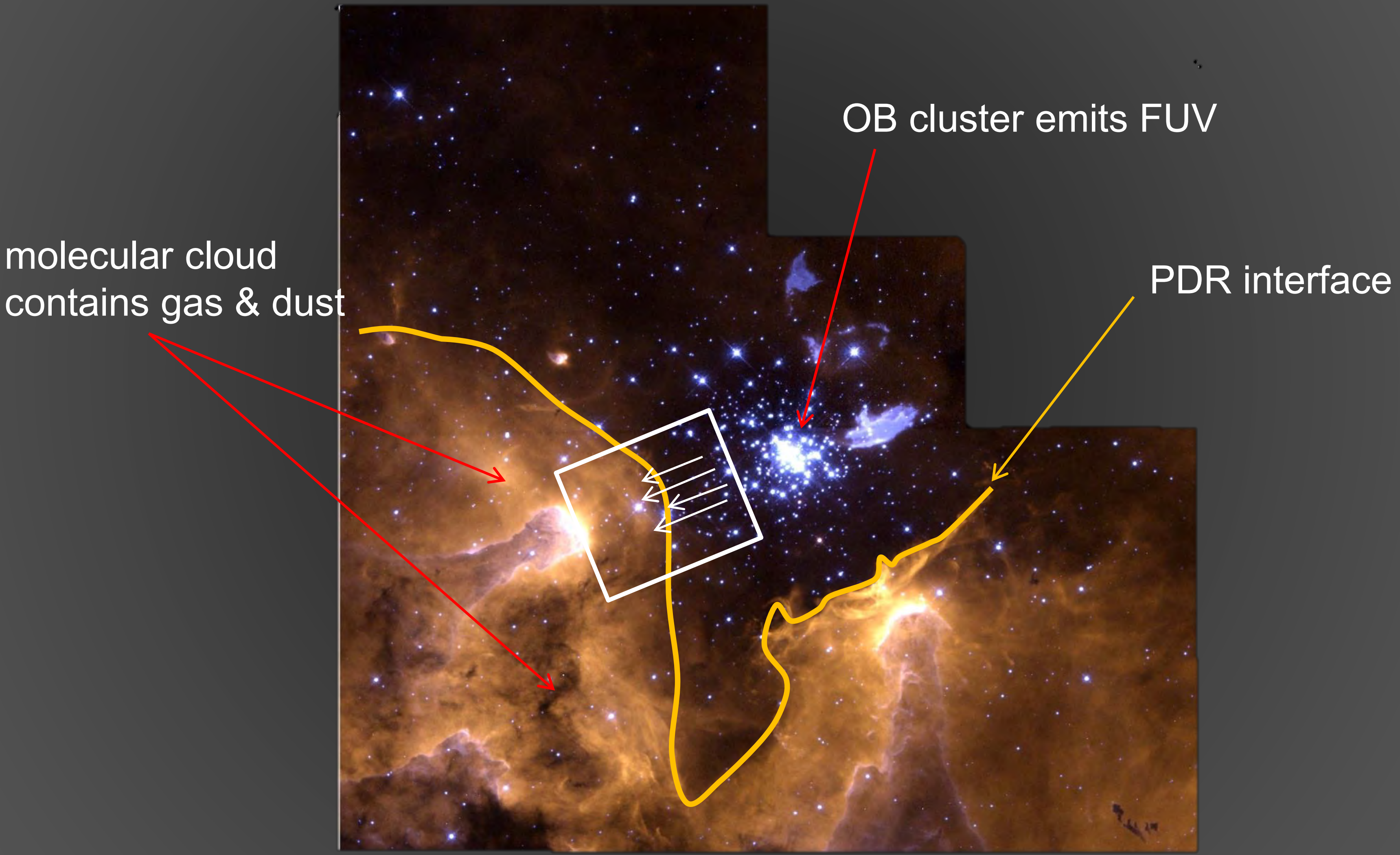

Introduction

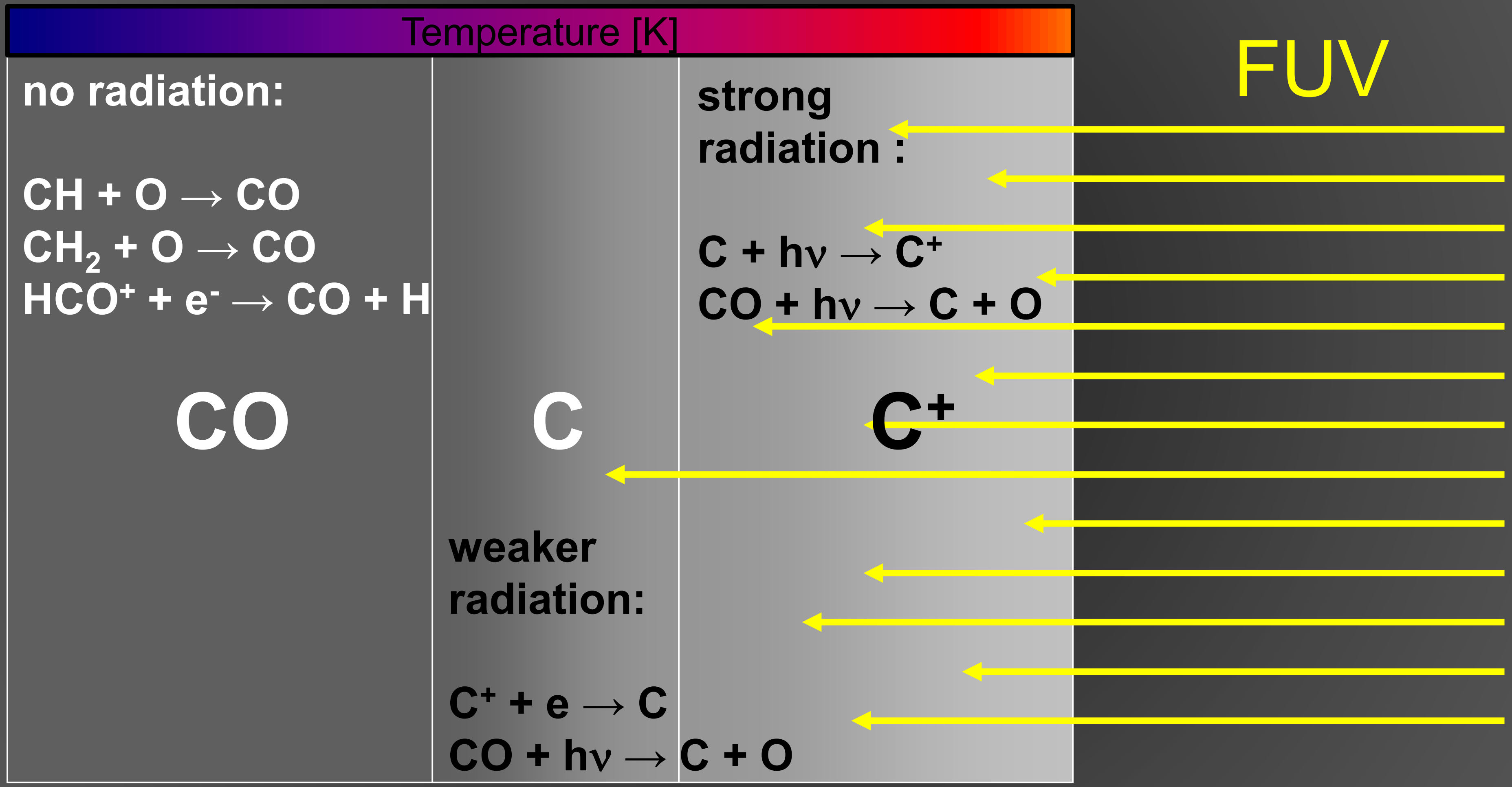

Interstellar cloud surface (cross section)

Basic structure

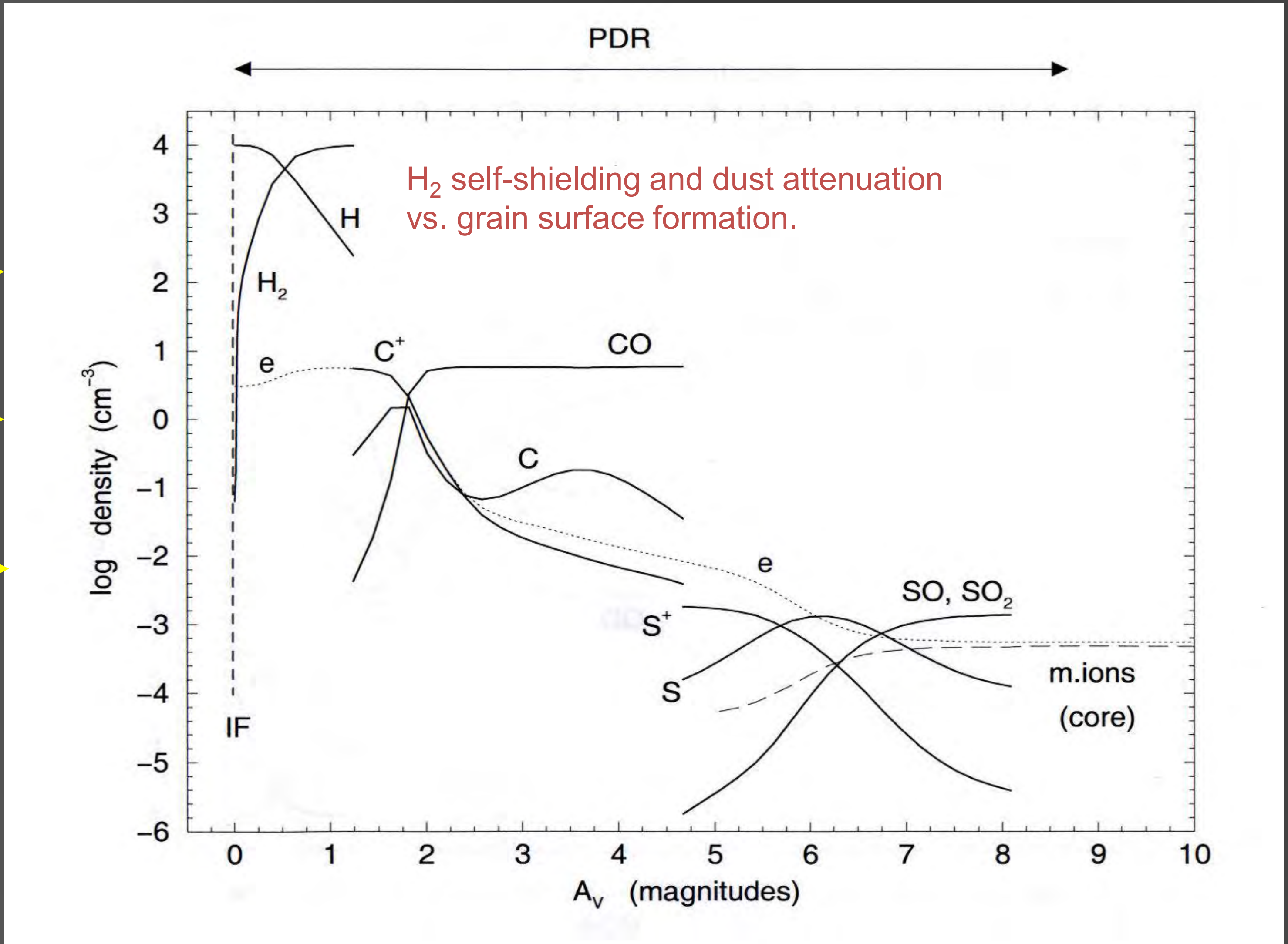

FUV
6-13.6 eV

Controlling parameters:

1) cloud density/pressure
2) FUV intensity
3) grain scattering properties
4) H_2 formation rate coefficient
5) geometry/clumpiness
6) gas phase abundances
7) magnetic field
8) cosmic ray ionization
9) turbulence
…

Sternberg & Dalgarno 1995

Physical structure

- Temperature
  - heating
  - cooling
- Density
- Geometry
- Dynamics

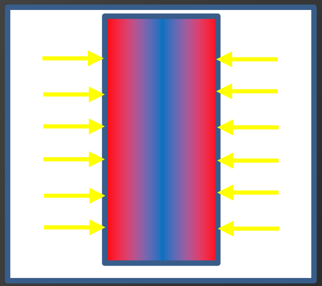

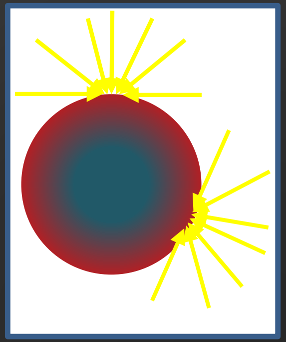

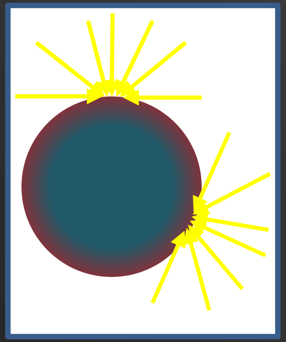

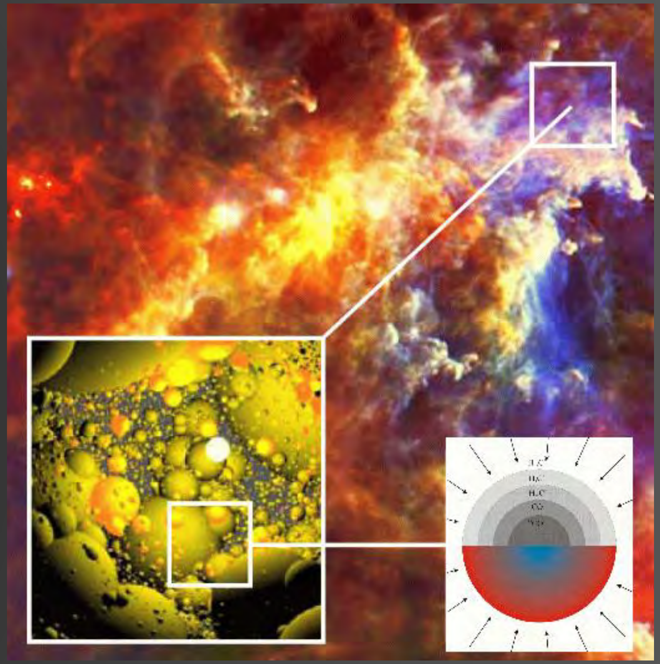

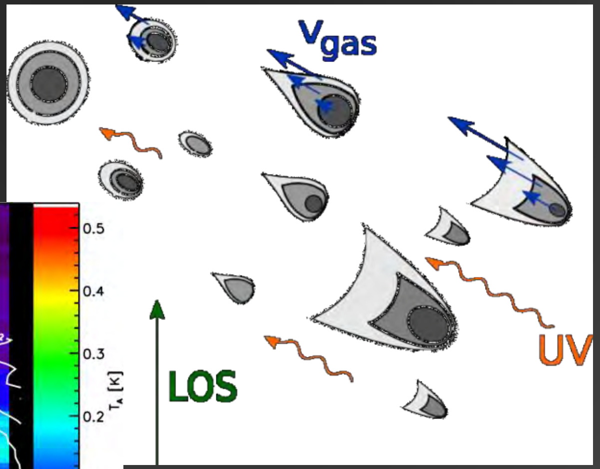

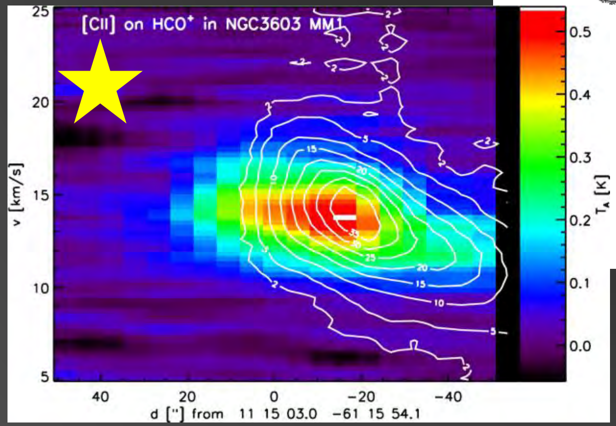

Gas heating

1. FUV photons
    1. Photoelectric heating
    2. vibrational deexcitation of electronically pumped H_2
    3. H_2 formation heating
    4. gas-grain collisions
    5. photodissociation of H_2
    6. ionization of atomic carbon
2. Cosmic rays/X-rays
3. Shocks (→Talk by A. Gusdorf)
4. Turbulence

Photoelectric heating

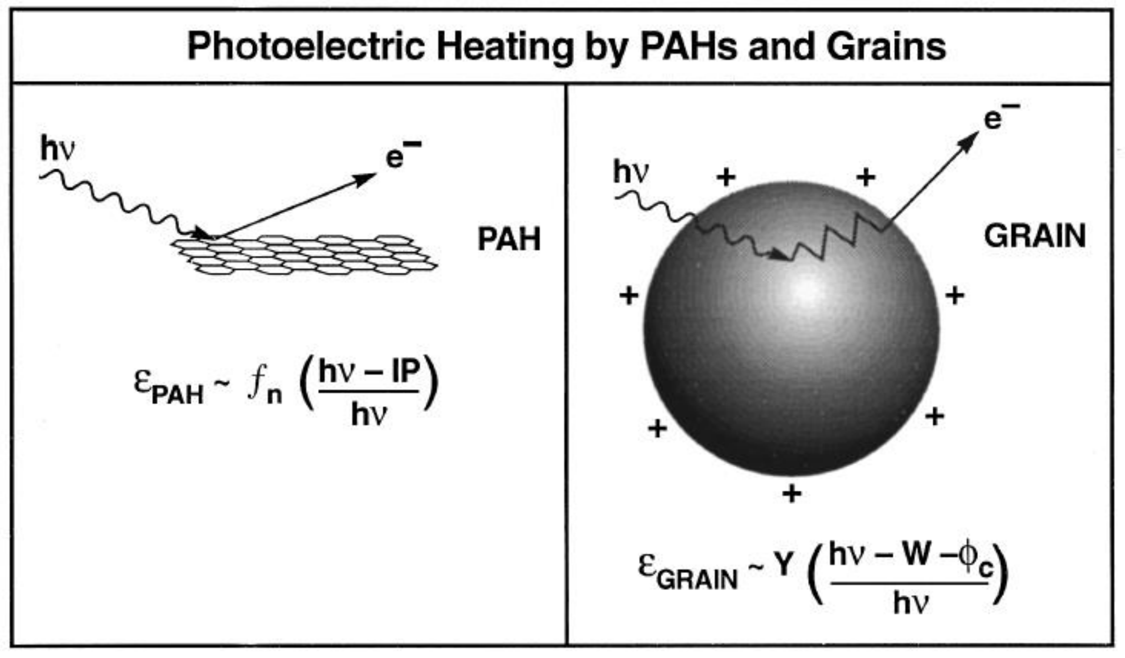

Hollenbach & Tielens, 1999, Rev. Mod. Phys., Vol. 71

"A far-ultraviolet photon absorbed by a dust grain creates a photoelectron which diffuses through the grain until it loses all its excess energy due to collisions with the matrix or finds the surface and escapes. For PAHs, the diffusion plays no role."

hv:	photon energy
W:	work function of the grain
ϕ_c:	Coulomp potential of the grain
IP:	ionization potential of the PAH
Y:	yield, i.e. probability that the photon escapes (~ 0.1 for large grains)
ε:	efficiency, i.e. fraction of escaping photon times fraction of energy carried away

Photoelectric heating

Draine & Weingartner 2001 ApJS, 234, 162

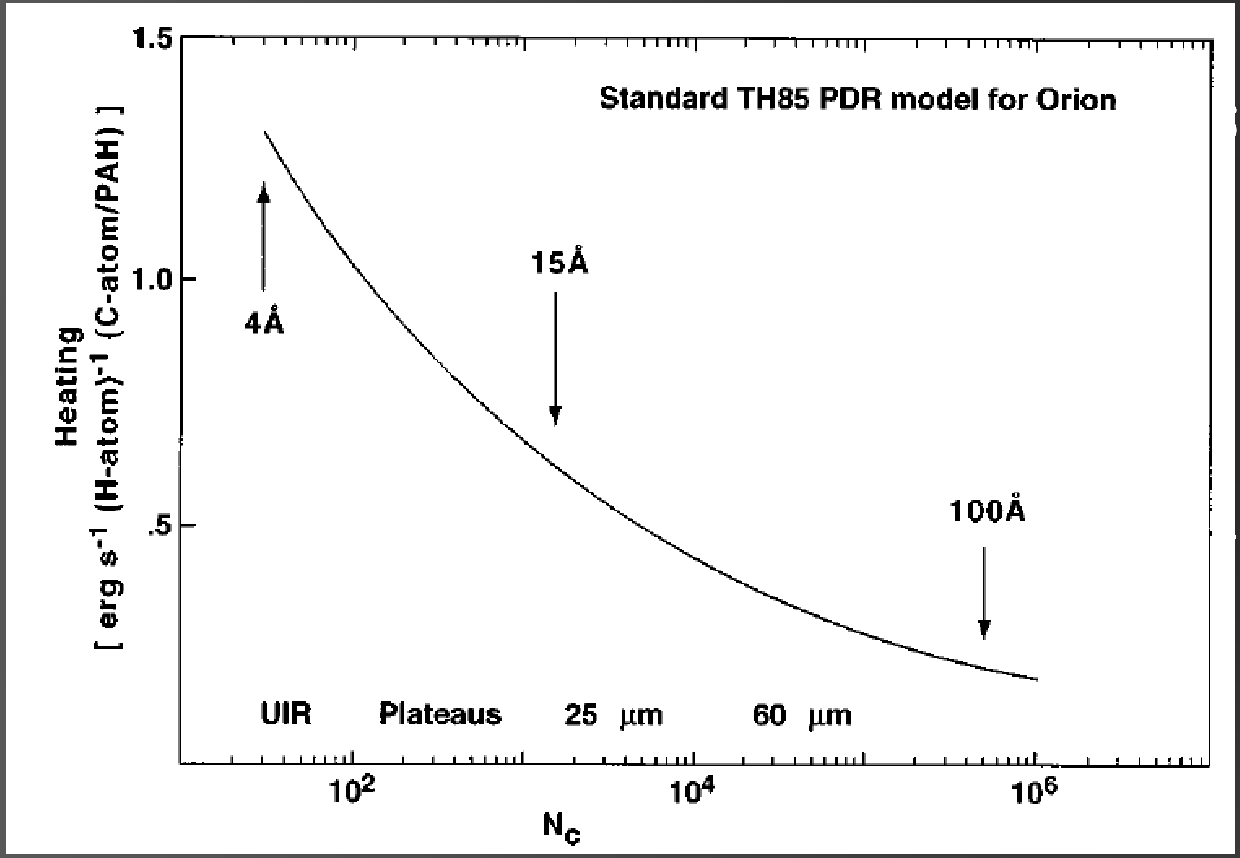

Tielens & Hollenbach 1999

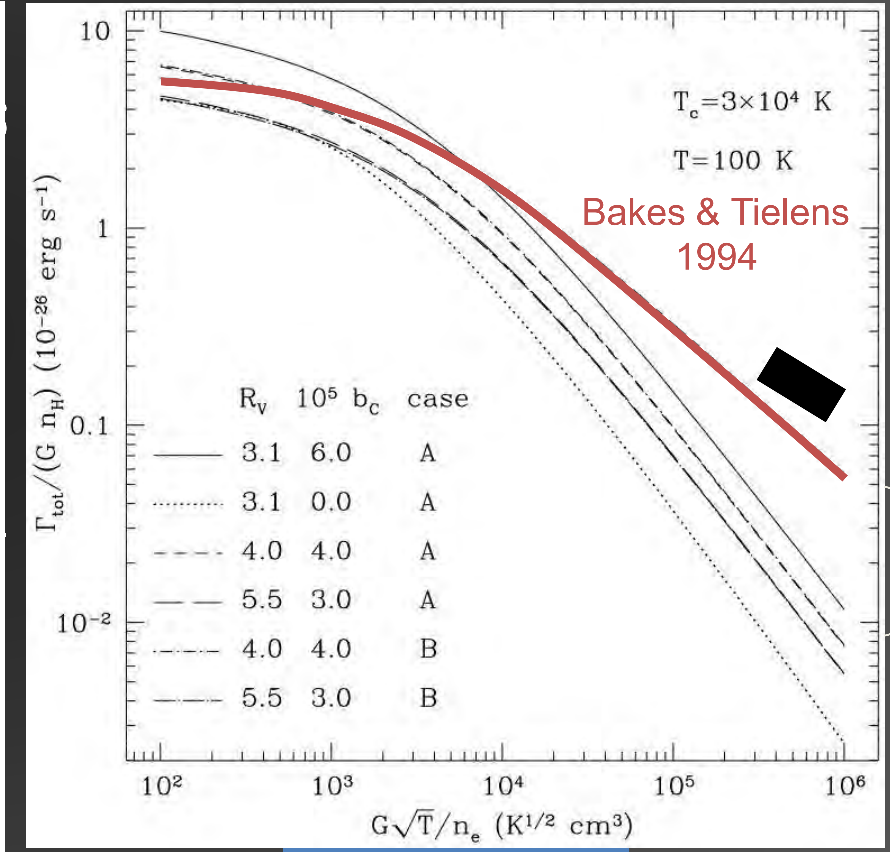

Different assumed electron-grain sticking coefficients.

grain charging →

Photoelectric heating

$$n\Gamma_{\rm pe} = 10^{-24} \epsilon n G_0 \, {\rm erg\, cm^{-3}\, s^{-1}}.$$

$$\epsilon = \frac{4.87 \times 10^{-2}}{1 + 4 \times 10^{-3} \gamma^{0.73}} + \frac{3.65 \times 10^{-2} (T/10^4)^{0.7}}{1 + 2 \times 10^{-4} \gamma}$$

$$\gamma = G_0 T^{1/2} / n_{\rm e}$$

charging parameter: photo-ionization over recombination rate

see also:
Bakes & Tielens 1994
Weingartner & Draine 2001

The work function of grains is ~ 5-7 eV.

50% of the PE heating is contributed by grains < 15 Å.

PAH‘s heat more efficiently than large grains.

H_2 pumping

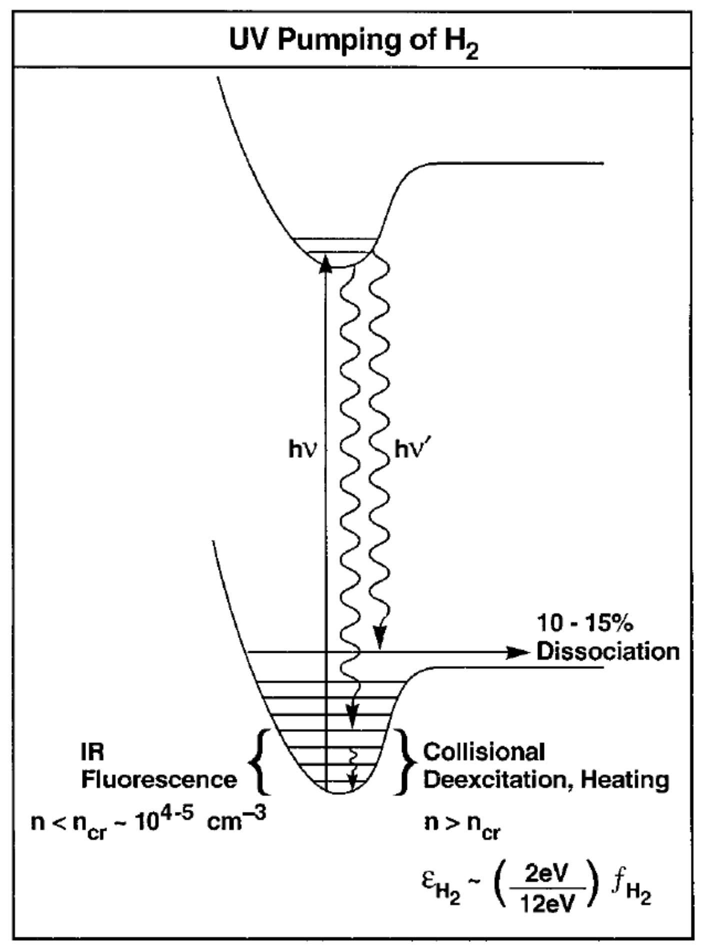

Tielens & Hollenbach 1999

- line absorption of FUV photons pumps electronically excited state (Lyman, Werner bands)
  - 10-15 % fluoresce back to vib. continuum of the ground el. state → photo-dissociation
  - 85-90 % fall back to bound vib. states of the el. ground state → E_{vib}~ 2 eV available for heating
- efficient at high densities

$$n\Gamma_{H_2} \simeq 2.9 \times 10^{-11} n n_{H} k_d \left[1 + \left(\frac{n_{cr}}{n}\right) + \frac{4.4 \times 10^2\, G_0}{n\, T^{1/2} \exp[-1000/T]}\right]^{-1} \mathrm{erg\ cm^{-3}\ s^{-1}}$$

H_2 formation heating

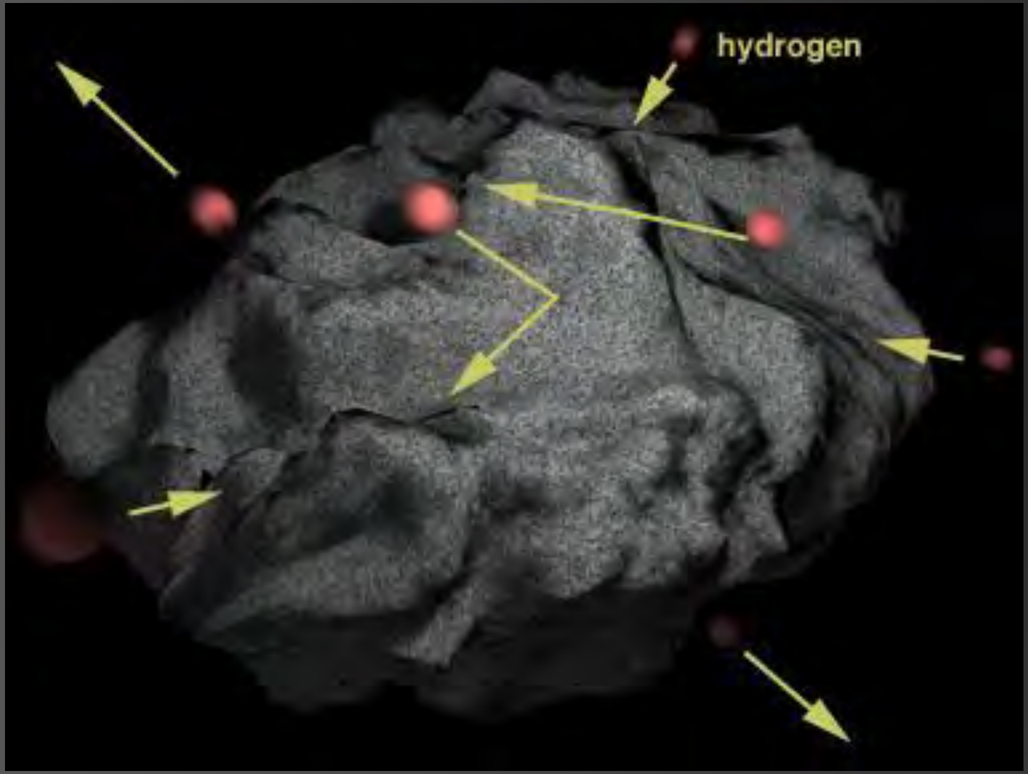

- H_2 forms on dust surfaces
- binding energy of H_2 ~ 4.5 eV
- newly formed H_2 molecules are released into the gas-phase and carry away part of the binding energy as kinetic and internal energy
  → heating via collisions

$$\Gamma_{\mathrm{H_2\ form}} = 2.4 \times 10^{-12} R_{\mathrm{H_2\ form}}\, n_{\mathrm{H}}\ \mathrm{erg\ cm^{-3}\ s^{-1}}$$

R_{H2form}: H_2 formation rate

H_2 formation heating

formation efficiency

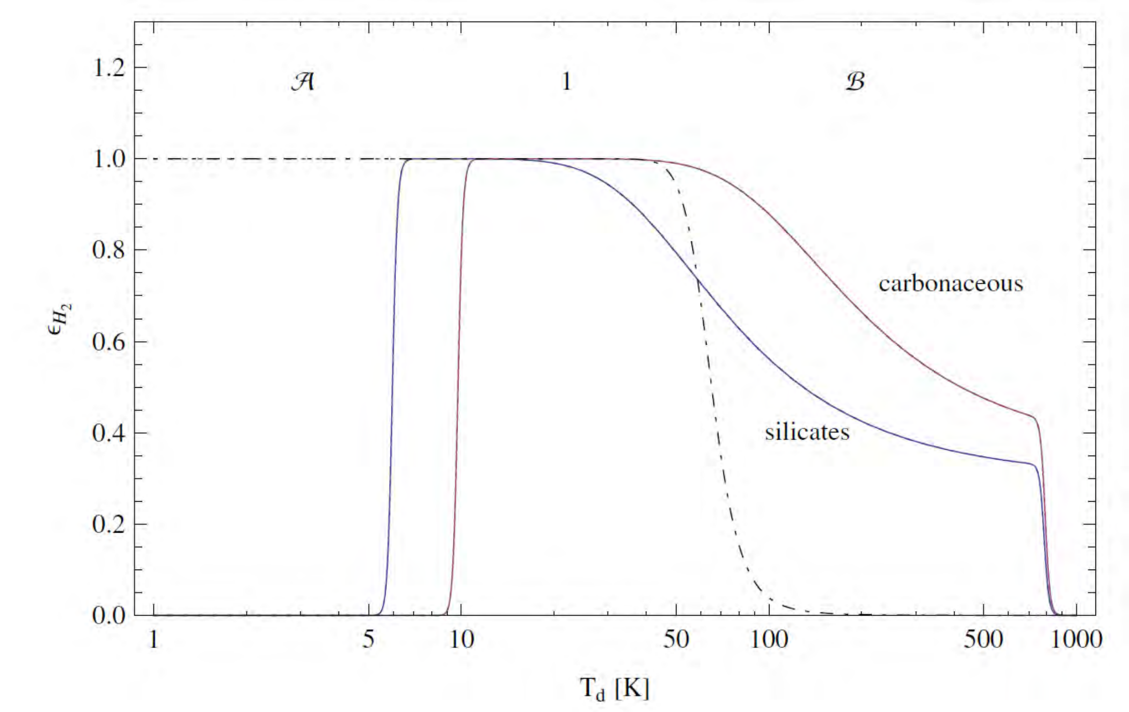

Cazaux & Tielens (2004,2010)

- H-binding to the grain surface determines its mobility and resistance against thermal desorption
  - weak binding (physisorption), T<50-80K
  - strong binding (chemisorption), T<~500-800 K

Chemisorption leads to efficient H_2 formation at high temperatures

H_2 formation heating

formation efficiency

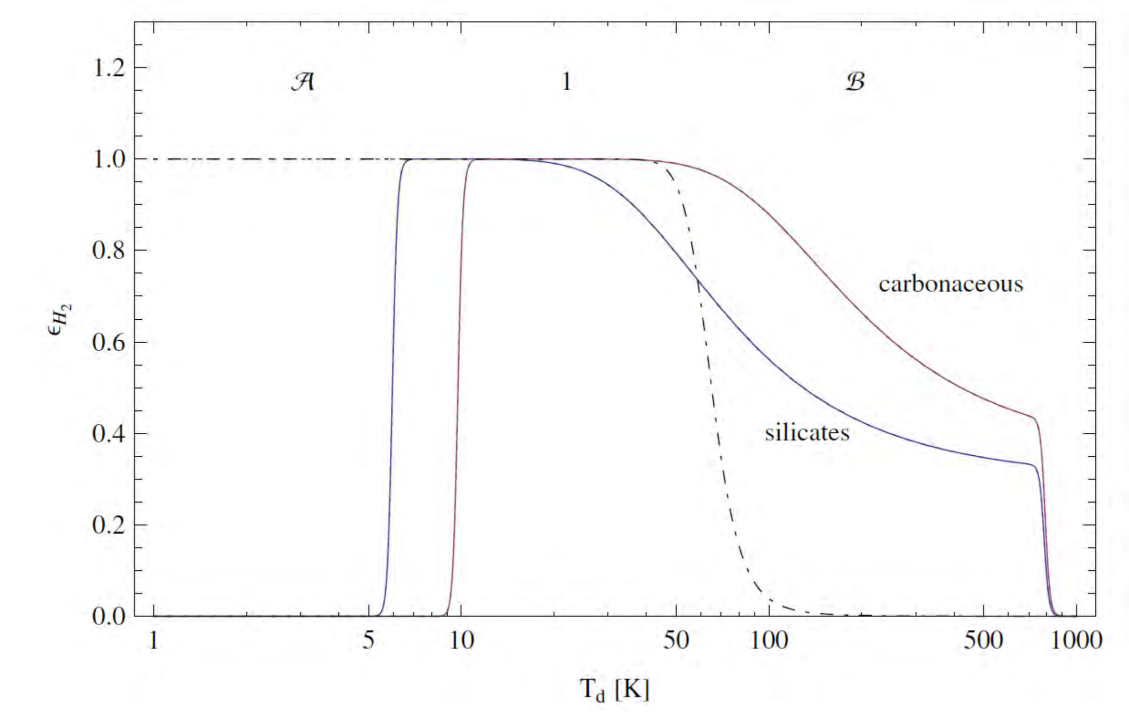

Cazaux & Tielens (2004,2010)

formation rate

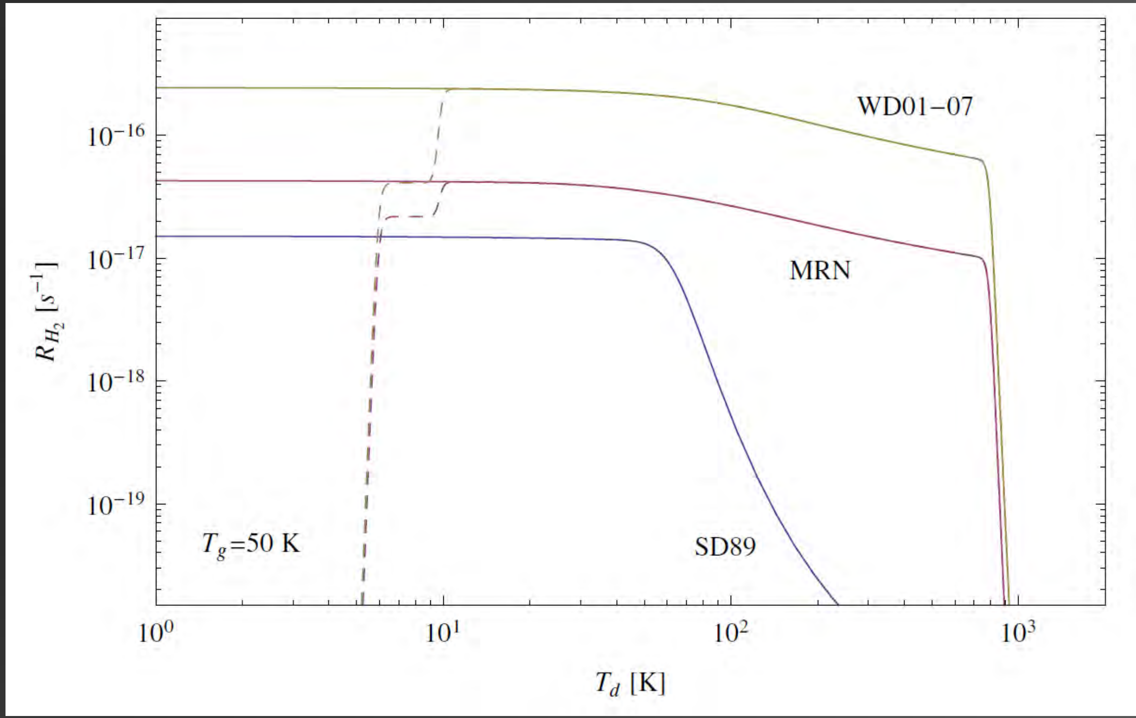

Chemisorption leads to efficient H_2 formation at high temperatures

H_2 formation heating

heating rate

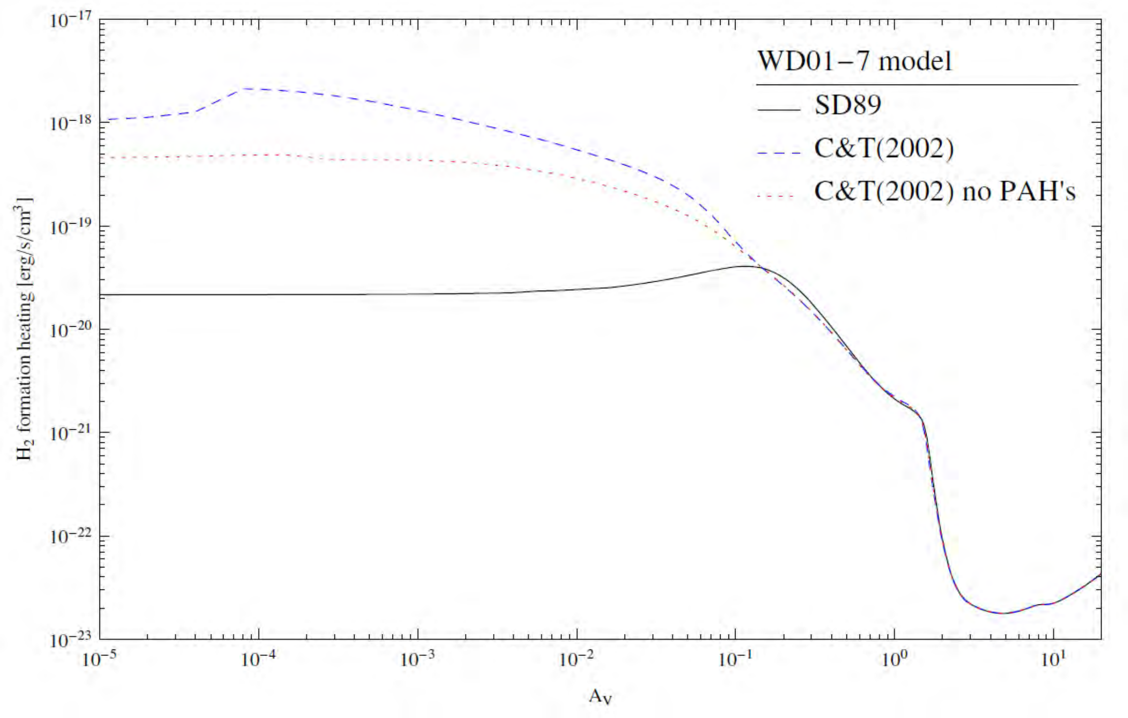

formation rate

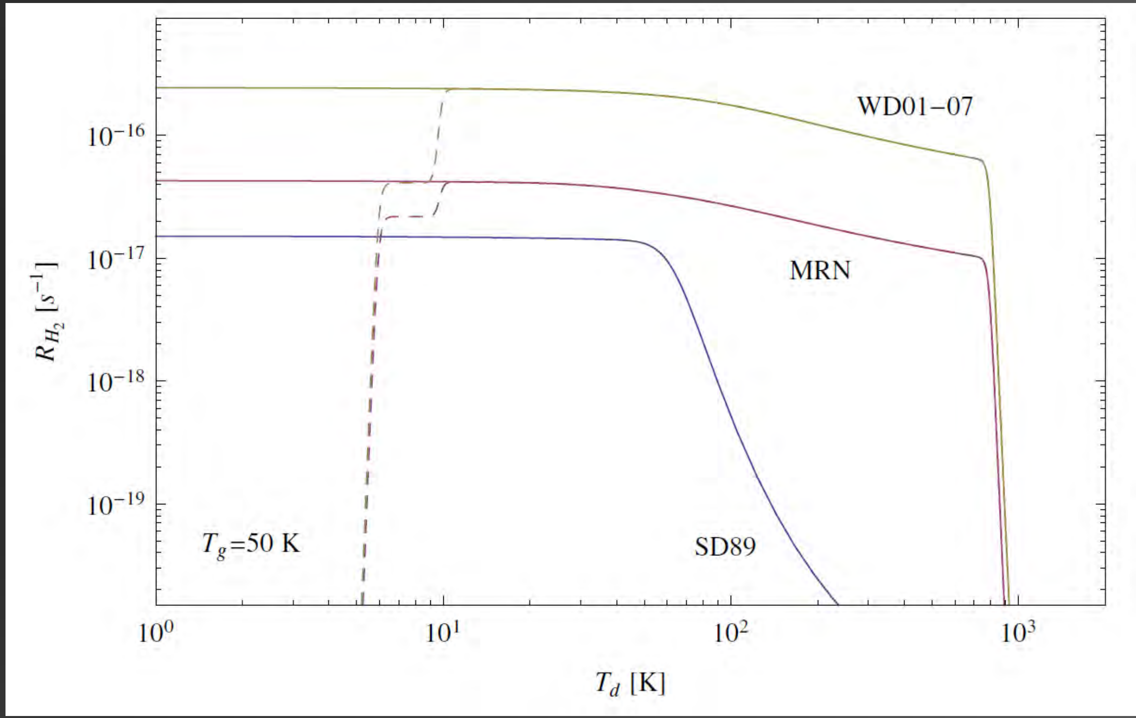

More efficient H2 formation leads to stronger gas heating.

H_2 formation heating

heating rate

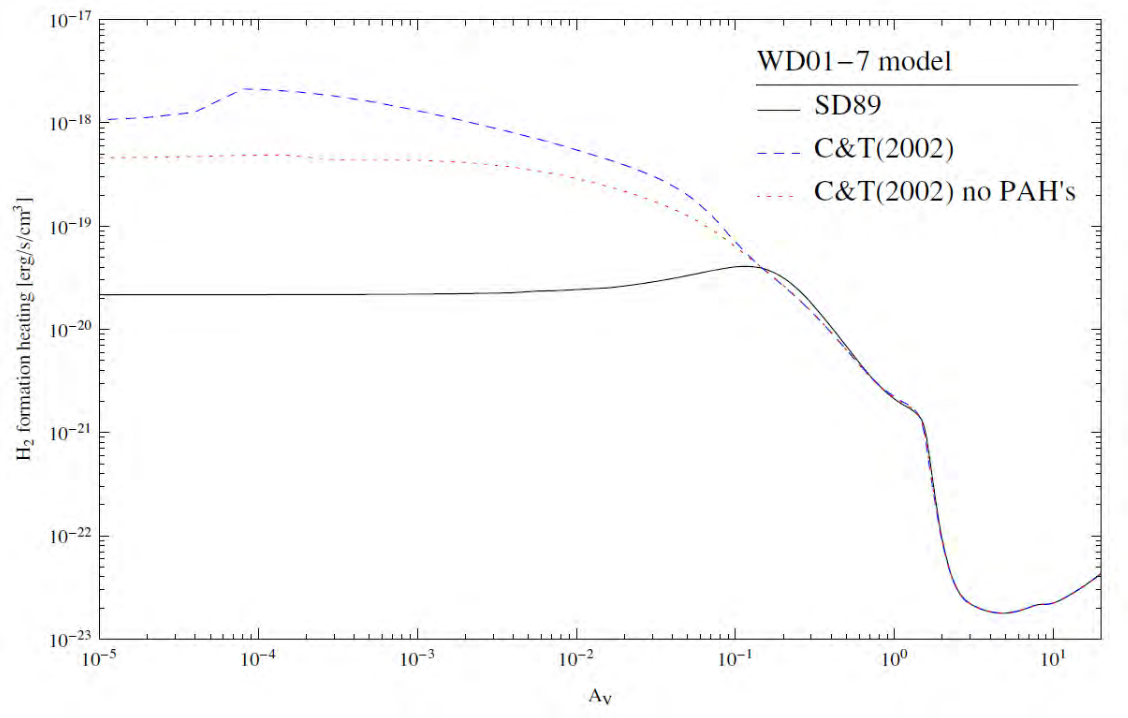

gas temperature

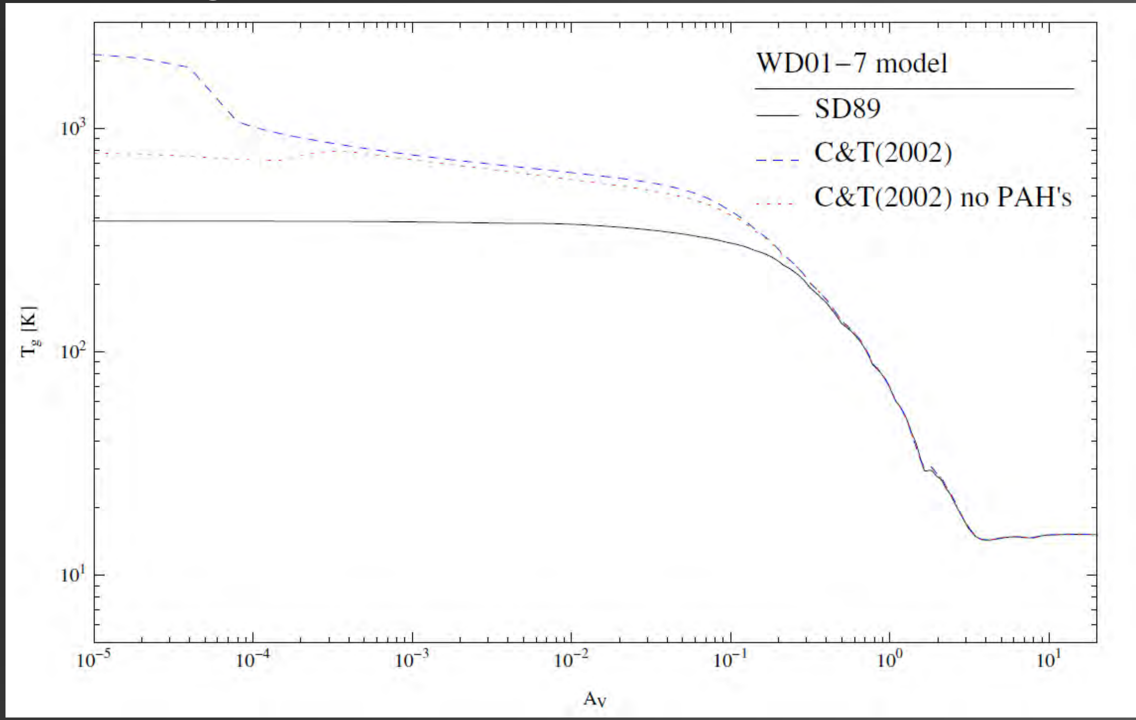

Röllig et al. 2013

More efficient H2 formation leads to stronger gas heating.

H_2 formation heating

CO line emission

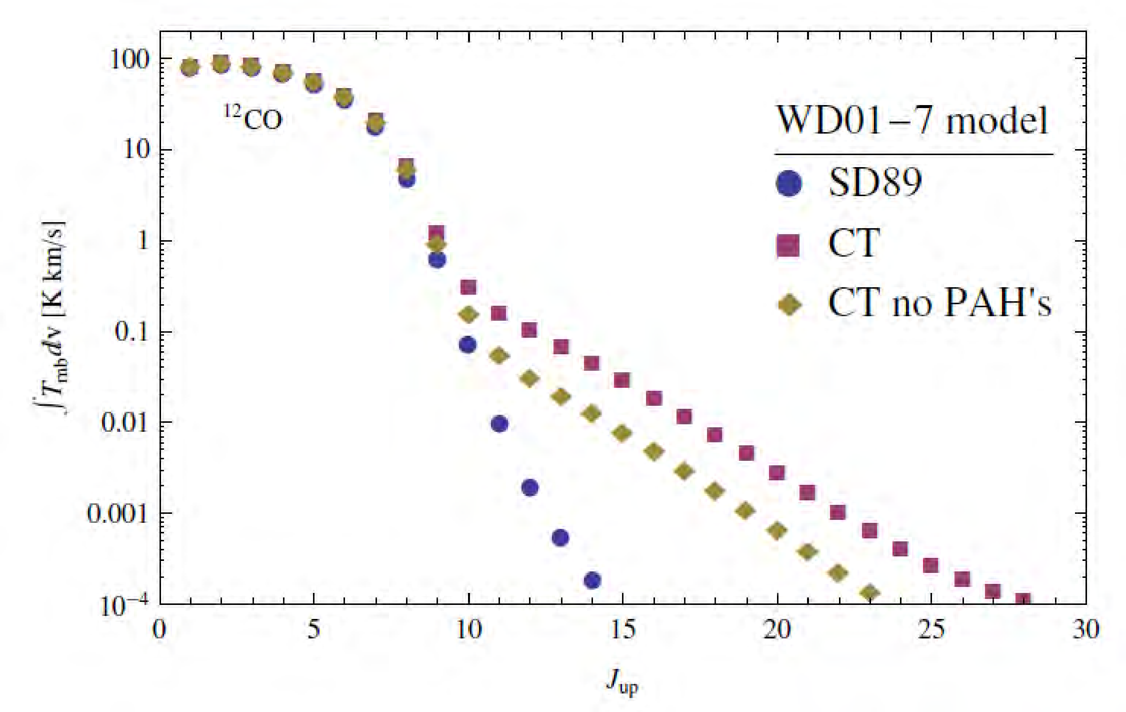

gas temperature

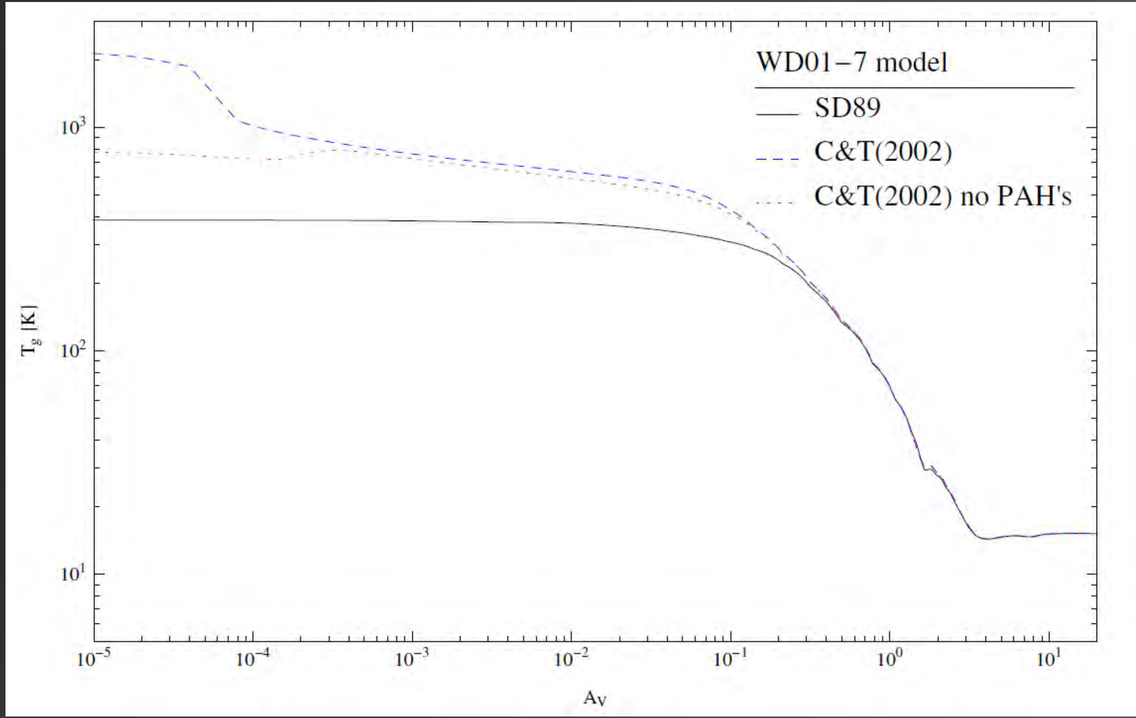

Röllig et al. 2013

Dust content & physics influences high-J CO emission

H_2 dissociation heating

- When H_2 is excited into the Lyman and Werner bands, there is about 10% chance that it will decay into the vibrational continuum, thus dissociating the molecule.
- Each of the H atoms created this way carries approximately 0.4 eV.

$$\Gamma_{H_2\ \mathrm{diss}} = 6.4 \times 10^{-13}\, n\,(H_2)\; R_{H_2\ \mathrm{diss}}\ \mathrm{erg\,cm^{-3}\,s^{-1}}$$

Gas-grain collisions

- If $T_{gas} \neq T_{dust}$ collisions between the two components will transport energy from the hotter to the cooler.

$$\Lambda_{\text{g-gr}} = n_{\text{gr}}\, n_{\text{H}}\, \sigma_{\text{gr}} \left(\frac{8kT_g}{\pi m_{\text{H}}}\right)^{1/2} \bar{\alpha}_T (2kT_g - 2kT_{\text{gr}})$$

Burke & Hollenbach 1983

α_T: accomodation factor, i.e. average energy transfer fraction (=1 if incoming particle fully thermalizes with the surface)

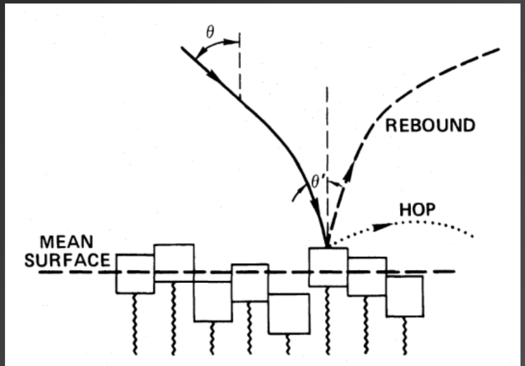

Gas-grain collisions

accomodation factor

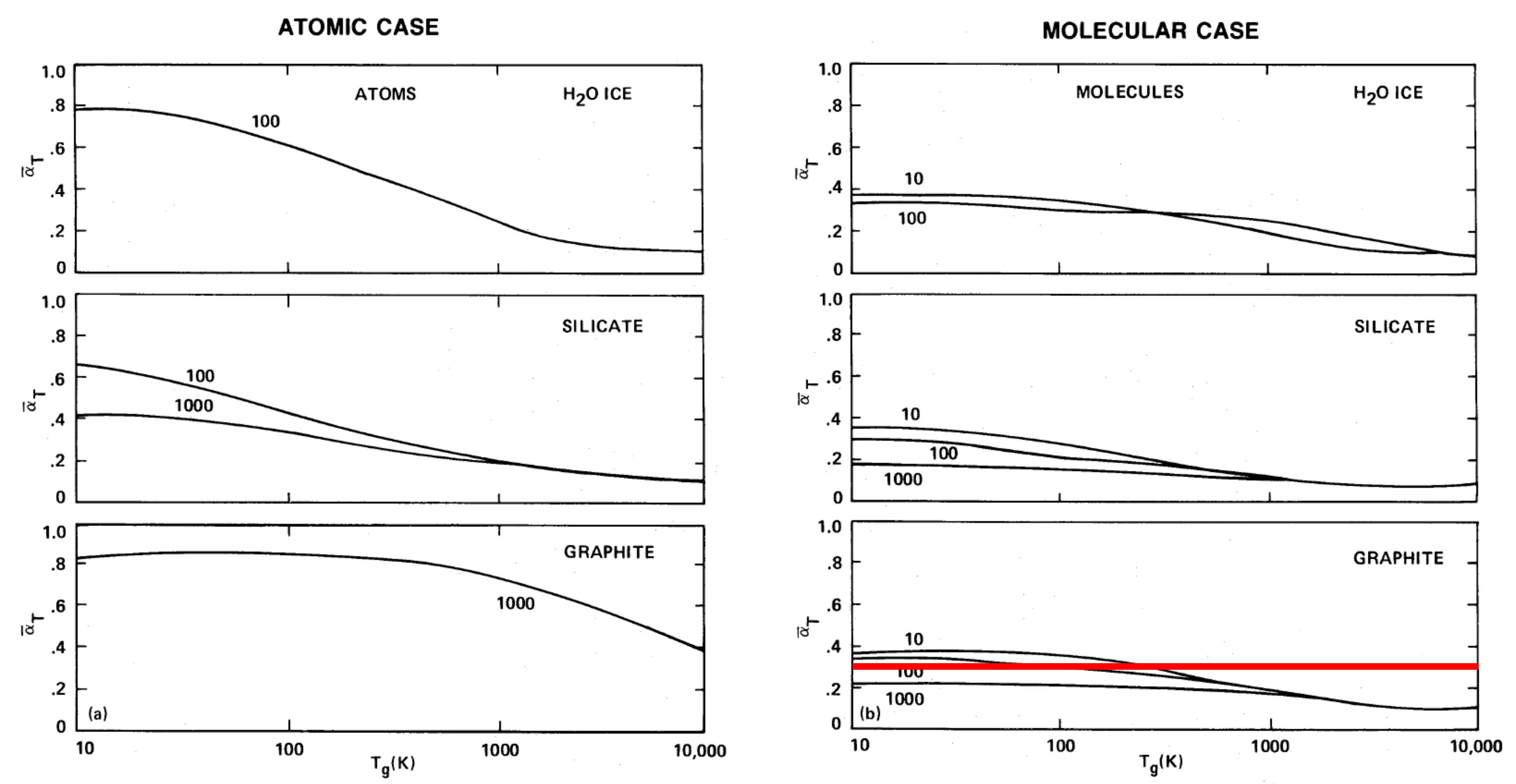

Burke & Hollenbach 1983

Carbon ionization

$$\Gamma_{\mathrm{C\ ion}} = 1.7 \times 10^{-12} R_{\mathrm{C\ ion}}\, n(\mathrm{C})\ \mathrm{erg\ cm^{-3}\ s^{-1}}$$

- Photo-ionization of atomic carbon releases a hot electron (~ 1 eV), heating the gas via collisions.

  R_{Cion}: carbon ionization rate

Cosmic ray heating

- Cosmic rays (e.g.: high energy 2-10 MeV) ionize the gas (H_2, He, HD) and inject hot e^- into the gas.
- The efficiency depends on the gas composition, density and ionization degree. Ionization of H and H2 contributes 3.5 and 8 eV respectively.
- Cosmic rays can penetrate much deeper into a molecular cloud (~ A_v=100) than UV photons (A_v<10). CR's are the dominant heating term at high optical depths.

$$\Gamma_{\rm CR} = \zeta_{\rm CR}\left(5.5\times10^{-12}n_{\rm H} + 2.5\times10^{-11}n_{\rm H_2}\right)$$

$$\xi_{\rm CR} \simeq 3\times10^{-16}\ {\rm s}^{-1}$$

Radiative line cooling

- When a transition of a species is excited collisionally and decays radiatively, the transition energy is carried away by photons and the gas is cooled.
- Coolant conditions:
  - abundant
  - collisionally excitable energy levels given ISM conditions
  - rapid decay times (large A_{ij})
- Good coolants:
  C^+, O, C, CO, H_2O

Radiative line cooling

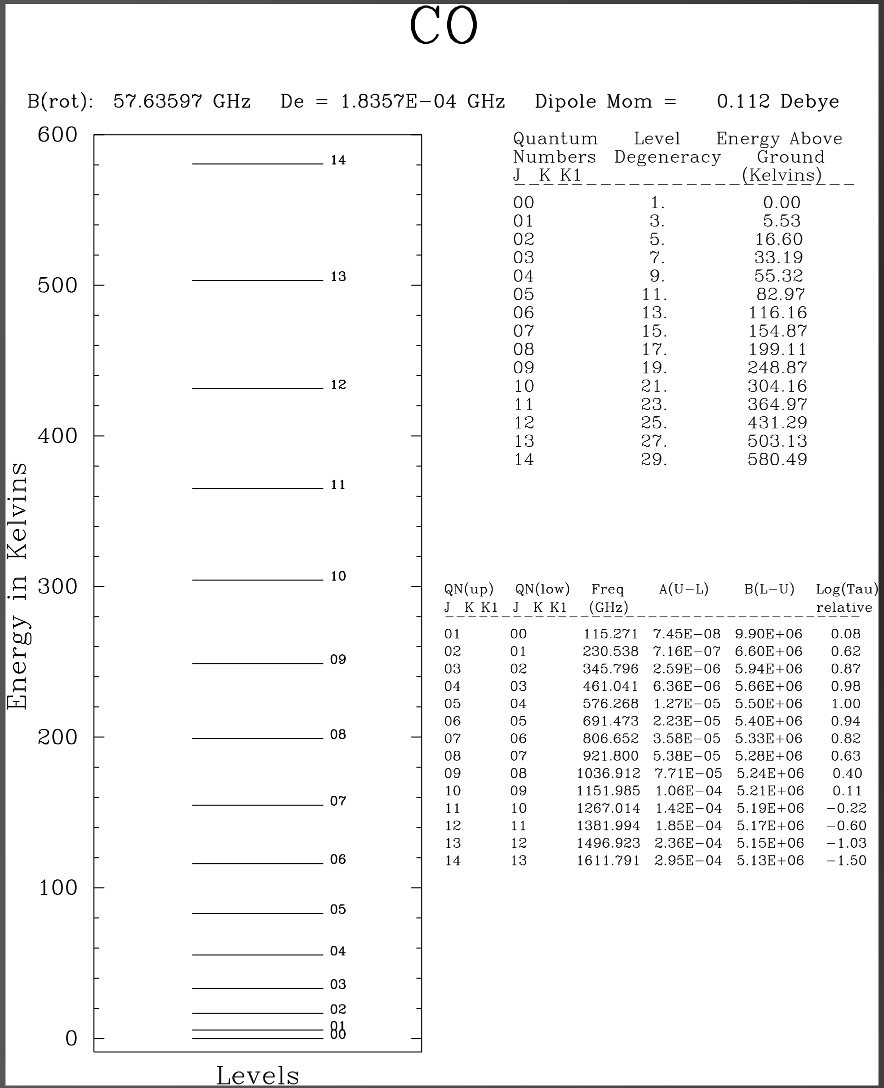

Quantum Numbers J K K1	Level Degeneracy	Energy Above Ground (Kelvins)
00	1.	0.00
01	3.	5.53
02	5.	16.60
03	7.	33.19
04	9.	55.32
05	11.	82.97
06	13.	116.16
07	15.	154.87
08	17.	199.11
09	19.	248.87
10	21.	304.16
11	23.	364.97
12	25.	431.29
13	27.	503.13
14	29.	580.49

QN(up) J K K1	QN(low) J K K1	Freq (GHz)	A(U-L)	B(L-U)	Log(Tau) relative
01	00	115.271	7.45E-08	9.90E+06	0.08
02	01	230.538	7.16E-07	6.60E+06	0.62
03	02	345.796	2.59E-06	5.94E+06	0.87
04	03	461.041	6.36E-06	5.66E+06	0.98
05	04	576.268	1.27E-05	5.50E+06	1.00
06	05	691.473	2.23E-05	5.40E+06	0.94
07	06	806.652	3.58E-05	5.33E+06	0.82
08	07	921.800	5.38E-05	5.28E+06	0.63
09	08	1036.912	7.71E-05	5.24E+06	0.40
10	09	1151.985	1.06E-04	5.21E+06	0.11
11	10	1267.014	1.42E-04	5.19E+06	−0.22
12	11	1381.994	1.85E-04	5.17E+06	−0.60
13	12	1496.923	2.36E-04	5.15E+06	−1.03
14	13	1611.791	2.95E-04	5.13E+06	−1.50

- When a transition of a species is excited collisionally and decays radiatively, the transition energy is carried away by photons and the gas is cooled.
- Coolant conditions:
  - abundant
  - collisionally excitable energy levels given ISM conditions
  - rapid decay times (large A_{ij})
- Good coolants:
  C^+, O, C, CO, H_2O

Fine-Structure Atomic Cooling Parameters

Species (0, 1, 2)[a]	$\frac{E_{ij}}{k}$ (K)[b]	λ_μ[c]	n_{cr}^{e} (cm^{-3})[d]	n_{cr}^{H} (cm^{-3})[d]	A_{ij} (s^{-1})[e]	γ_{ij}^{e} (cm^{-3} s^{-1})[f]	γ_{ij}^{H} (cm^{3} s^{-1})[f]	N_{τ} (cm^{-2})[g]
C I ($^3P_0$, $^3P_1$, $^3P_2$)	2.4(1)	609.2	3.9(0)$T_2^{-0.13}$	1.6(2)$T_2^{-0.34}$	7.9(−8)	3.0(−9)	1.6(−10)$T_2^{0.14}$	2.3(20)
	6.3(1)	229.9	1.3(1)	7.0(2)$T_2^{-0.26}$	2.0(−14)	5.0(−9)	9.2(−11)$T_2^{0.26}$	9.8(27)
	3.9(1)	369.0	...		2.7(−7)	1.5(−8)	2.9(−10)$T_2^{0.26}$	5.3(20)
C II ($^2P_{1/2}$, $^2P_{3/2}$)	9.2(1)	157.7	8.7(0)$T_2^{0.50}$	3.0(2)$T_2^{-0.07}$	2.4(−6)	2.8(−7)$T_2^{-0.5}$	8.0(−10)$T_2^{0.07}$	6.5(20)
Cl I ($^2P_{3/2}$, $^2P_{1/2}$)	1.3(3)	11.4	2.6(5)	1.4(7)$T_2^{-0.17}$	1.2(−2)	4.7(−8)	8.3(−10)$T_2^{0.17}$	1.1(24)
Cl II ($^3P_2$, $^3P_1$, $^3P_0$)	1.0(3)	14.4	1.4(4)$T_2^{0.45}$	5.4(6)	7.5(−3)	5.3(−7)$T_2^{-0.5}$	1.4(−9)	7.5(23)
	1.4(3)	10.0	1.6(3)$T_2^{0.50}$	8.1(5)	4.8(−7)	5.3(−7)$T_2^{-0.5}$	1.1(−9)	1.0(29)
	4.3(2)	33.4	...	...	1.4(−3)	3.2(−7)$T_2^{-0.5}$	6.3(−10)	5.7(23)
Fe I ($^5D_4$, $^5D_3$, $^5D_2$)	6.0(2)	24.0	2.1(4)$T_2^{-0.13}$	3.1(6)$T_2^{-0.28}$	2.5(−3)	1.2(−7)	8.0(−10)$T_2^{0.17}$	6.6(21)
	1.0(3)	14.2	7.5(3)	1.3(6)$T_2^{-0.17}$	1.0(−9)	1.2(−7)	6.9(−10)$T_2^{0.17}$	9.3(26)
	4.2(2)	34.2	...	...	1.6(3)	9.3(−8)	5.3(−10)$T_2^{0.17}$	3.7(21)
Fe II ($^6D_{9/2}$, $^6D_{7/2}$, $^6D_{5/2}$) ..	5.6(2)	26.0	1.2(3)$T_2^{0.41}$	2.2(6)$T_2^{-0.09}$	2.1(−3)	1.8(−6)$T_2^{-0.5}$	9.5(−10)	6.0(21)
	9.6(2)	15.0	6.0(2)$T_2^{0.50}$	1.5(6)	1.5(−9)	1.8(−6)$T_2^{-0.5}$	5.7(−10)	5.9(28)
	4.1(2)	35.4	...	...	1.6(−3)	8.7(−7)$T_2^{-0.5}$	4.7(−10)	3.3(21)
Ne II ($^2P_{3/2}$, $^2P_{1/2}$)	1.1(3)	12.8	5.4(4)$T_2^{0.50}$	6.6(6)	8.6(−3)	1.6(−7)$T_2^{-0.5}$	1.3(−9)	1.9(22)
Ni I ($^3F_4$, $^3F_3$, $^3F_2$)	1.9(3)	7.5	5.2(5)$T_2^{-0.06}$	7.8(7)$T_2^{-0.22}$	6.2(−2)	1.2(−7)	8.0(−10)$T_2^{0.17}$	1.1(23)
	3.2(3)	4.5	1.2(5)	2.0(7)$T_2^{0.17}$	3.6(−9)	1.2(−7)	6.9(−10)$T_2^{0.17}$	1.3(31)
	1.3(3)	11.3	...	...	2.5(−2)	9.3(−8)	5.3(−10)$T_2^{0.17}$	8.9(22)
Ni II ($^2D_{5/2}$, $^2D_{3/2}$)	2.2(3)	6.6	5.0(4)$T_2^{0.50}$	5.0(7)	5.5(−2)	1.1(−6)$T_2^{-0.5}$	1.1(−9)	2.2(23)
O I ($^3P_2$, $^3P_1$, $^3P_0$)	2.3(2)	63.1	6.3(3)$T_2^{-0.03}$	8.5(5)$T_2^{-0.69}$	9.0(−5)	1.4(−8)	9.2(−11)$T_2^{0.67}$	4.9(20)
	3.3(2)	44.2	8.9(2)	1.1(5)$T_2^{-0.57}$	1.0(−10)	1.4(−8)	4.3(−11)$T_2^{0.80}$	3.8(27)
	9.8(1)	145.6	...		1.7(−5)	5.0(−9)	1.1(−10)$T_2^{0.44}$	3.7(20)
S I ($^3P_2$, $^3P_1$, $^3P_0$)	5.7(2)	25.2	4.2(4)$T_2^{-0.03}$	1.8(6)$T_2^{-0.22}$	1.4(−3)	3.3(−8)	7.5(−10)$T_2^{0.17}$	2.0(22)
	8.2(2)	17.4	6.7(3)	2.7(5)$T_2^{-0.17}$	7.1(−8)	3.3(−8)	7.1(−10)$T_2^{0.17}$	3.7(27)
	2.5(2)	56.6	...	...	3.0(−4)	1.2(−8)	4.2(−10)$T_2^{0.17}$	1.5(22)
Si I ($^3P_0$, $^3P_1$, $^3P_2$)	1.1(2)	129.6	7.2(2)$T_2^{-0.50}$	1.9(4)$T_2^{-0.47}$	8.4(−6)	7.2(−9)	3.5(−10)$T_2^{-0.03}$	2.3(21)
	3.2(2)	44.8	1.4(3)	6.3(4)$T_2^{-0.17}$	2.4(−10)	7.2(−9)	1.7(−10)$T_2^{0.17}$	2.0(27)
	2.1(2)	68.4	...	...	4.2(−5)	2.2(−8)	5.0(−10)$T_2^{0.17}$	5.6(21)
Si II ($^2P_{1/2}$, $^2P_{3/2}$)	4.1(2)	34.8	1.2(2)$T_2^{0.50}$	3.2(5)	2.1(−4)	1.7(−6)$T_2^{-0.5}$	8.0(−10)$T_2^{-0.07}$	7.1(21)

[a] The levels are arranged as follows: 0 = ground state, 1 = first excited state, and 2 = second excited state.

[b] For three-level systems, the energies listed are E_{10}, E_{20}, and E_{21}, respectively.

[c] The wavelength in microns; note that the 2→0 transition is generally forbidden.

[d] The critical densities (*see text*) are listed to achieve LTE in levels 1 and 2, respectively, $T_2 = T/100$ K. The power law fits for the three level systems are accurate to 30% in the temperature range 30 K < T < 3000 K.

[e] The spontaneous transition rates listed in order A_{10}, A_{20}, and A_{21}. These are taken from Aller (1984), Garstang 1958, 1962, 1964, 1968; Grevesse, Nussbaumer, and Swings 1971; and Wiese *et al.* 1966, 1969.

[f] The rate coefficients for collisional deexcitation are listed in the same order. They are calculated from formulae given by Bahcall and Wolf 1968 with the exceptions C I and O I (Launay and Roueff 1977*a*), C II (Launay and Roueff 1977*b*), Fe II (Aannestad 1973), Ne II (Osterbrock 1974). Proton rates are substituted for electron rates for neutral target atoms.

[g] N_τ is the column density of hydrogen nuclei which provide unit optical depth at line center, assuming solar abundances of the species in the lower state of the transition.

Hollenbach & Mckee, 1989, ApJ 342, 306

Radiative line cooling

$$\Lambda_X(\nu_{ij}) = n_i A_{ij} h\nu_{ij} \beta_{\rm esc}(\tau_{ij}) \frac{S(\nu_{ij}) - P(\nu_{ij})}{S(\nu_{ij})}$$

- radiative cooling rate due to transition *i*→*j* of a species *x*

$$S(\nu_{ij}) = \frac{2h\nu_{ij}^3}{c^2} \left(\frac{g_i n_j}{g_j n_i} - 1 \right)^{-1}$$

- local source function

$$\frac{{\rm d}n_i}{{\rm d}t} = \sum_{j \neq i} n_j R_{j \to i} - n_i \sum_{j \neq i} R_{i \to j} = 0$$

- level populations from the equations of statistical equilibrium

$$P(\nu_{ij}) = B_{\nu_{ij}}(T_{\rm CMB}) + \tau_{\rm dust} B_{\nu_{ij}}(T_0)$$

- background radiation

Radiative line cooling

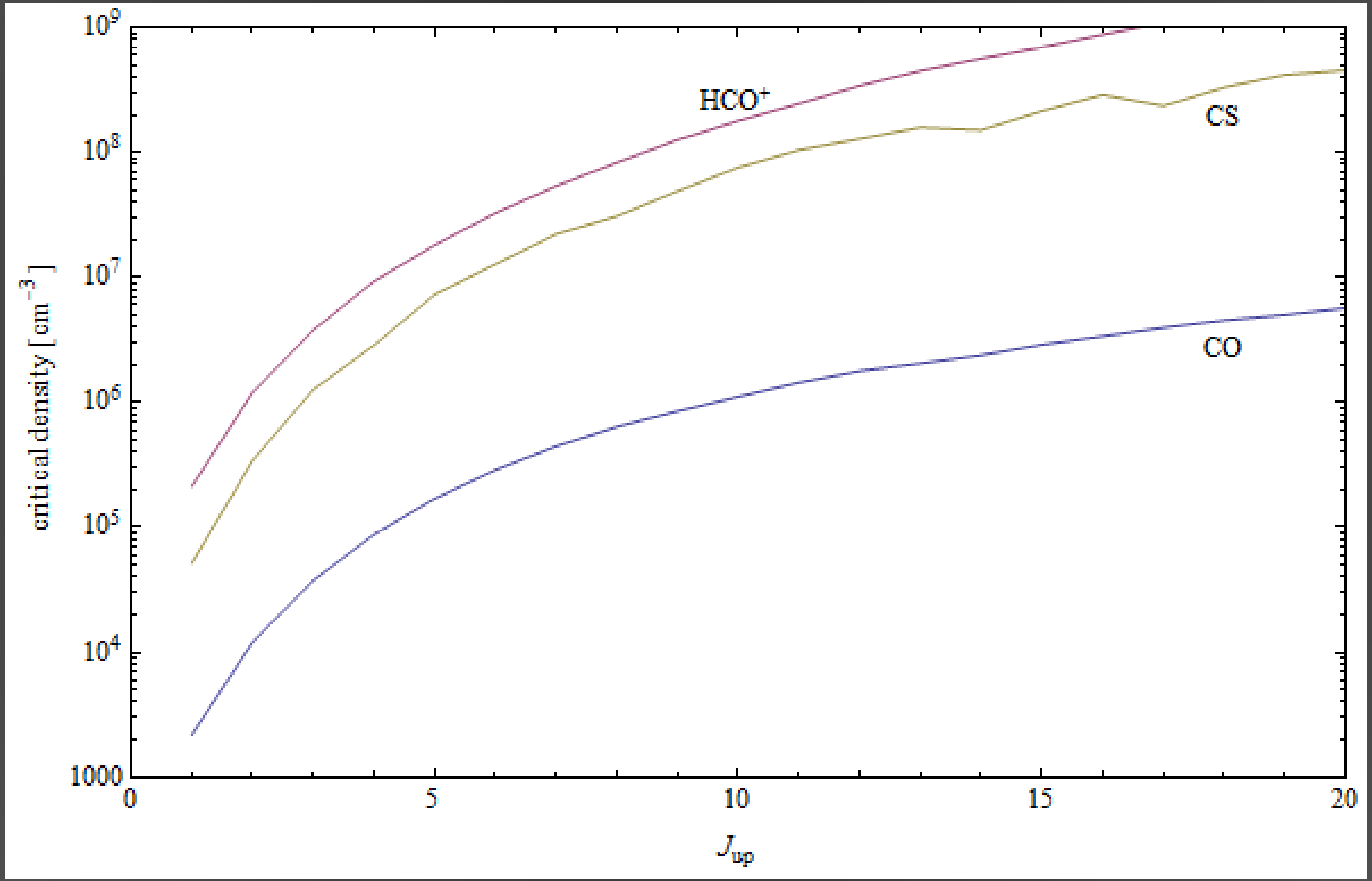

PDR heating/cooling

$\chi=100$ $\chi=10^5$

$n=10^3$

$n=10^5$

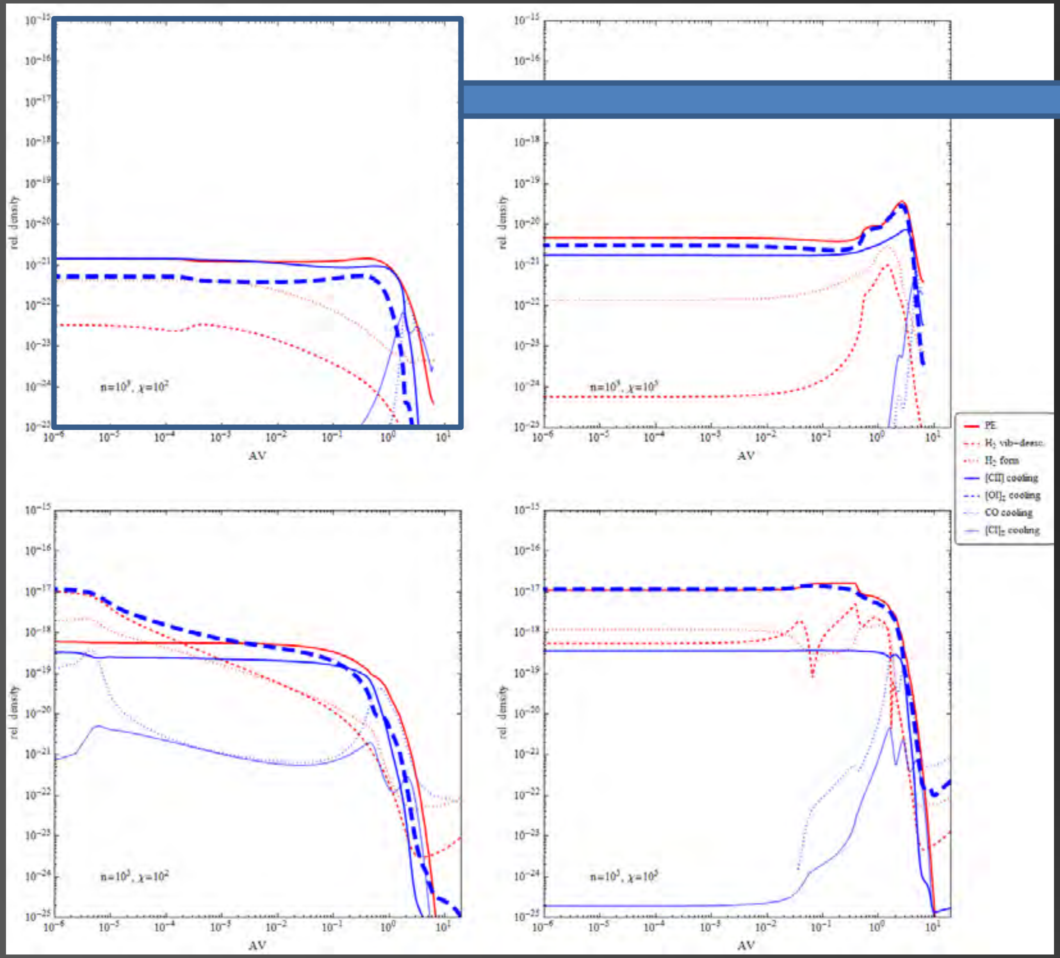

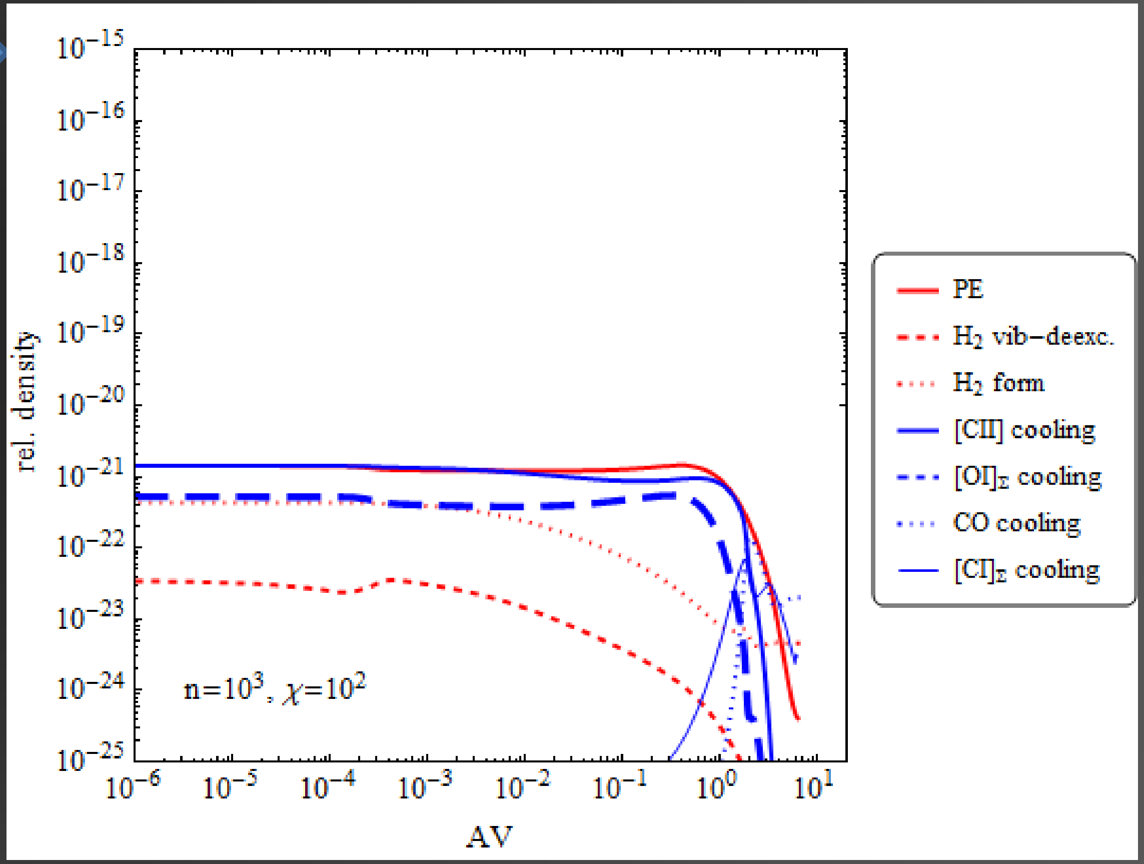

PDR heating/cooling

χ=100 χ=10^5

n=10^3

n=10^5

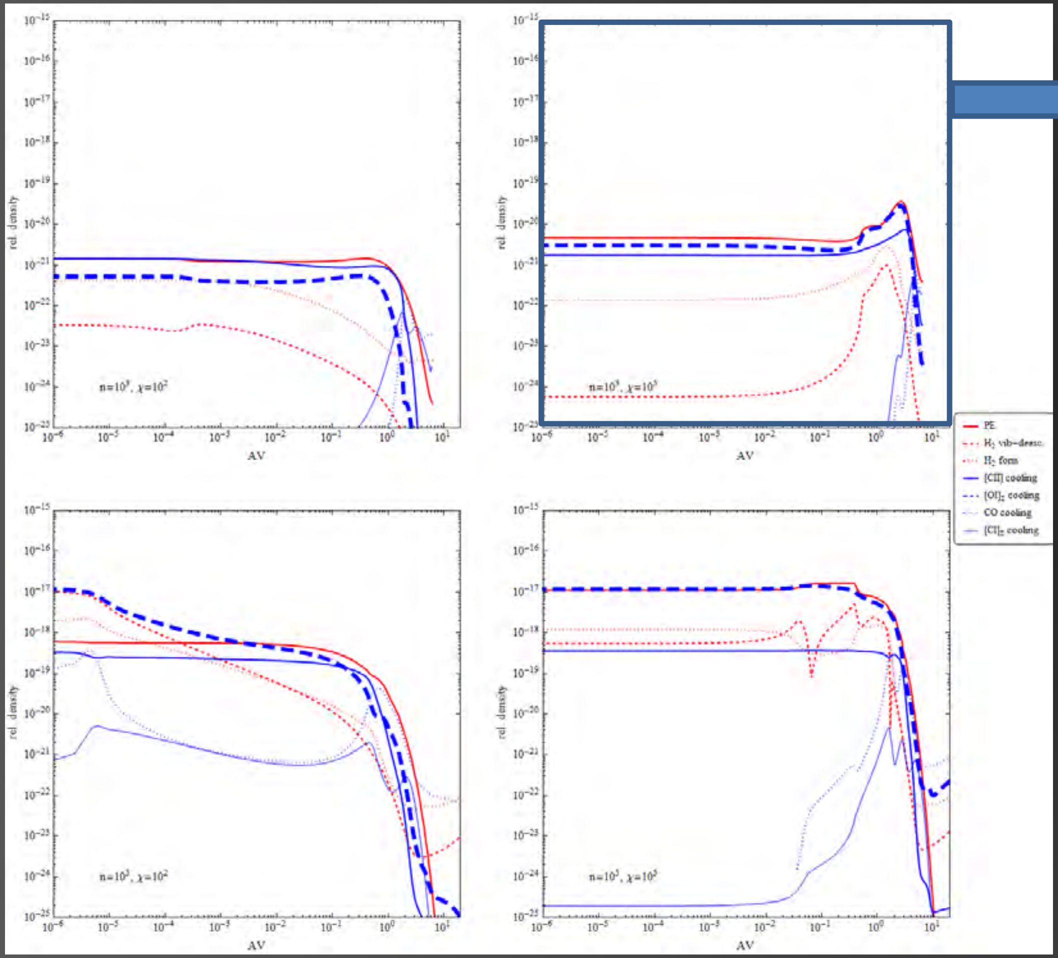

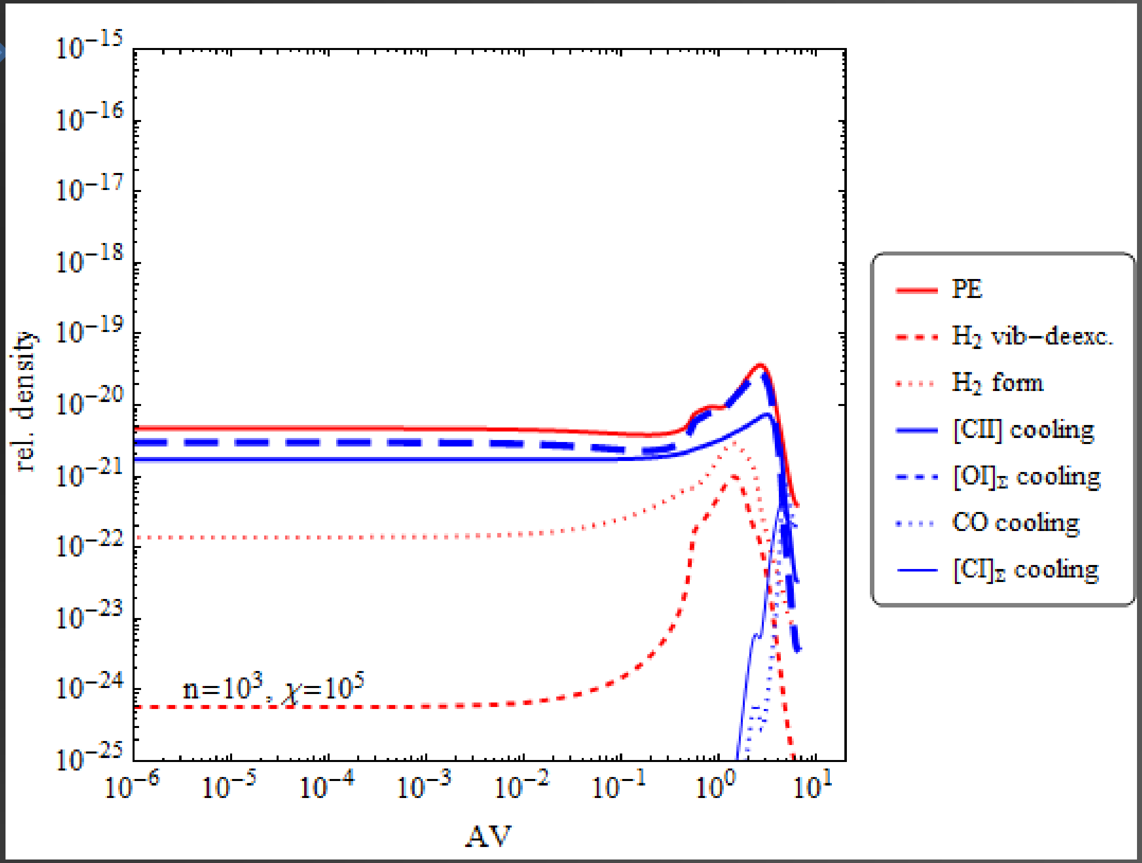

PDR heating/cooling

χ=100 $\chi=10^5$

$n=10^3$

$n=10^5$

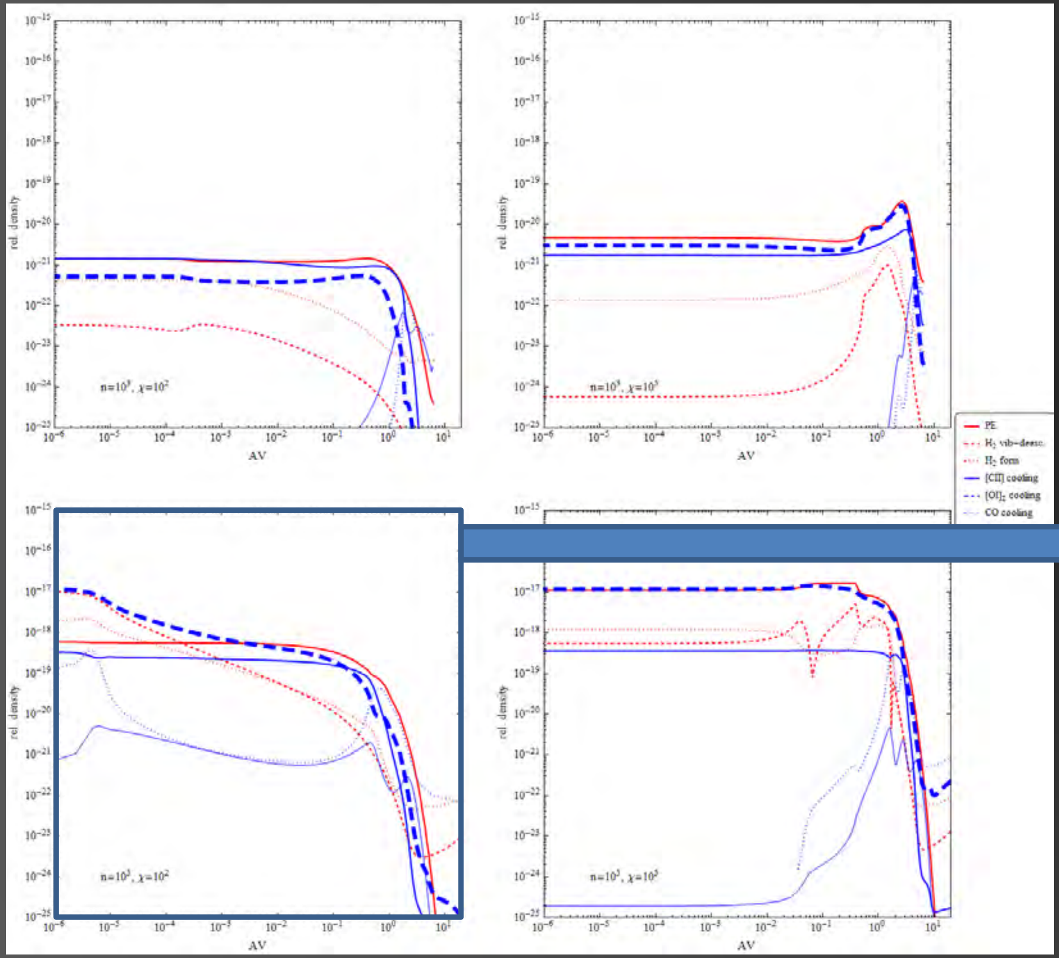

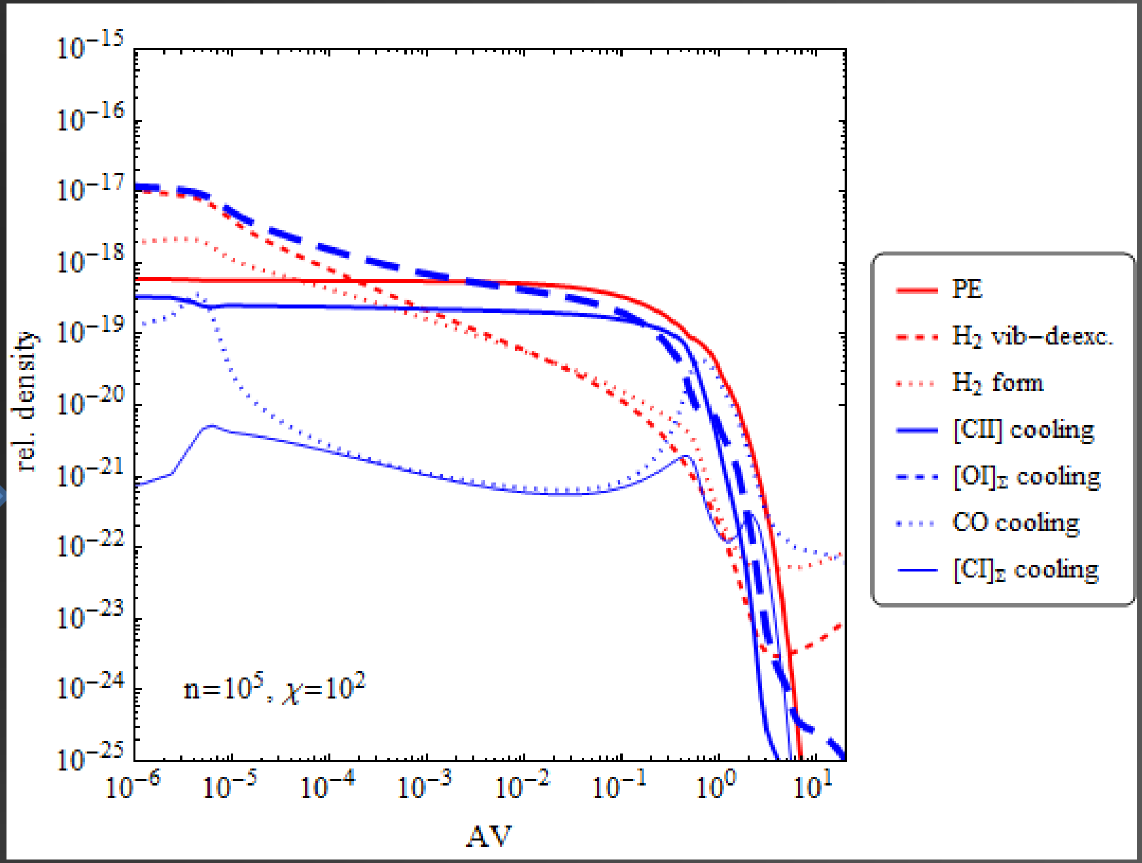

PDR heating/cooling

$\chi=100$ $\chi=10^5$

$n=10^3$

$n=10^5$

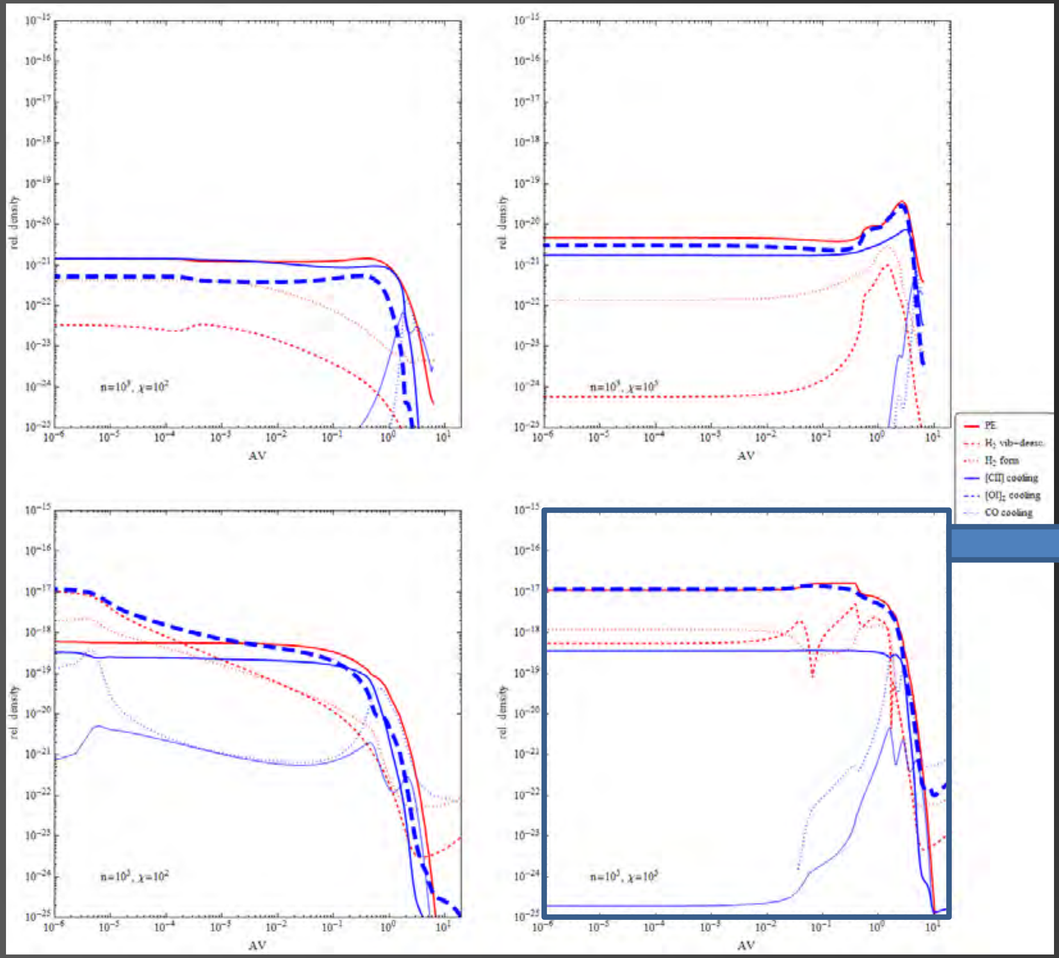

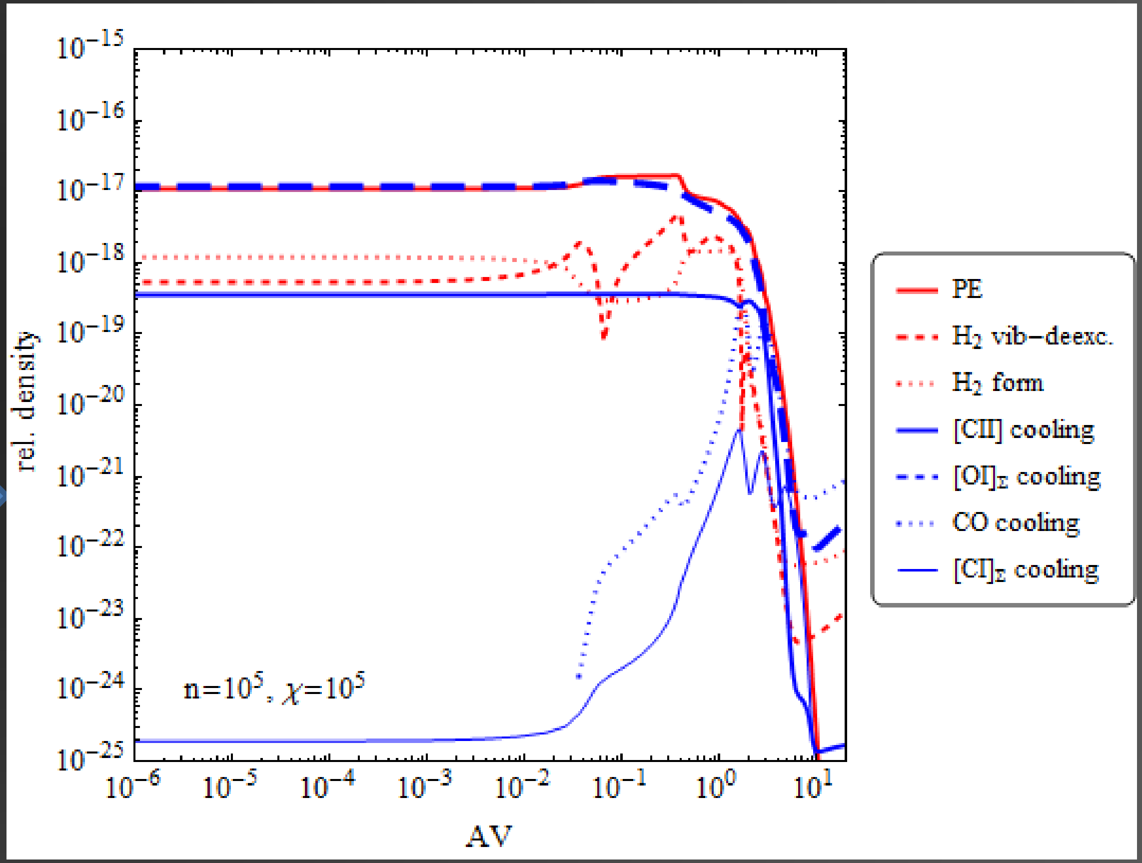

H_2 excitation

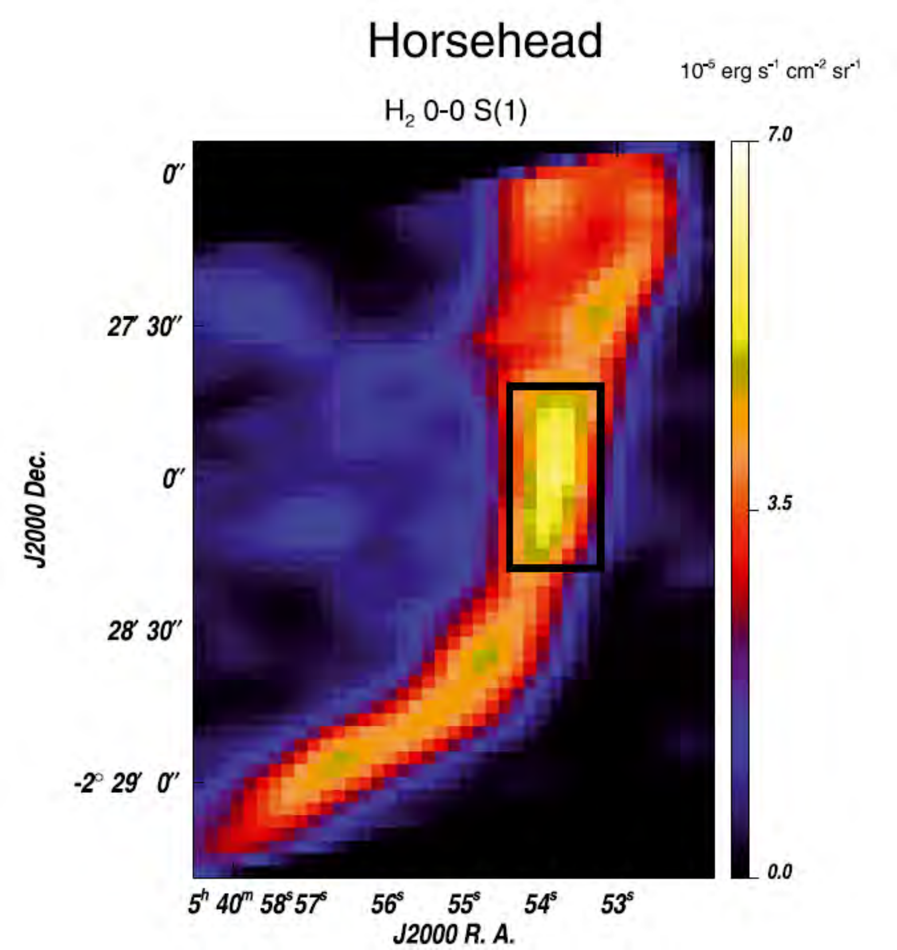

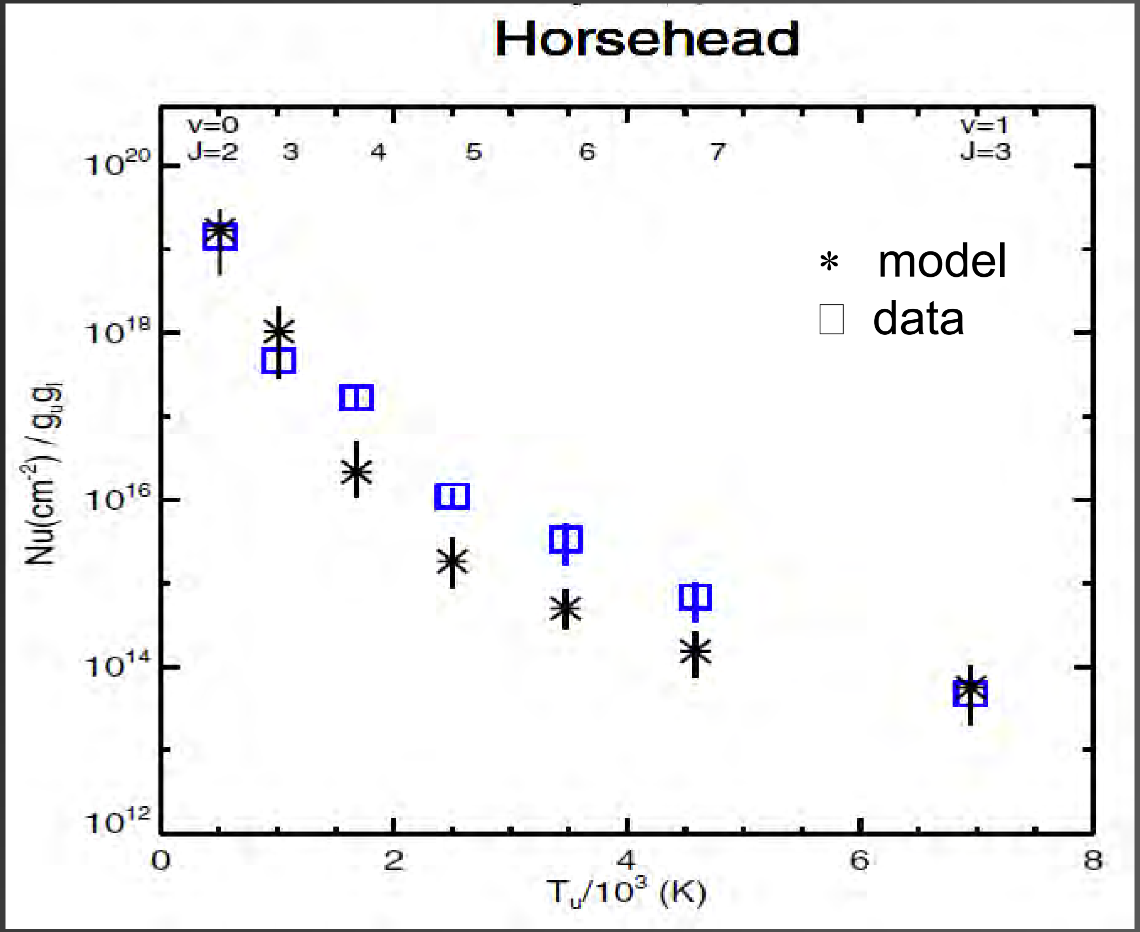

Habart et al. 2011

H_2 excitation

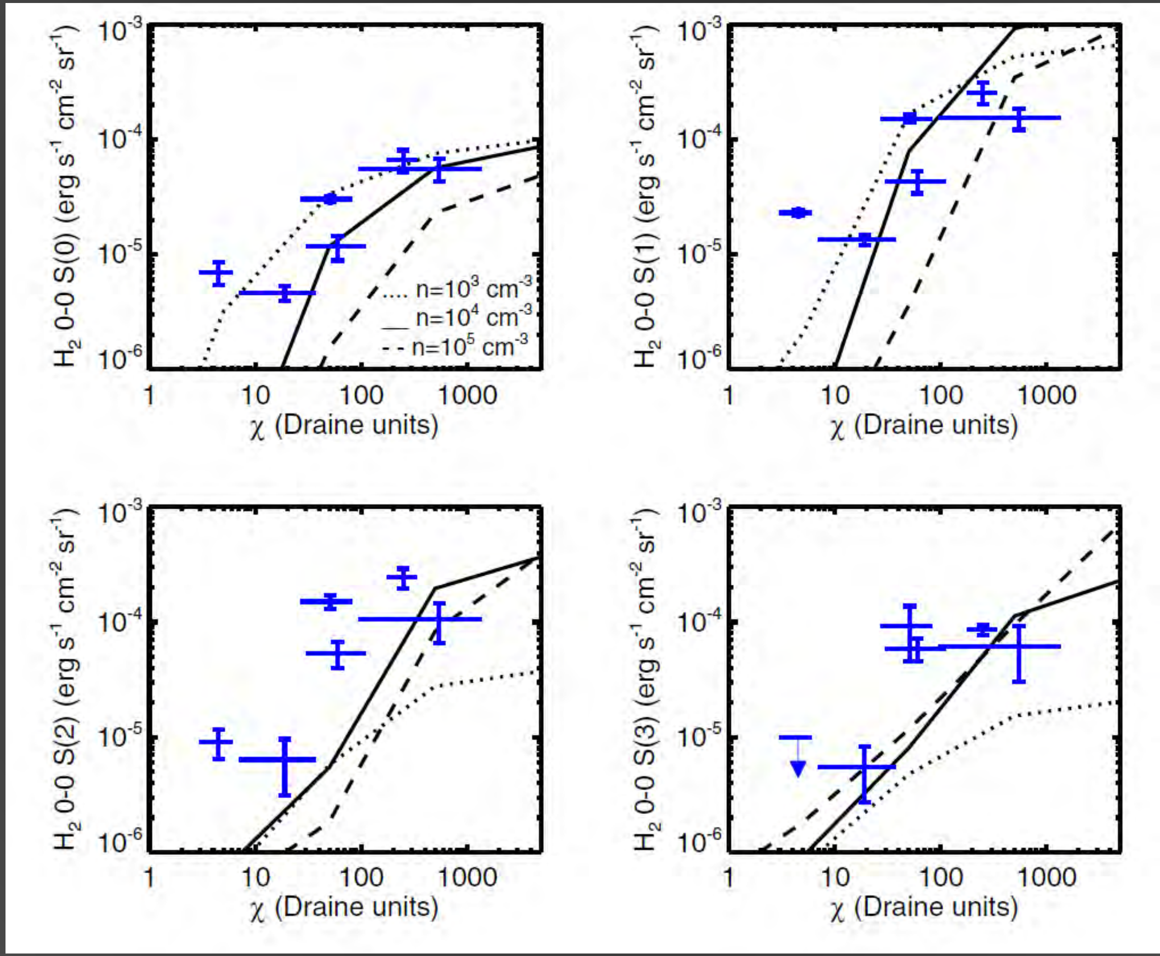

Habart et al. 2011

higher H_2 transition (J_{up}>3) can not easily be reproduced by PDR models

CO Dissociation

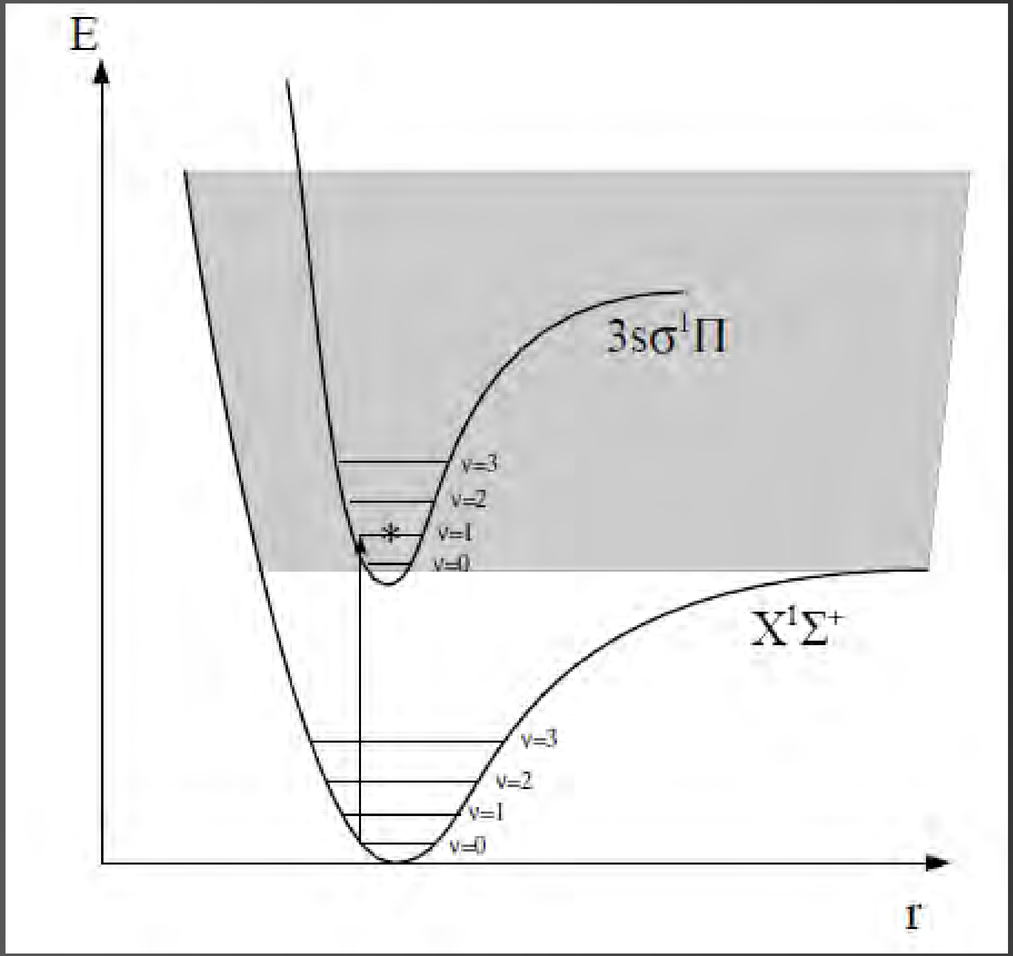

- CO dissociation occurs via line absorption!
- Absorbed photons excite *predissociated* electronic states that can decay into unbound continuum of the ground elect. state radiationless.
- More than 30 absorption bands in the range 913 Å ≤ λ ≤ 1077 Å
- Line absorption leads to optical thickness effects (self-shielding)

Warin et al. 1996

CO Dissociation

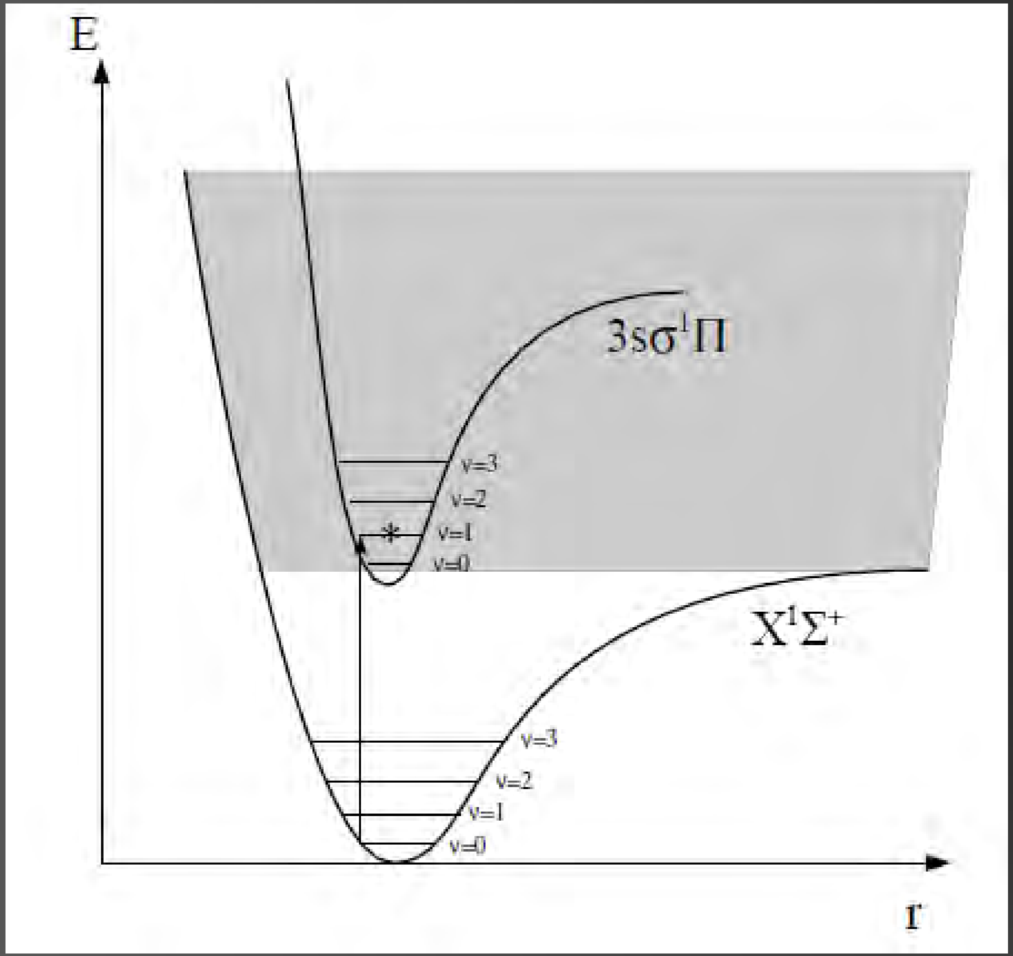

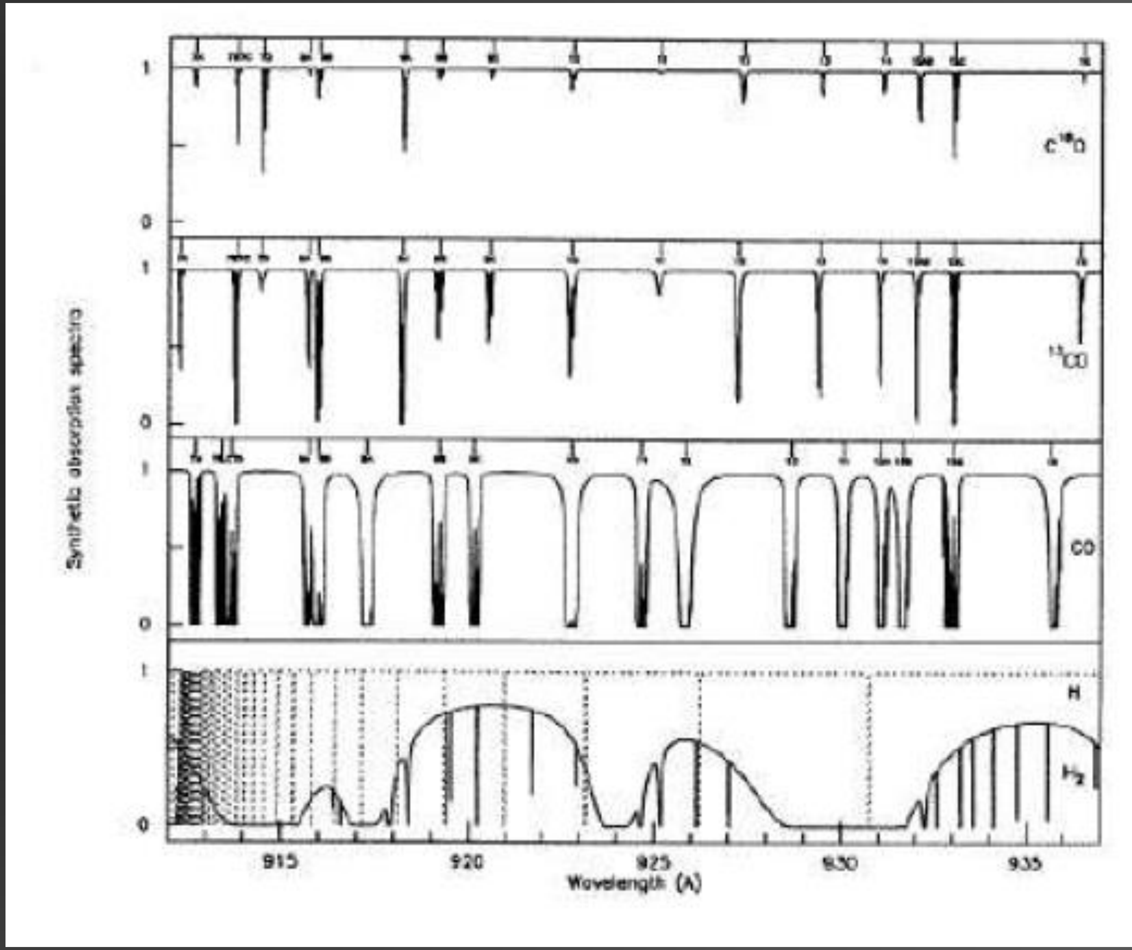

Warin et al. 1996

Chemistry

The carbon roadmap

- Like any roadmap, this network describes *how to get from A to B*.
- Like on any roadmap, *some paths are quick some are slow*.
- Unlike any normal roadmap some *slow paths may become very quick* under certain conditions

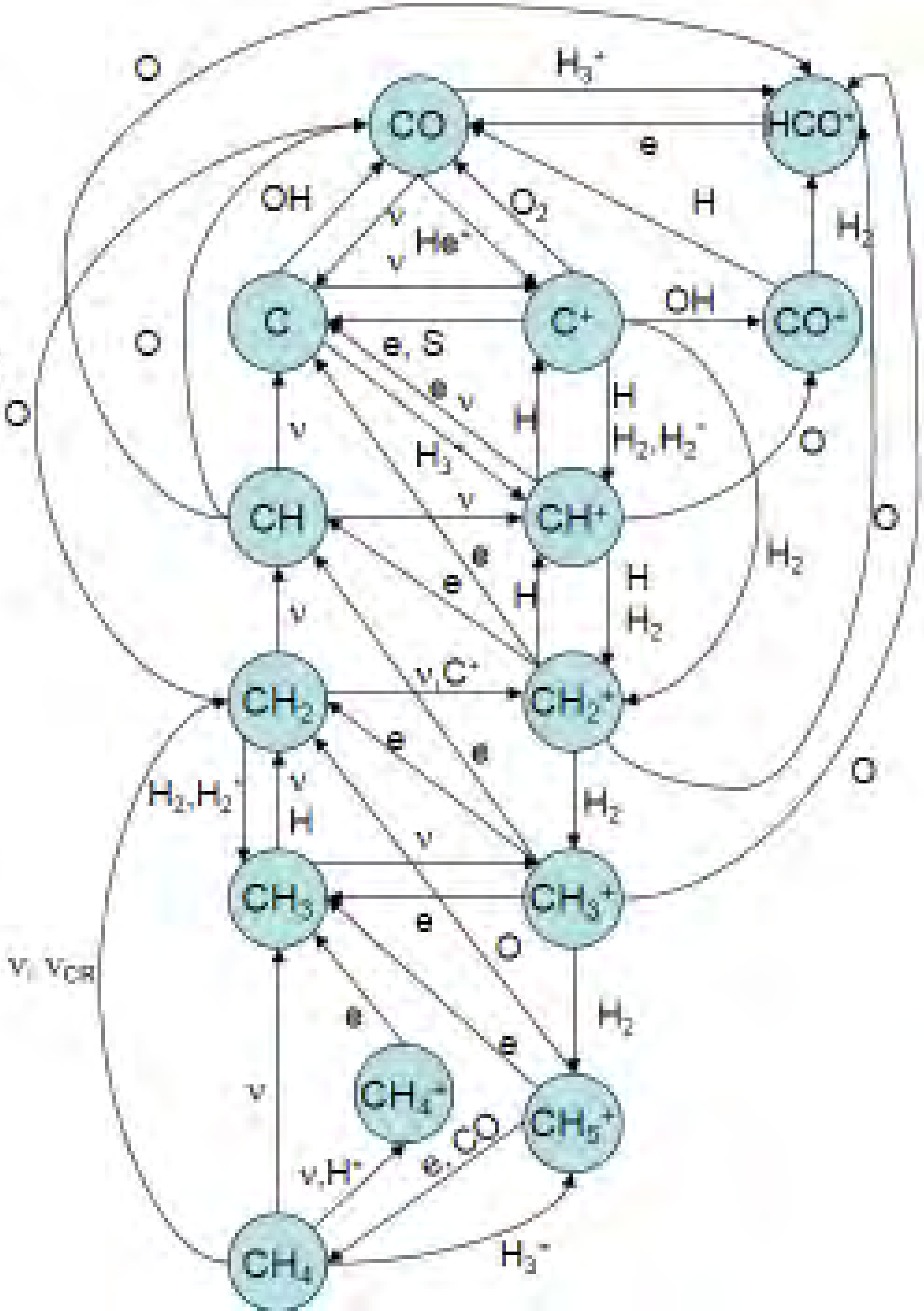

Example: **Diffuse Cloud**

starting point: C^+

collision with H_2:

~~$C^+ + H_2 \rightarrow CH^+ + H$~~ ΔE=4600K

instead:

k ≈ 10^{-15} cm³s⁻¹

$C^+ + H_2 \rightarrow CH_2^+ + \nu$

k ≈ 10^{-9} cm³s⁻¹

$CH_2^+ + H_2 \rightarrow CH_3^+ + H$

then:

k ≈ 10^{-7} cm³s⁻¹

$CH_n^+ + e \rightarrow CH_{n-1} + H$

and:

k ≈ 10^{-10} cm³s⁻¹

$CH_n + O \rightarrow CO + n\,H$

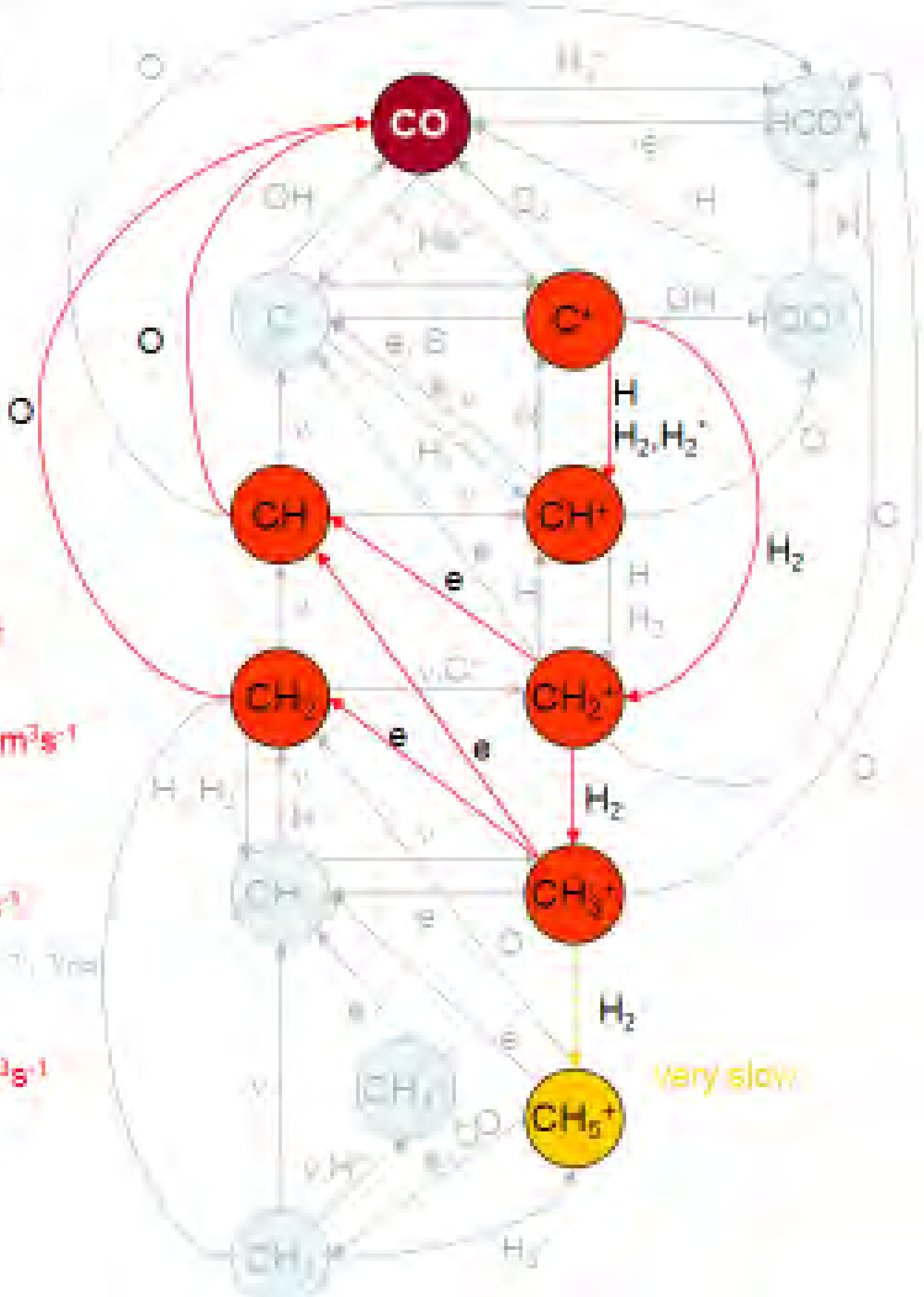

Example: **PDR**

high FUV intensity heats the gas at the surface

→ some slow routes become quick

$C^+ + H_2 \rightarrow CH^+ + H$

$C^+ + H_2^* \rightarrow CH^+ + H$

endothermic reactions become possible

activation energy barriers become surmountable

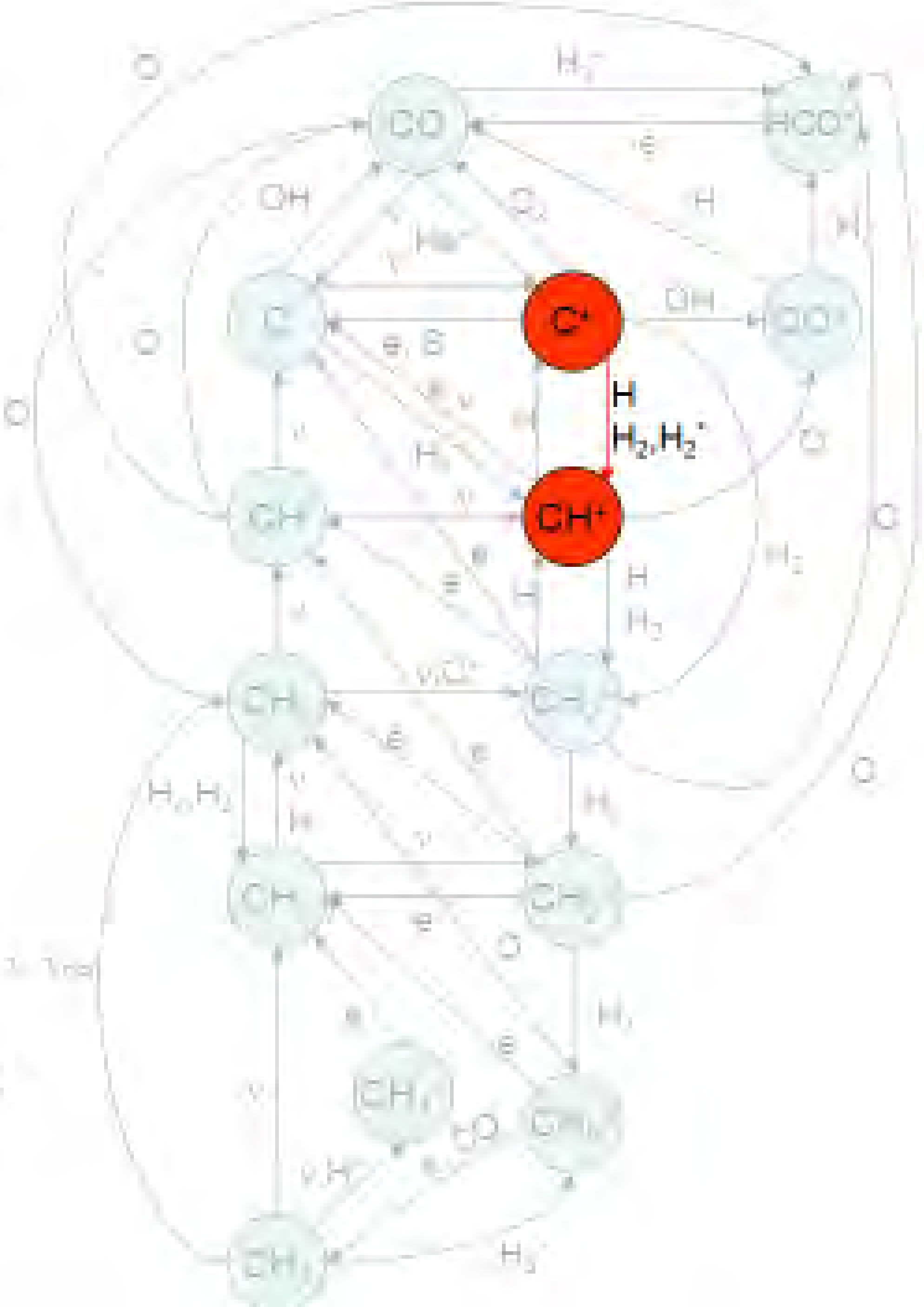

Example: **Dark Cloud**

cold and dense:

$T=10$ K, $n=10^4$-10^5 cm^{-3}

carbon locked in CO

$He + c.r \rightarrow He^+ + e$

$He^+ + CO \rightarrow C^+ + O + He$

FUV fully absorbed

some roads vanish

some roads become slow

e.g. reactions with e$^-$

but:

$CH_5^+ + CO \rightarrow CH_4 + HCO^+$

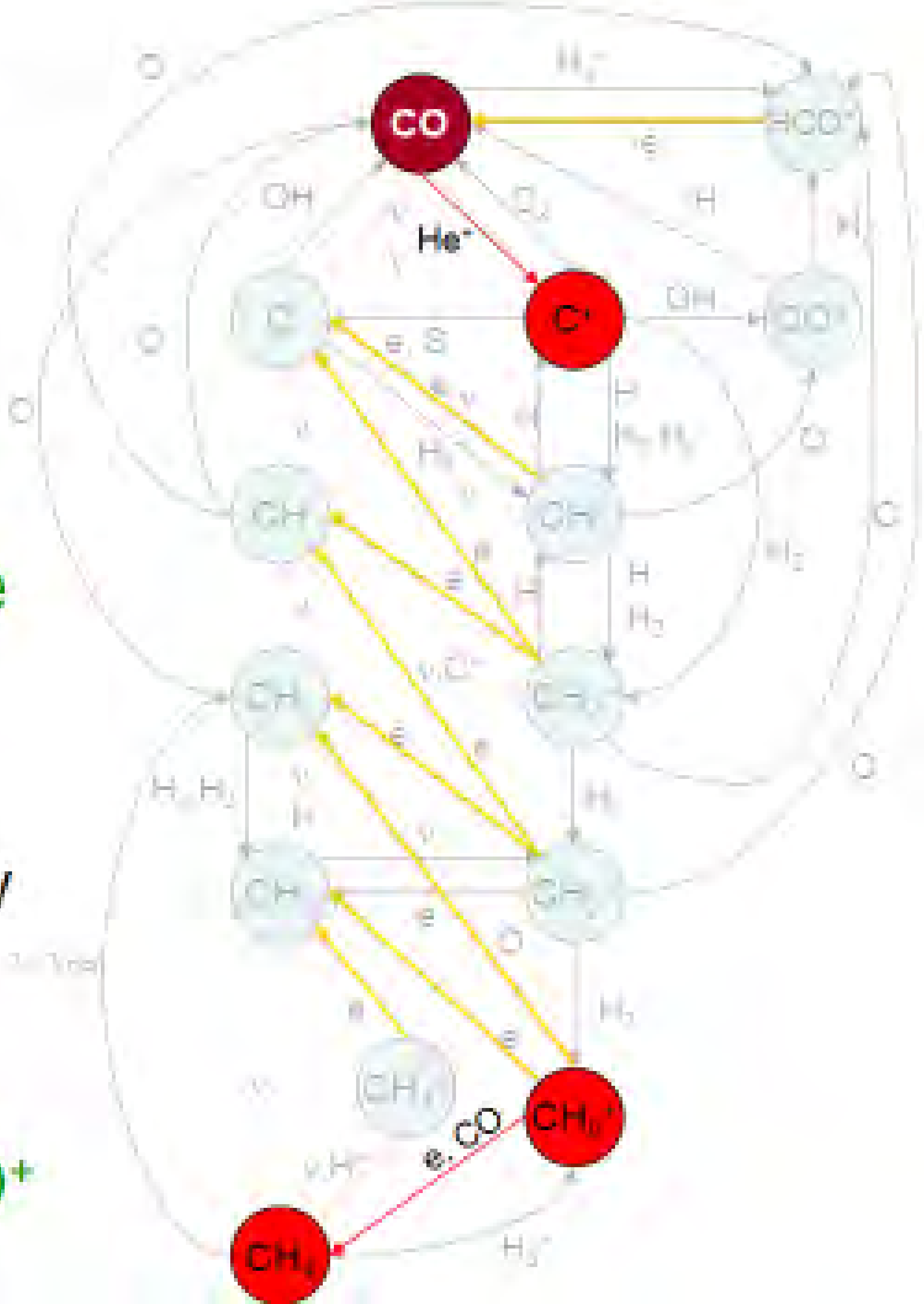

Looks 'simple', but:

CH^+ a factor 100 too low

H_2 formation not fully understood

…

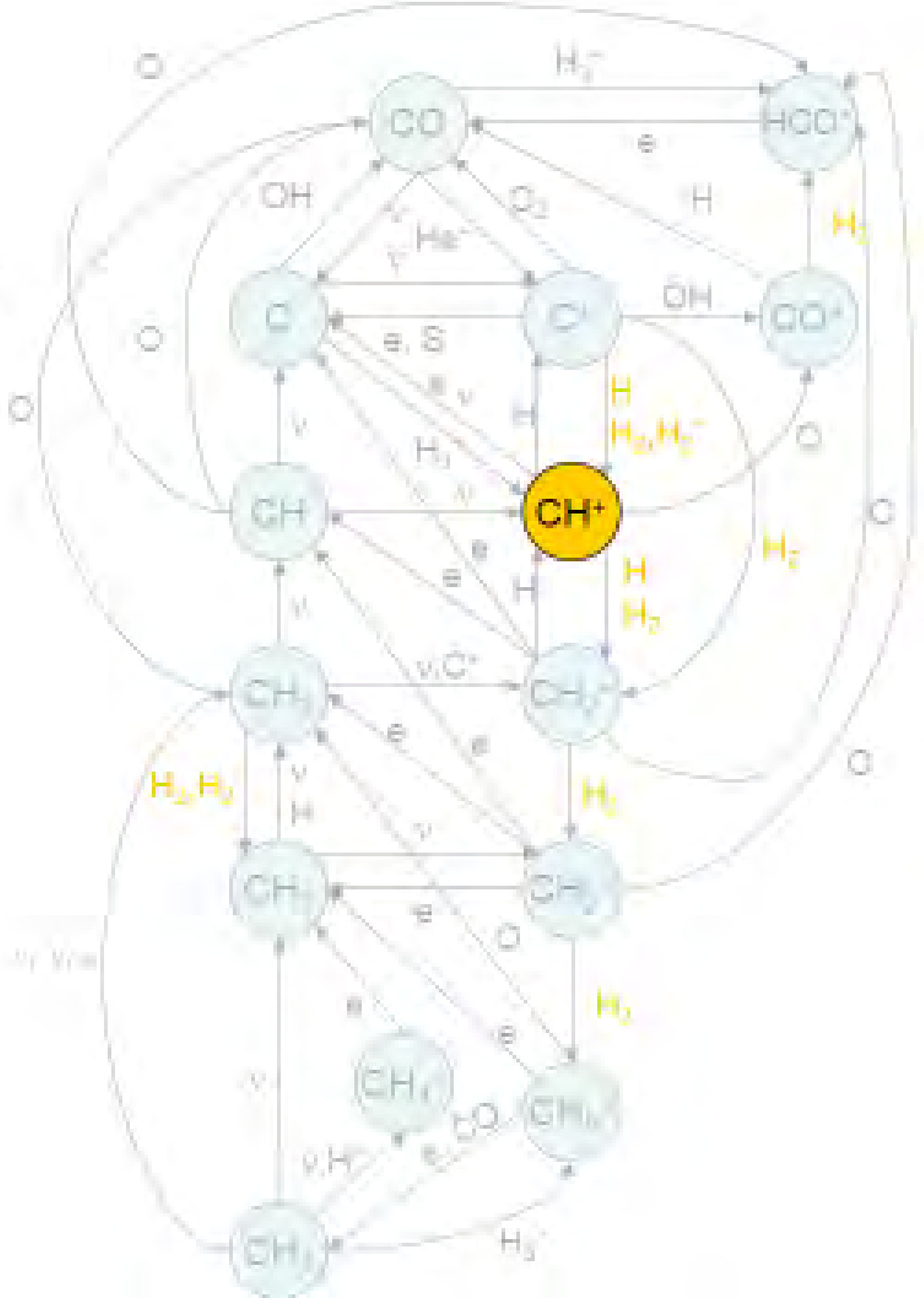

A_V is not a spatial coordinate

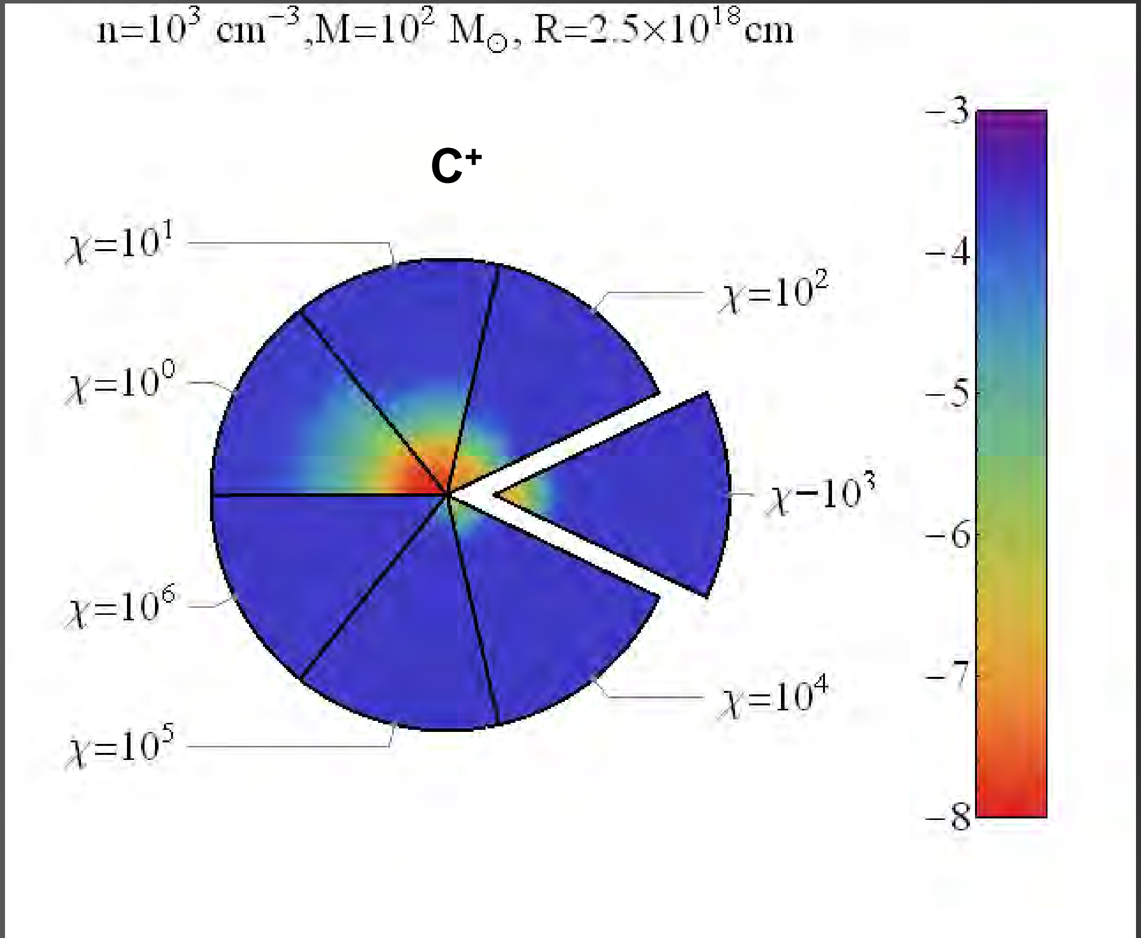

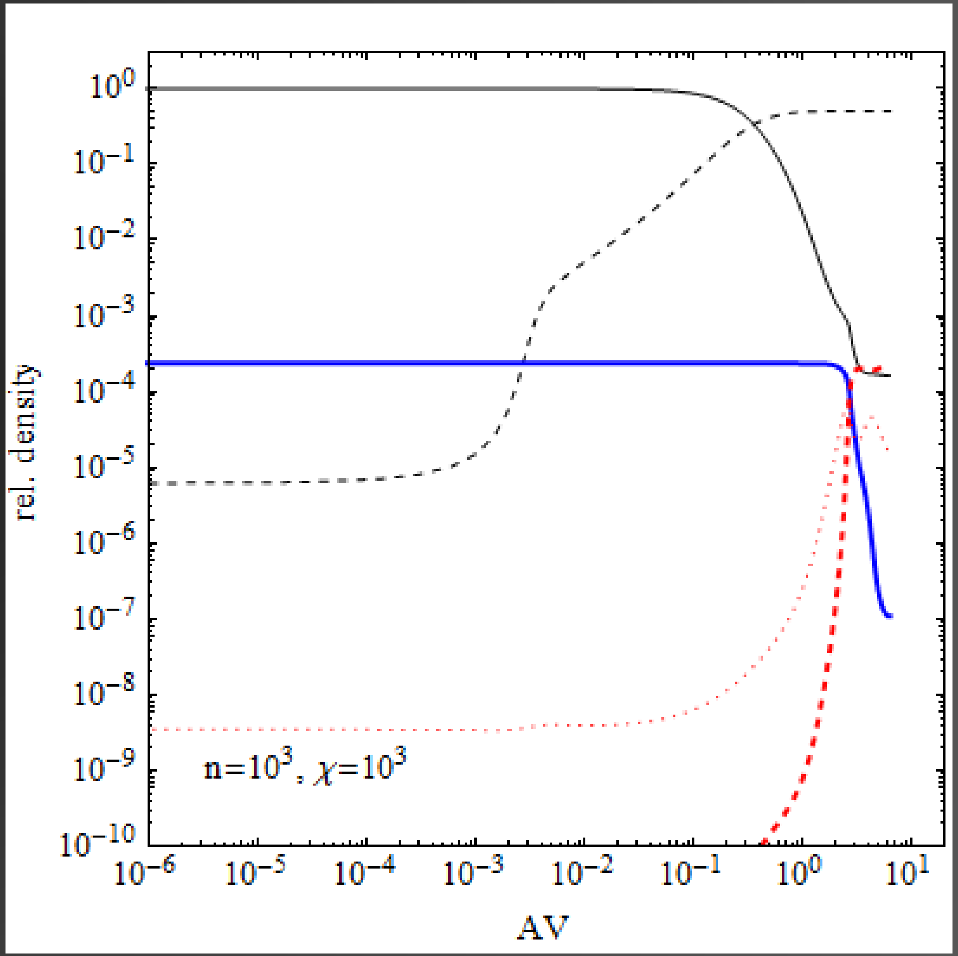

A_V is not a spatial coordinate

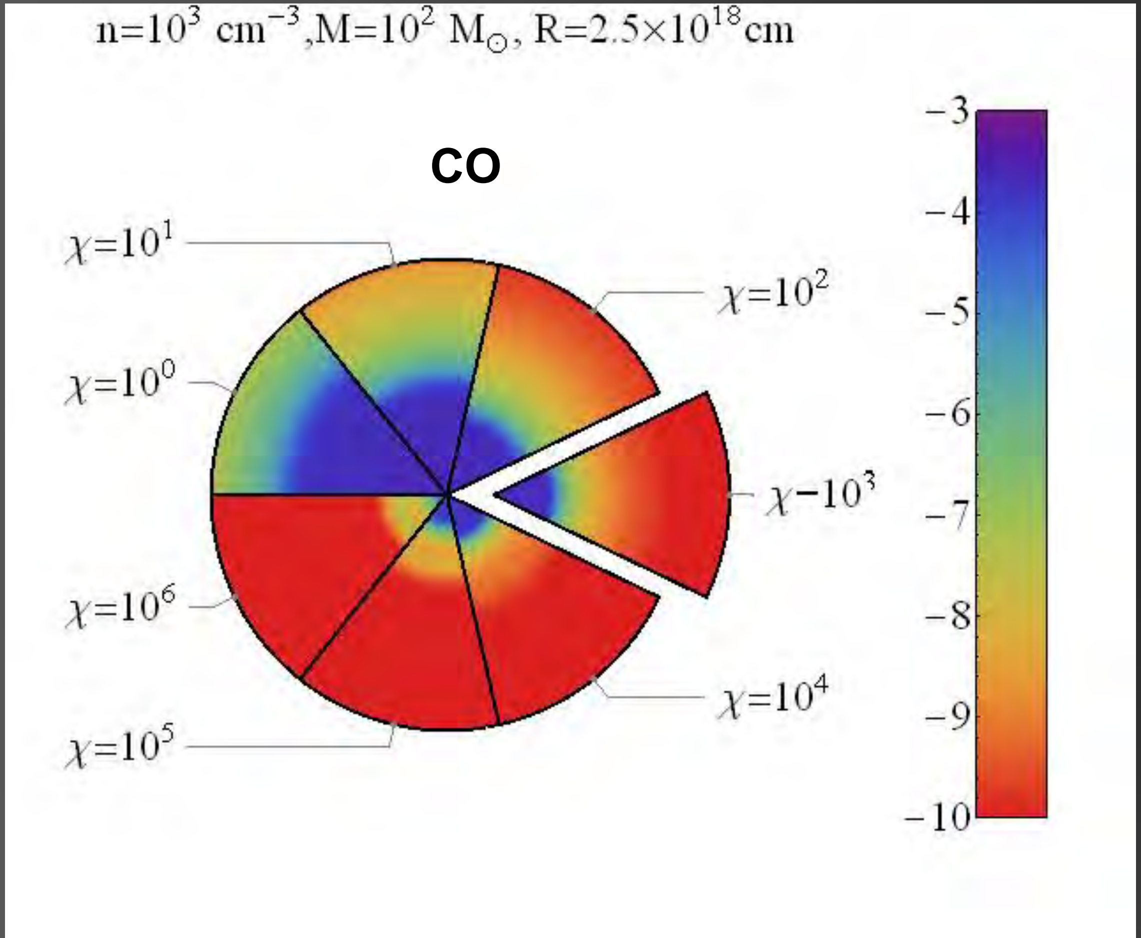

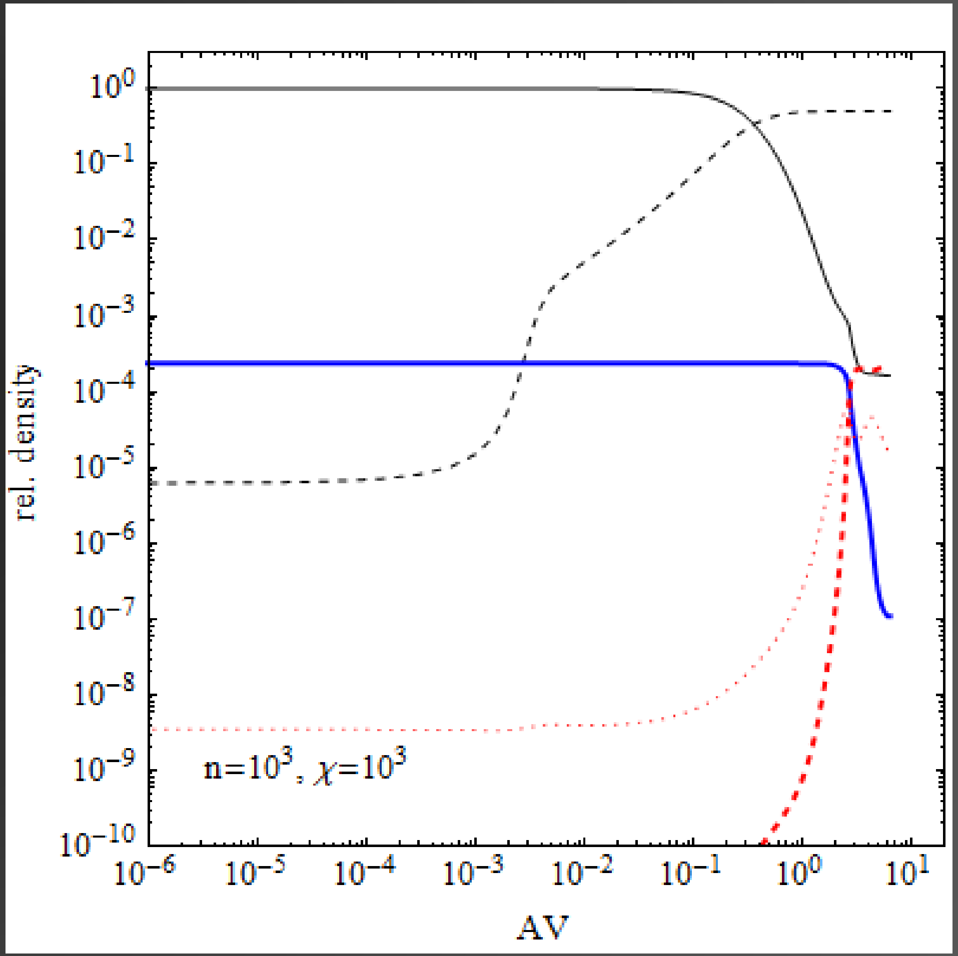

A_V is not a spatial coordinate

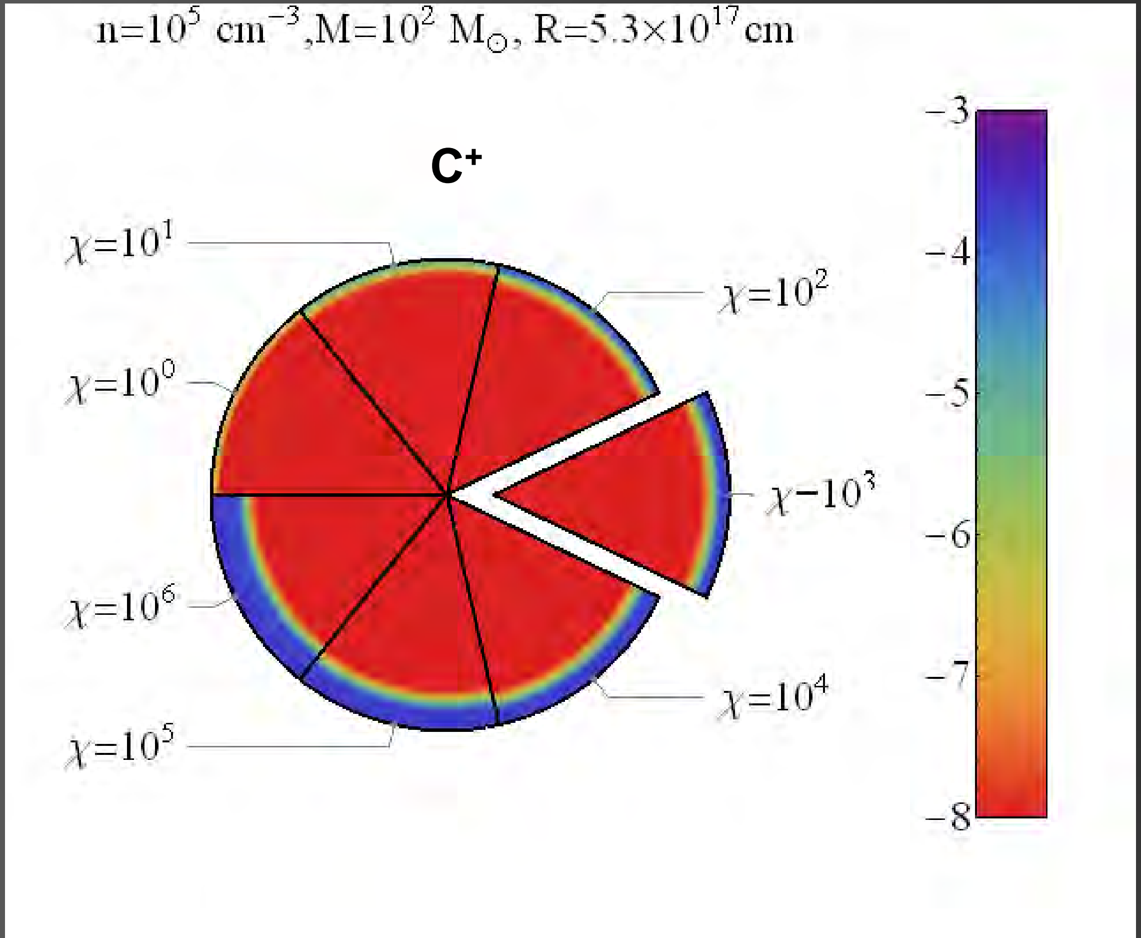

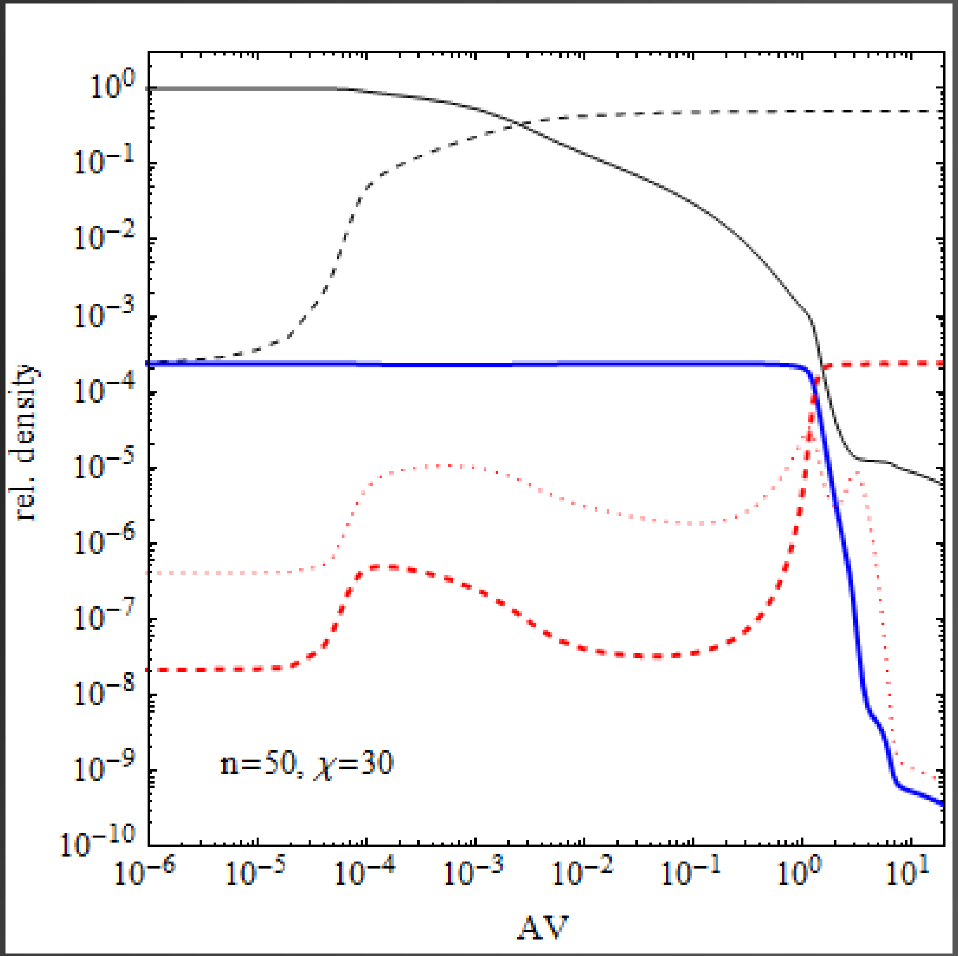

A_V is not a spatial coordinate

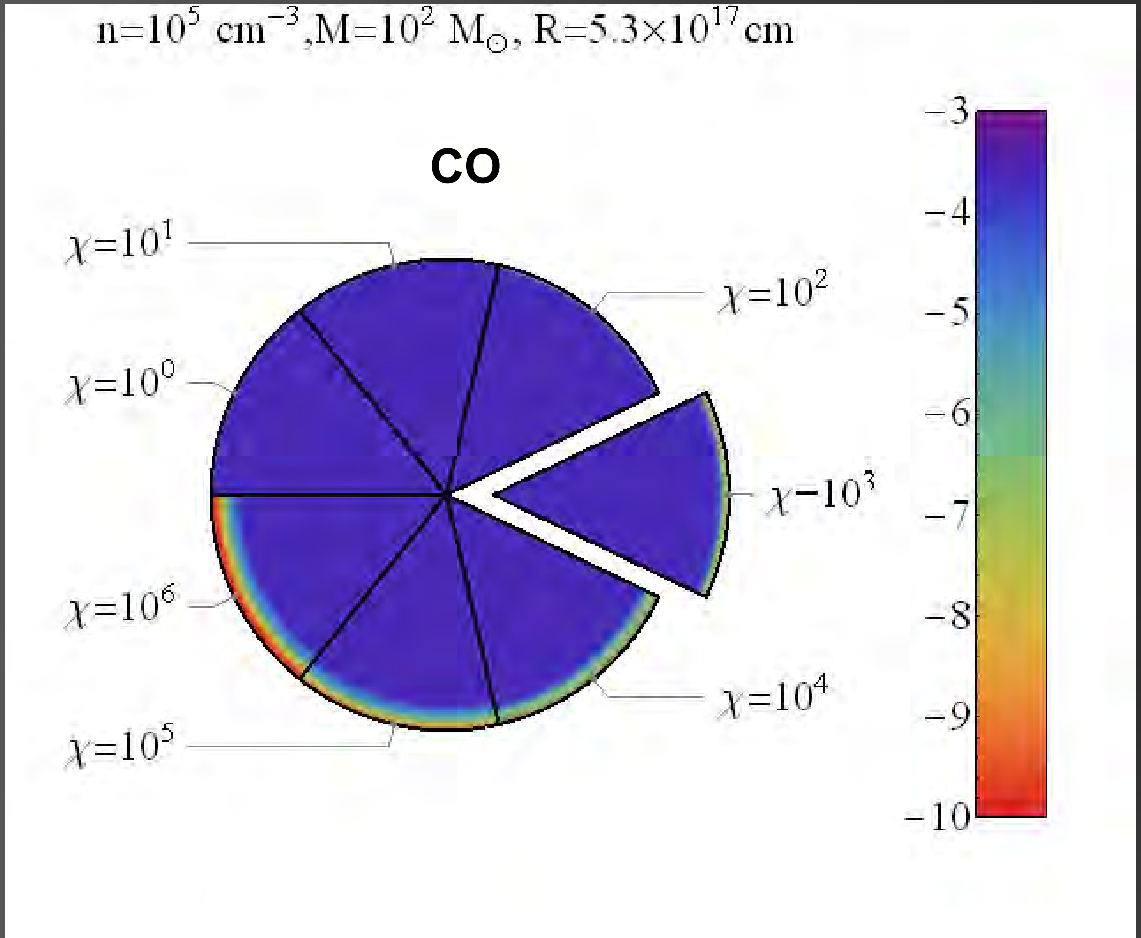

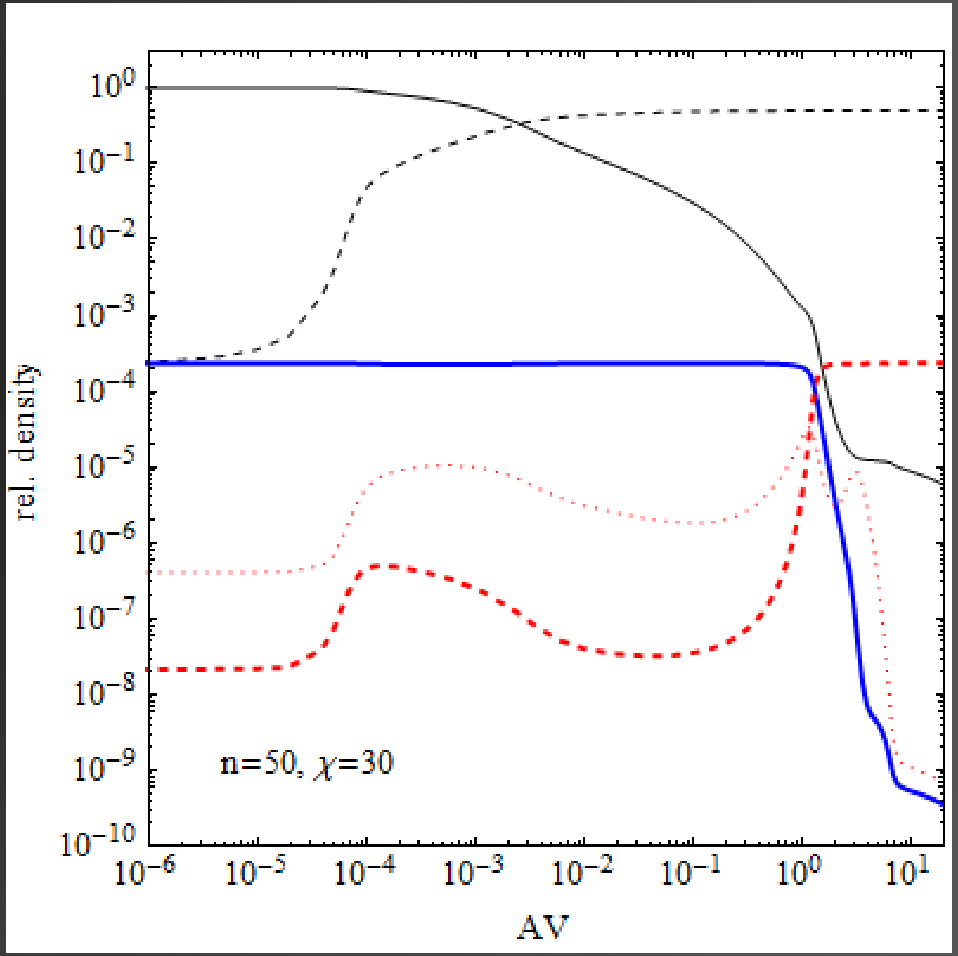

PDR Model Chemistry

$\chi=100$ $\chi=10^5$

$n=10^3$

$n=10^5$

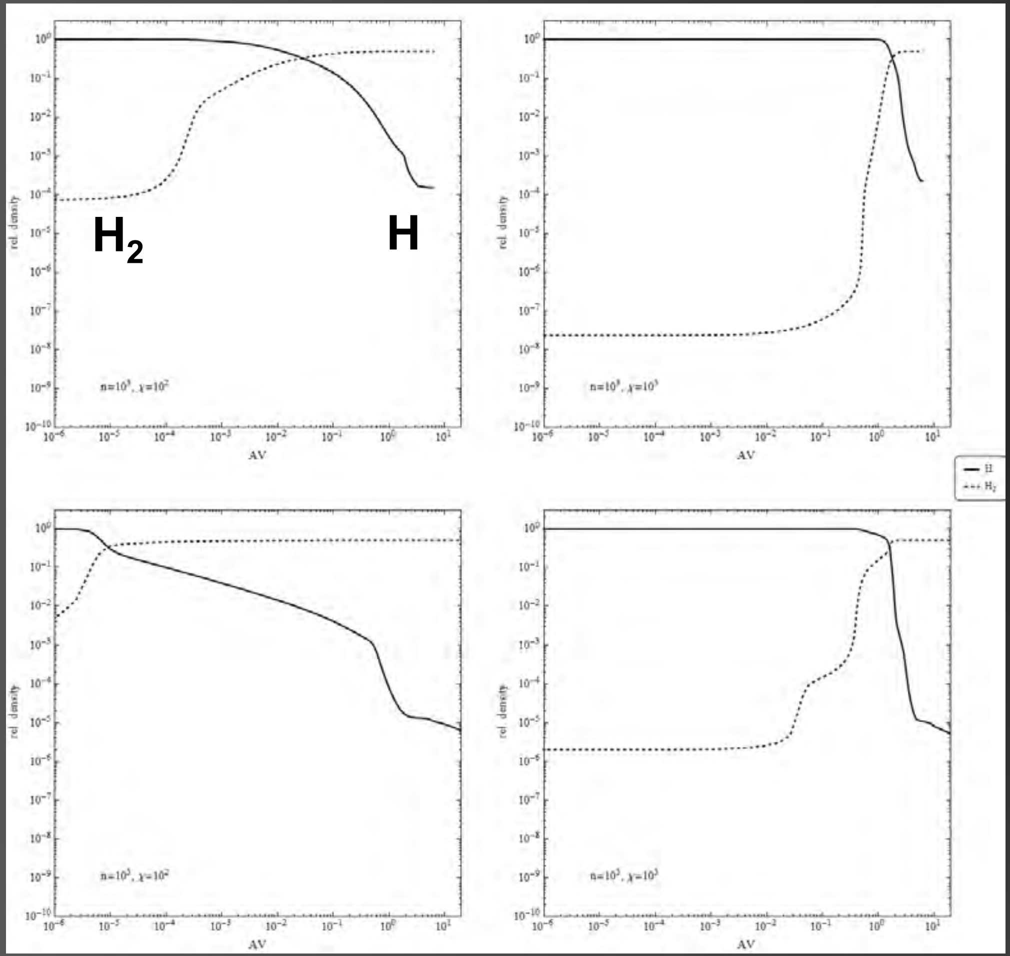

- H_2 photodissociation is a line absorption process. Once the absorption lines become optically thick, photodissociation becomes inefficient
- Density and UV field strength determine the depth of the H-H_2 transition zone

PDR Model Chemistry

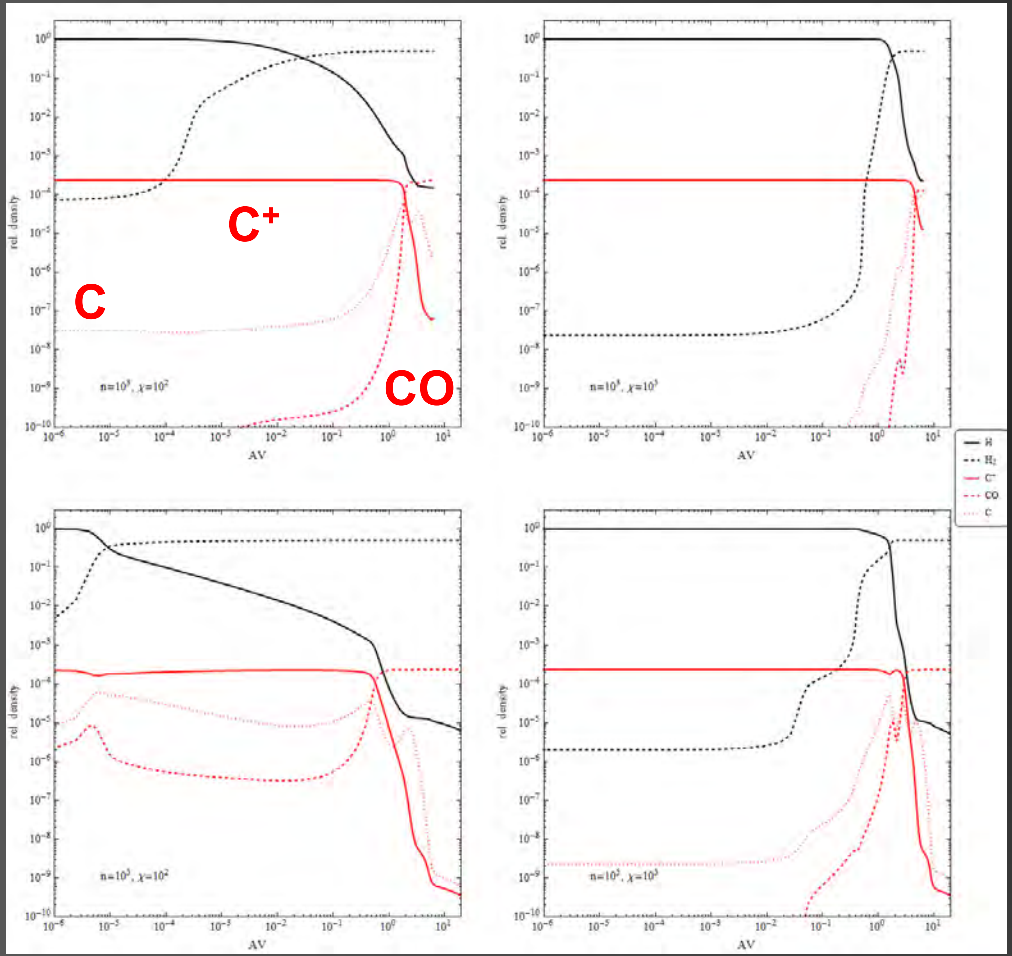

- CO photodissociation is shielded by
  - itself (self-shielding)
  - CO isotopologues (mutual shielding)
  - overlapping H2 lines
  - dust attenuation
- CO photodissociation becomes inefficient for $N_{CO} > 10^{16}$ cm^{-2}

PDR Model Chemistry

$\chi=100$ $\chi=10^5$

$n=10^3$

$n=10^5$

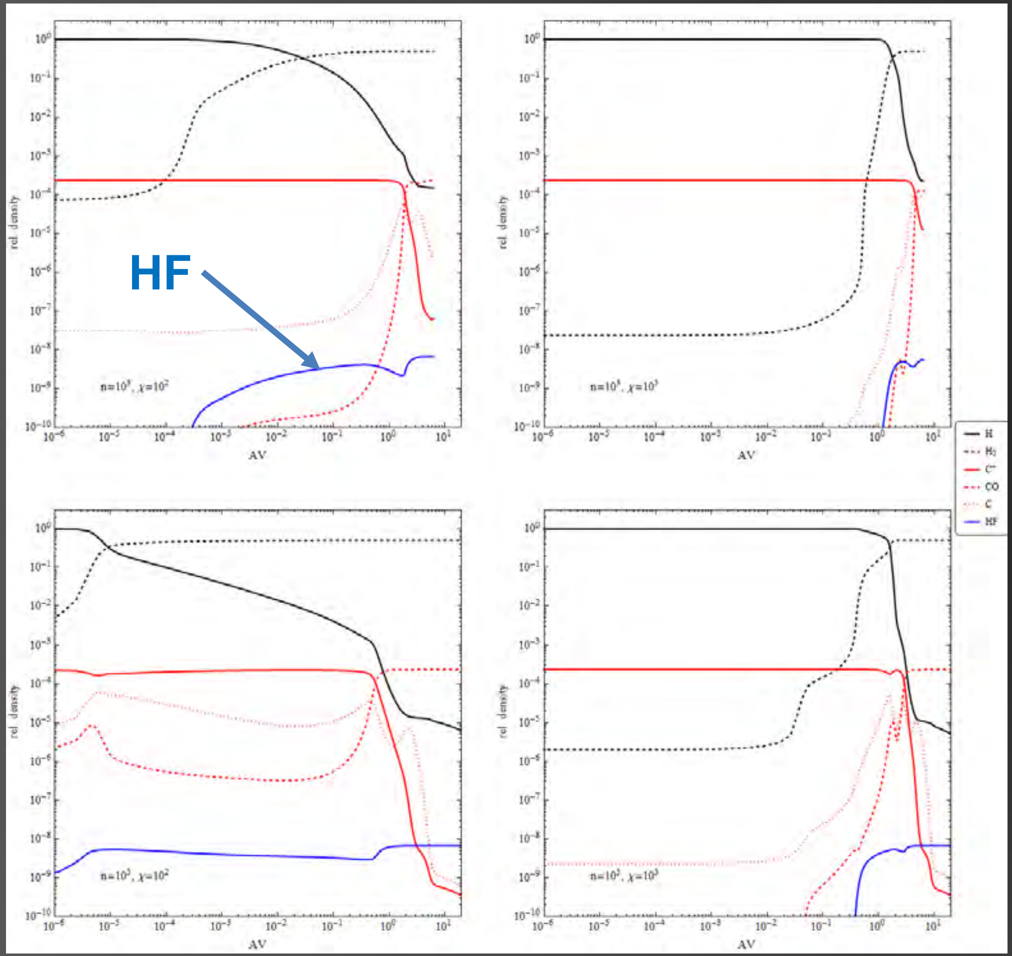

- „Standard“ models show a good H2-HF correlation (agreement with empirical findings)

PDR Model Chemistry

χ=100 χ=10^5

n=10^3

n=10^5

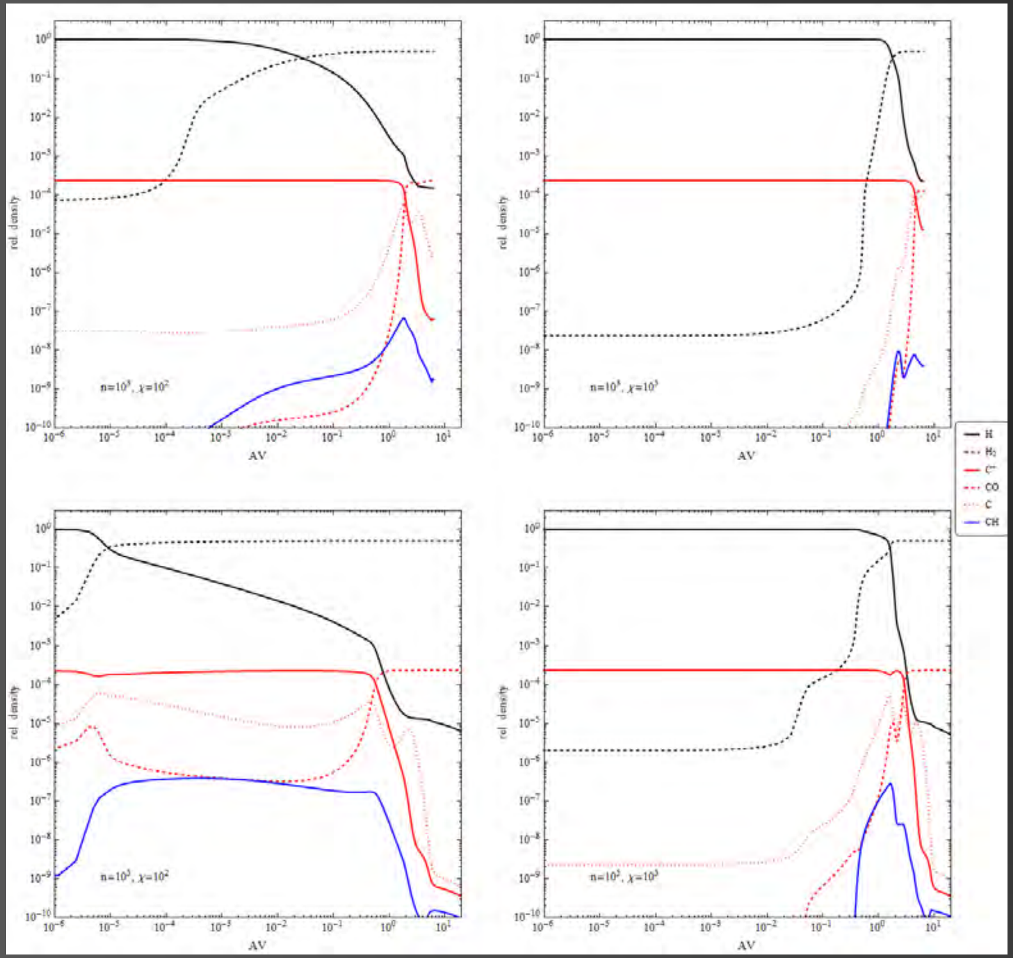

- H_2-CH correlation changes from diffuse to denser clouds

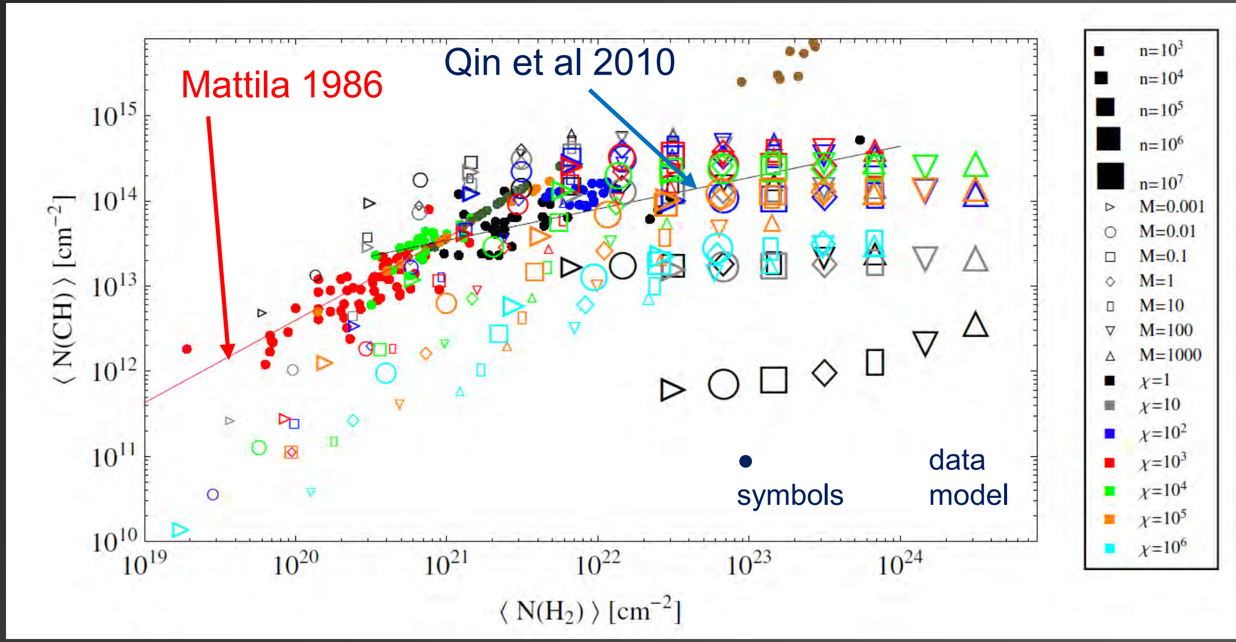

Röllig & Ossenkopf 2013, A&A 550, A56

PDR Model Chemistry

χ=100 $\chi=10^5$

$n=10^3$

$n=10^5$

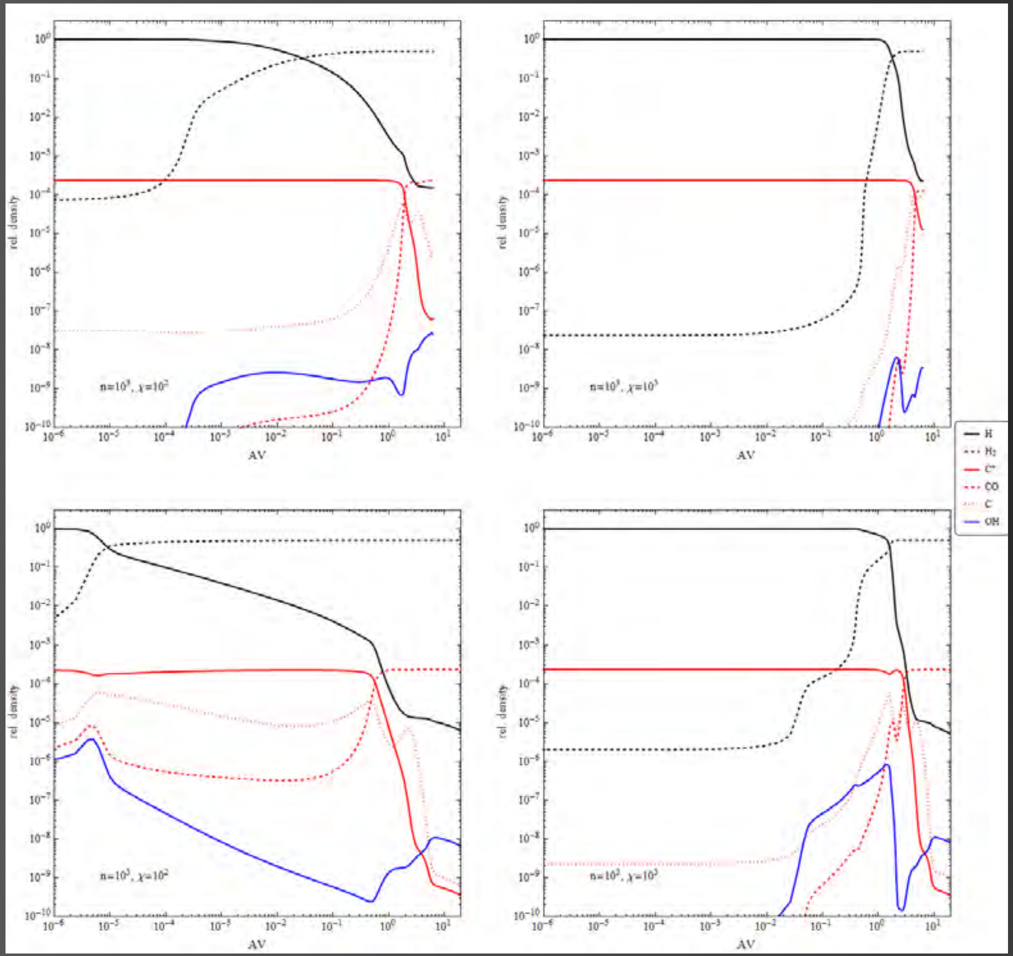

- OH appears to be a reasonable PDR interface tracer
- column densities not well modelled

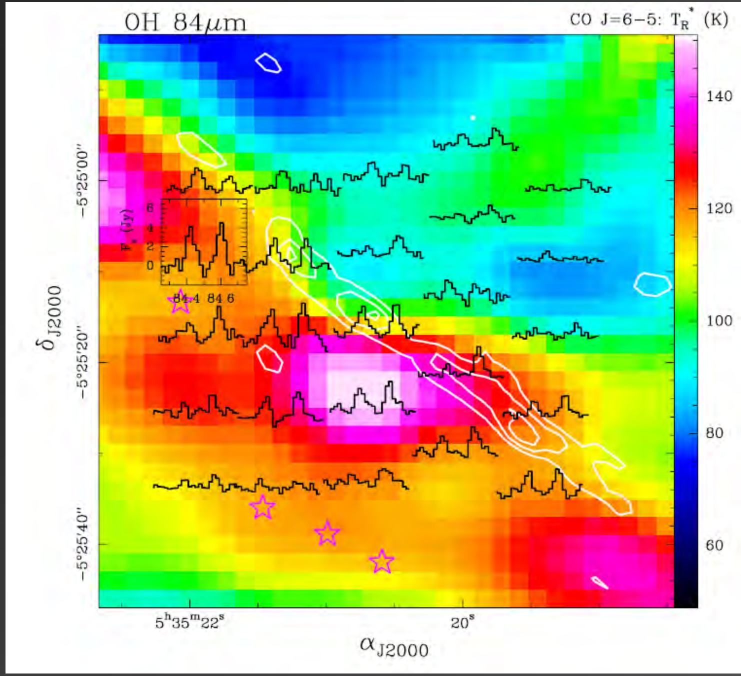

Orion bar

contours: OH 84 μm (E_u/k = 291 K)

colors: CO (6-5)

Goicoechea et al. 2011

XDR or PDR?

(Spaans & Meijerink 2007, ApJ 664, L23)

TABLE 1

Column Densities and Column Density Ratios

N_H	$N(CO^+)$	$N(HOC^+)$	$N(HCO^+)$	$N(CN)$	$N(HCN)$	CO^+/HCO^+	HCO^+/HOC^+	CN/HCN
XDR: $n = 10^5$ cm^{-3} and $F_X = 5.1$ ergs s^{-1} cm^{-2}								
1.0E22	3.0E12	3.3E12	4.3E13	1.1E15	6.0E12	0.07	13.2	181
2.0E22	4.8E12	5.0E12	1.6E14	2.7E15	2.8E13	0.03	31.5	95.4
3.0E22	5.7E12	5.9E12	2.7E14	4.7E15	5.9E13	0.02	46.4	78.9
XDR: $n = 10^{3.5}$ cm^{-3} and $F_X = 1.6$ ergs s^{-1} cm^{-2}								
3.0E22	1.2E12	5.7E11	1.5E12	5.2E13	3.2E10	0.8	2.6	1.6E3
6.0E22	8.3E12	6.9E12	3.7E13	5.1E14	9.4E11	0.2	5.4	543
9.1E22	1.8E13	1.5E13	1.3E14	1.5E15	3.8E12	0.14	8.5	400
PDR: $n = 10^5$ cm^{-3}, $G_0 = 10^{3.5}$, and $\zeta = 5 \times 10^{15}$ s^{-1}								
1.0E22	1.6E10	1.0E10	2.8E14	2.3E15	3.5E14	5.6E−5	2.8E4	6.6
2.0E22	1.7E10	1.5E10	7.8E14	4.5E15	9.5E14	2.2E−5	5.2E4	4.7
3.0E22	1.9E10	2.0E10	1.3E15	6.7E15	1.6E15	1.4E−5	6.5E4	4.3

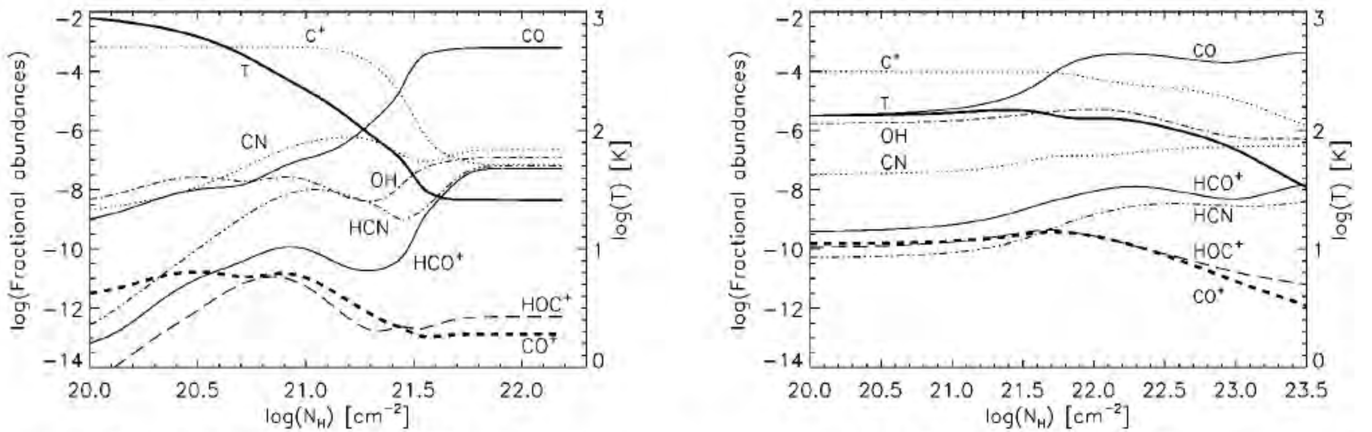

FIG. 2.—Chemical and thermal structure of a PDR with an enhanced cosmic ionization rate ($\zeta = 5 \times 10^{-15}$ s^{-1}) and an XDR model. Density $n = 10^5$ cm^{-3}, and $G_0 = 10^{3.5}/F_X = 1.6$ ergs s^{-1} cm^{-2}). The CO^+ abundance is at least an order of magnitude larger in the XDR.

Credit: Slide by
A. Fuente

XDR vs. PDR

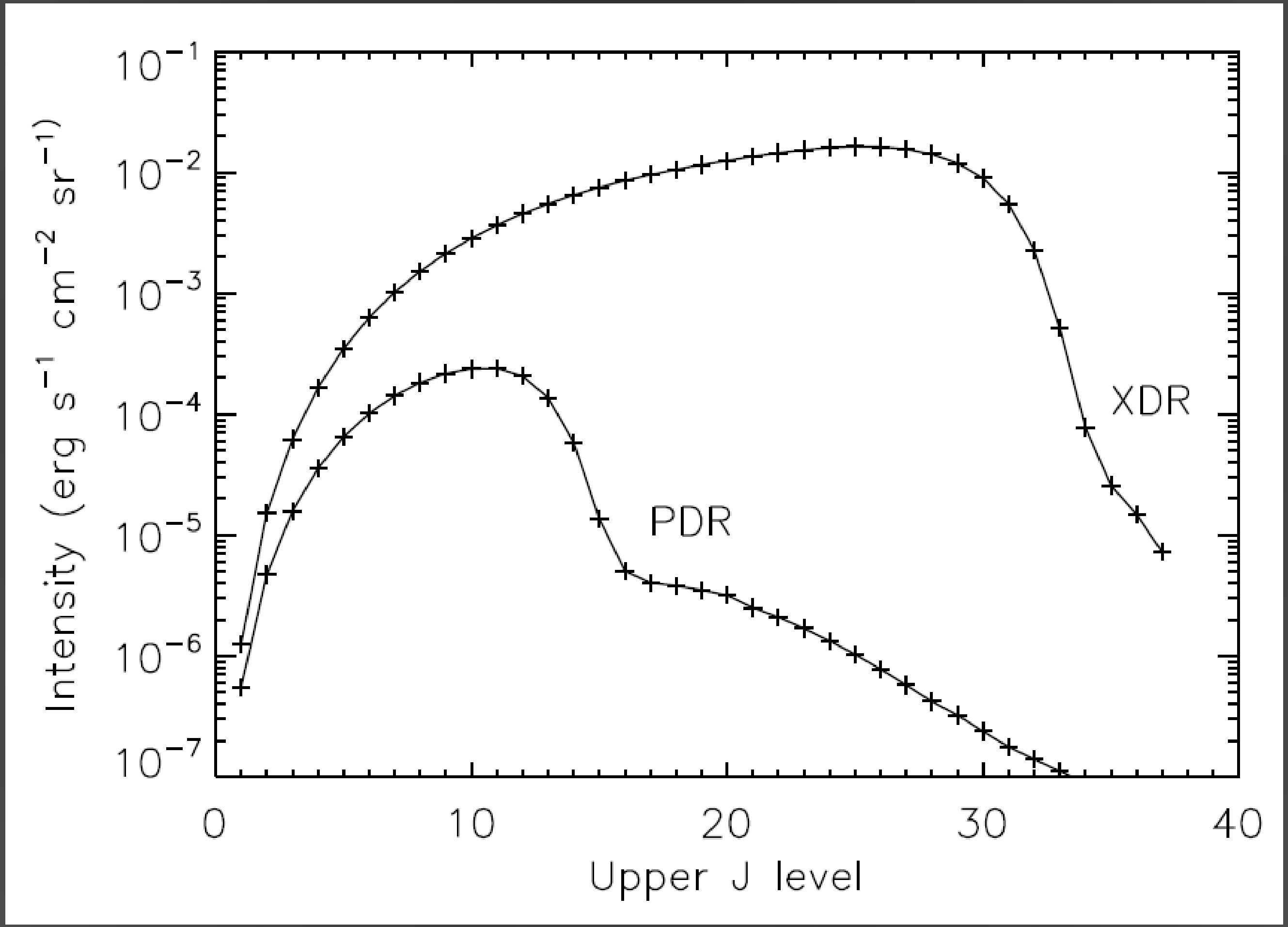

Spaans & Meijerink 2008

PDR Emission

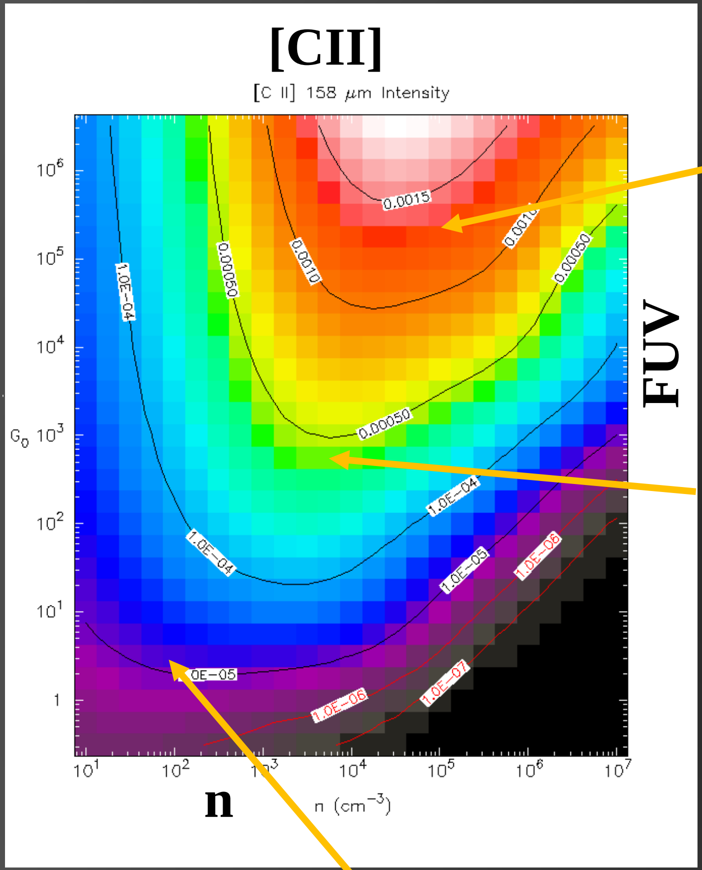

Kaufman et al. 1999

Orion PDR

Classic PDRs

G_0/n = const

Diffuse Gas

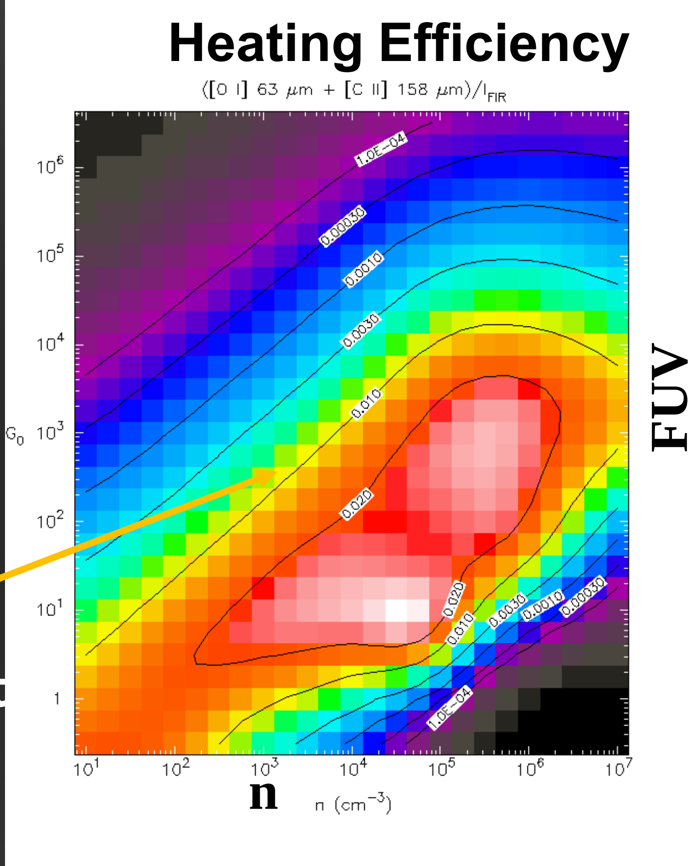

Kaufman et al. 1999

PDR Emission

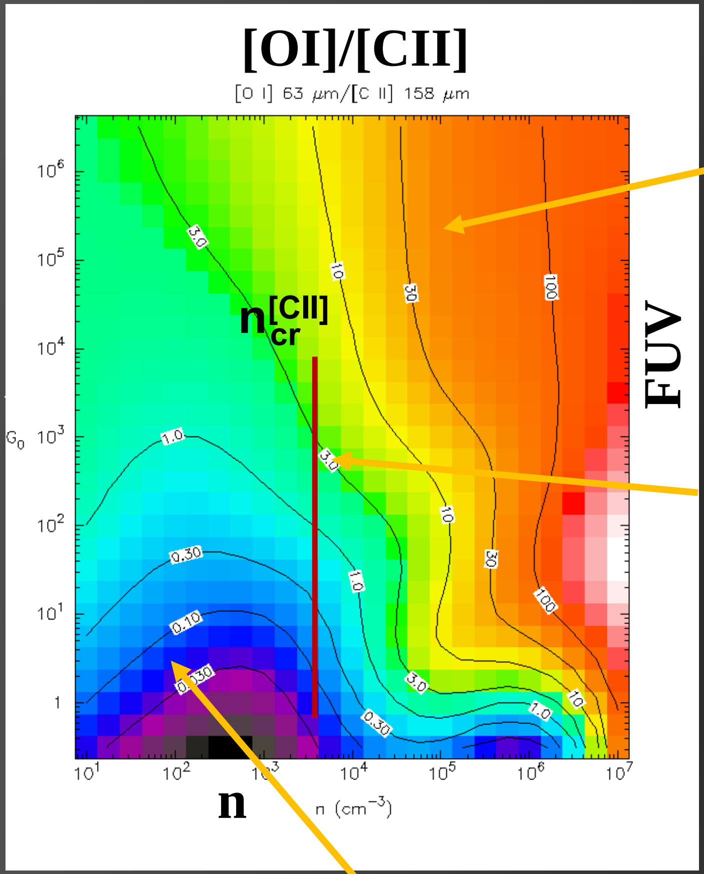

Kaufman et al. 1999

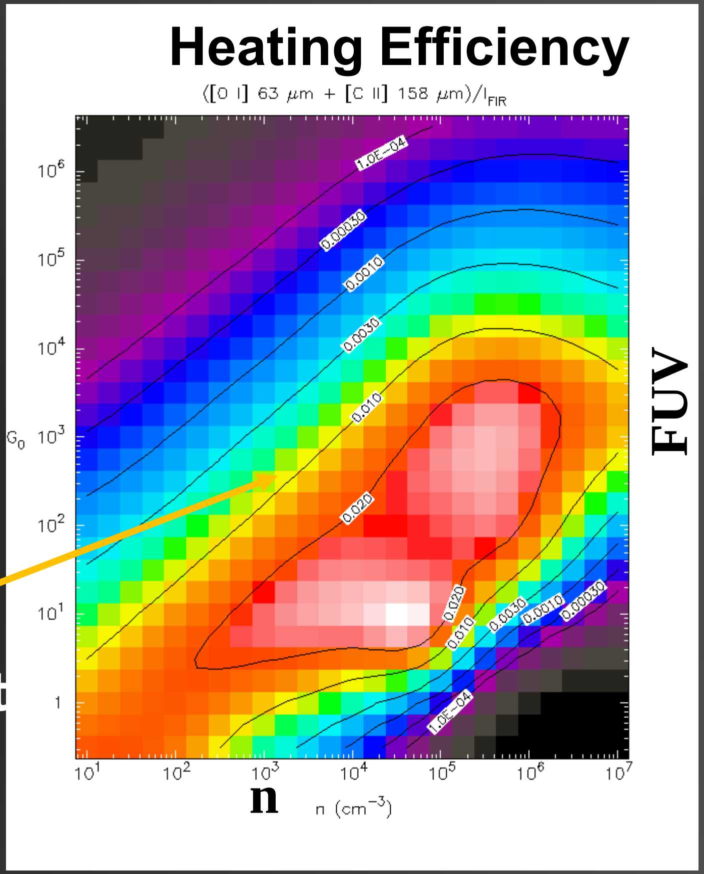

Kaufman et al. 1999

Orion PDR

Classic PDRs

G_0/n = const

Diffuse Gas

PDR diagnostics

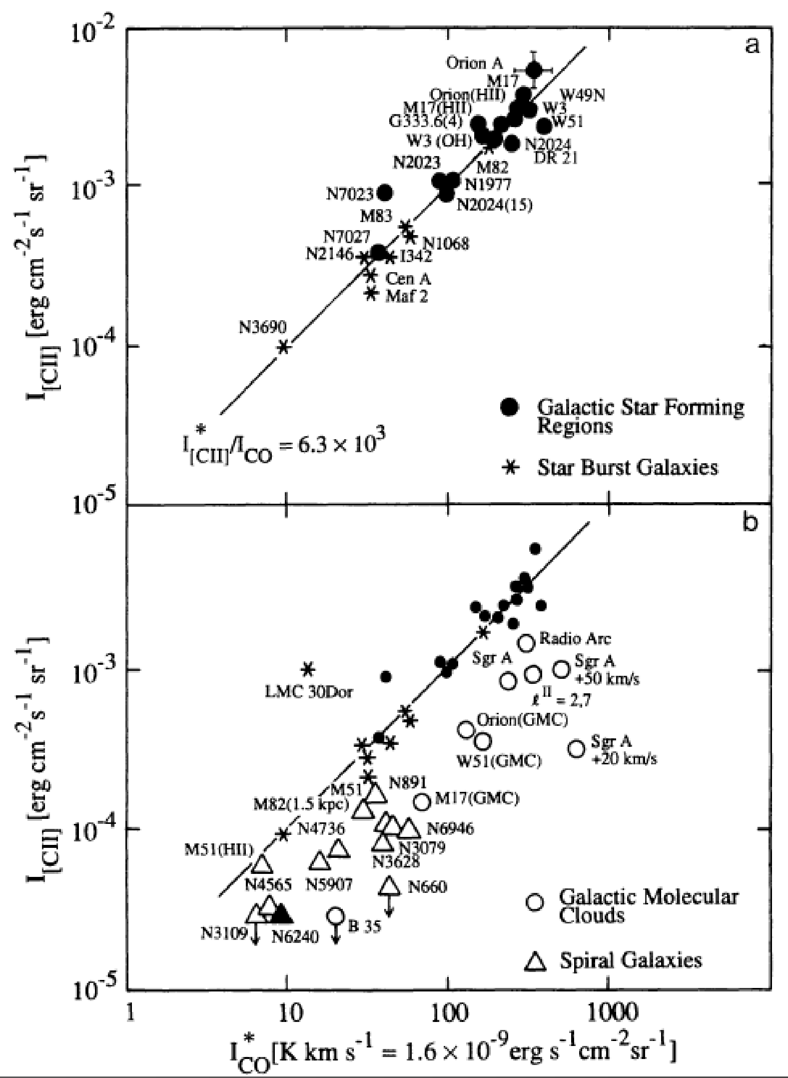

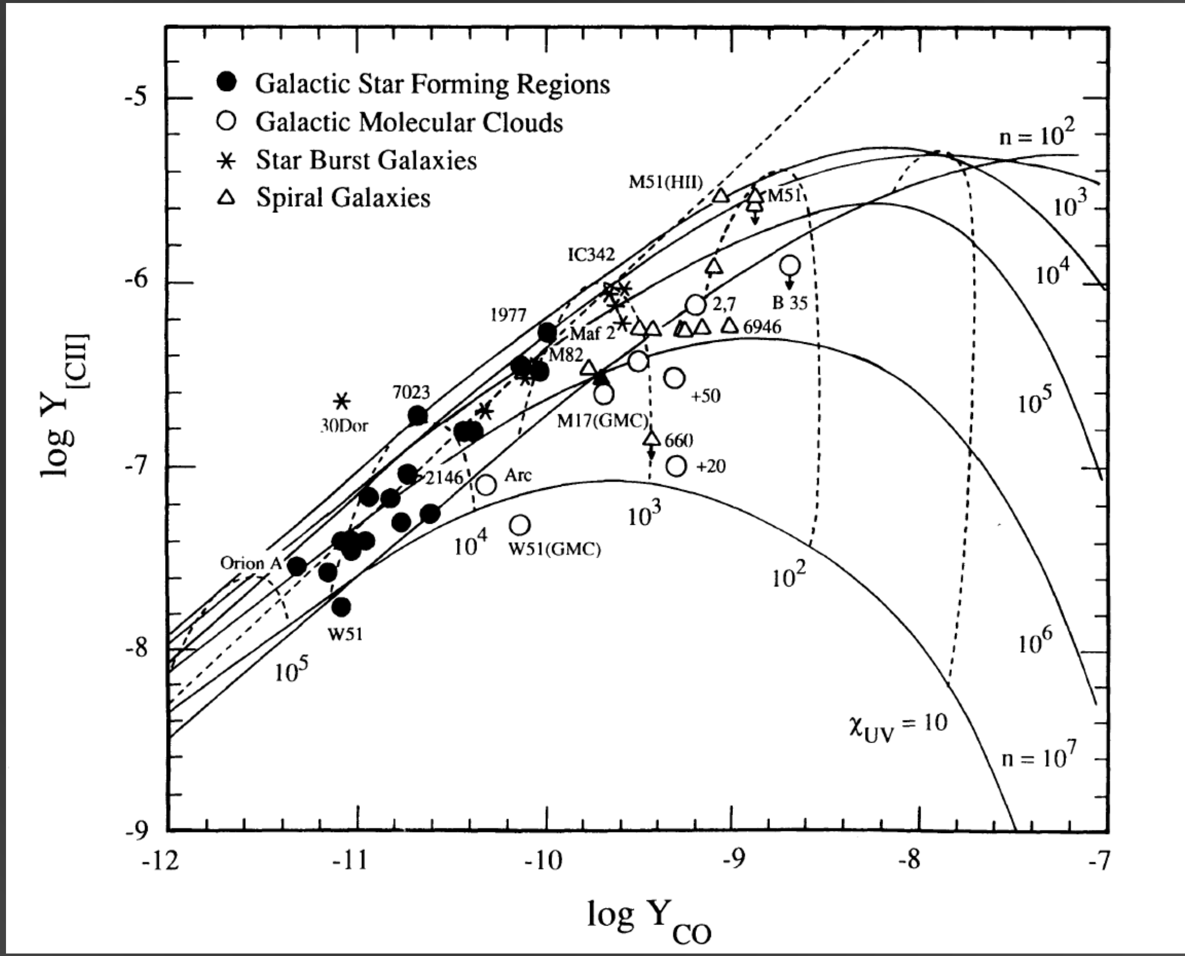

Stacey et al. 1991

$Y_{[CII]}=I_{[CII]}/I_{FIR}$
$Y_{CO}=I_{CO}/I_{FIR}$

PDR diagnostic model diagrams

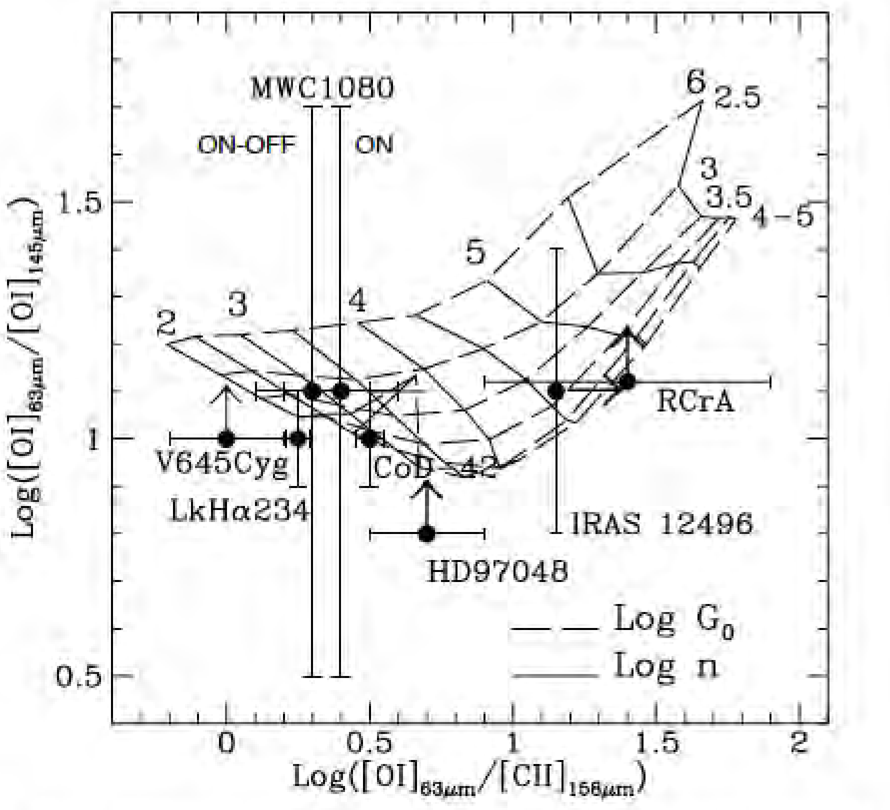

Fig. 4. Observed line ratios superimposed to PDR model (see text).

- Absolute intensities always involve an (unknown) filling factor
- Lorenzetti et al (1999) used the $[OI]_{63\mu m}/[CII]_{157\mu m}$ and $[OI]_{63\mu m}/[OI]_{145\mu m}$ intensity ratios to derive the physical conditions of the PDRs associated with Herbig Ae/Be stars based on ISO data.

PDR diagnostic model diagrams

PDR diagmostic diagrams are useful to derive global properties. If the main heating mechanism is the photoelectric effect, heating efficiency depends on the grain charge which is itself governed by the paramter $G_0\, T^{1/2} / n_e$.

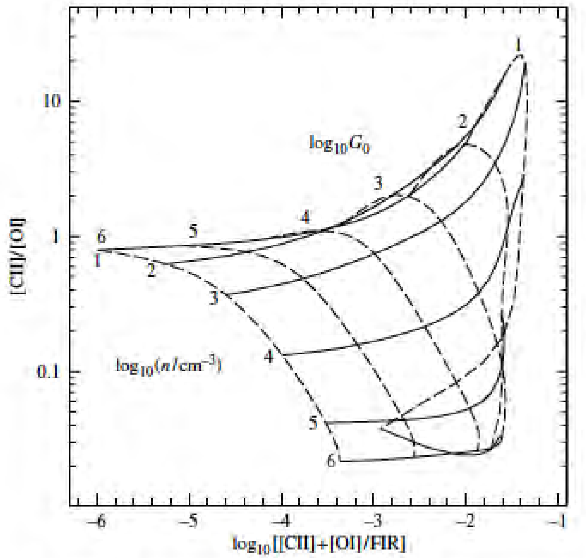

Figure 9.9 A diagnostic diagram for PDRs based on the observed intensity ratio of the [CII] 158 μm and [OI] 63 μm lines and the overall cooling efficiency. The lines present the results of detailed model calculations for different densities and incident FUV fields. Figure kindly provided by M. J. Kaufman; derived from the models described in M. J. Kaufman, M. G. Wolfire, D. Hollenbach, and M.L. Luhman, 1999, *Ap. J.*, **527**, p. 795.

$$\frac{F_{\mathrm{OI}} + F_{\mathrm{CII}}}{2F_{\mathrm{IR}}}$$

Gas heating efficiency

Since the [CII] 158 μm and [OI 63 μm lines have different critical densities, their intensity ratio is a good measure of the density.

Diagnostic Plots

Kaufmann et al. 1999

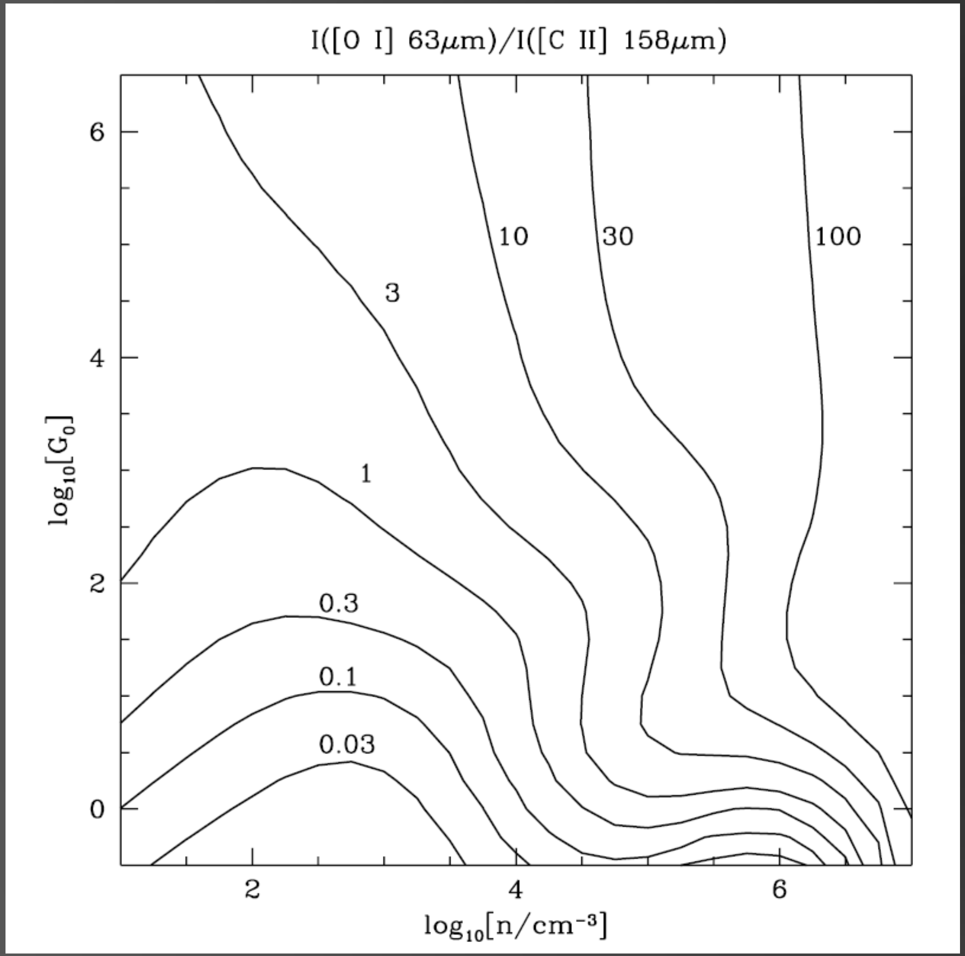

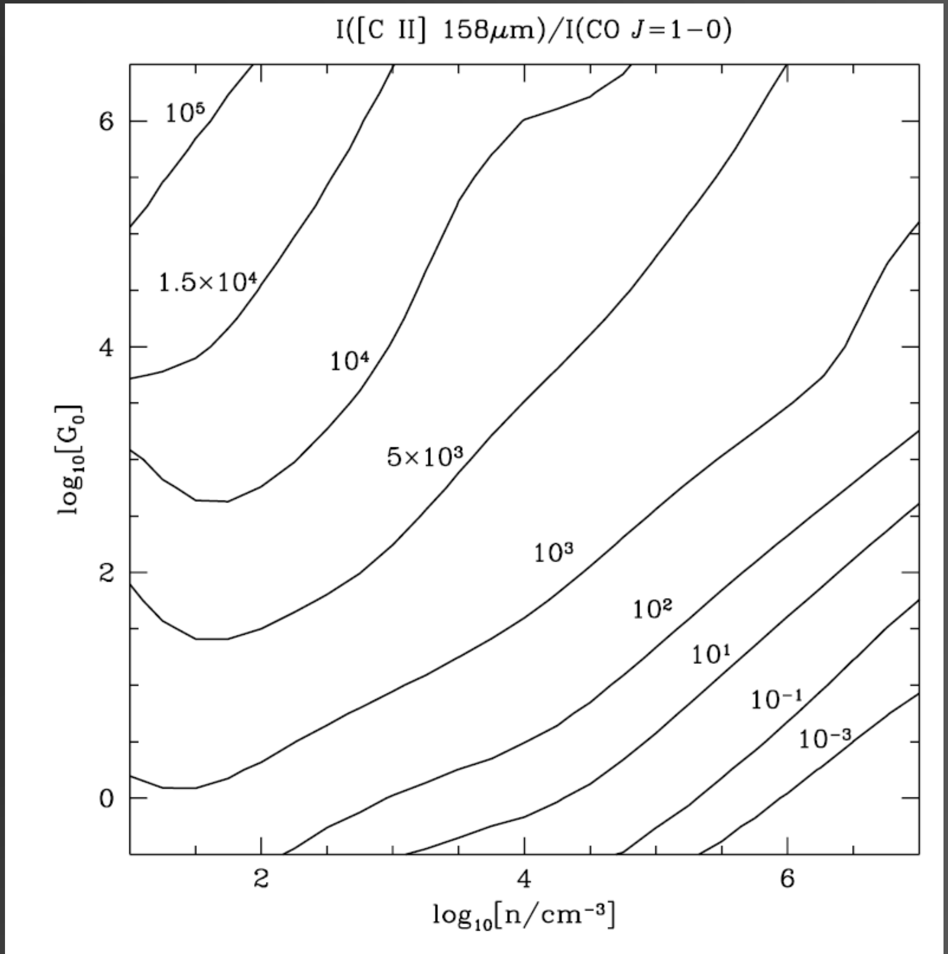

[CII] contribution from HII regions

Teff= 42000 K

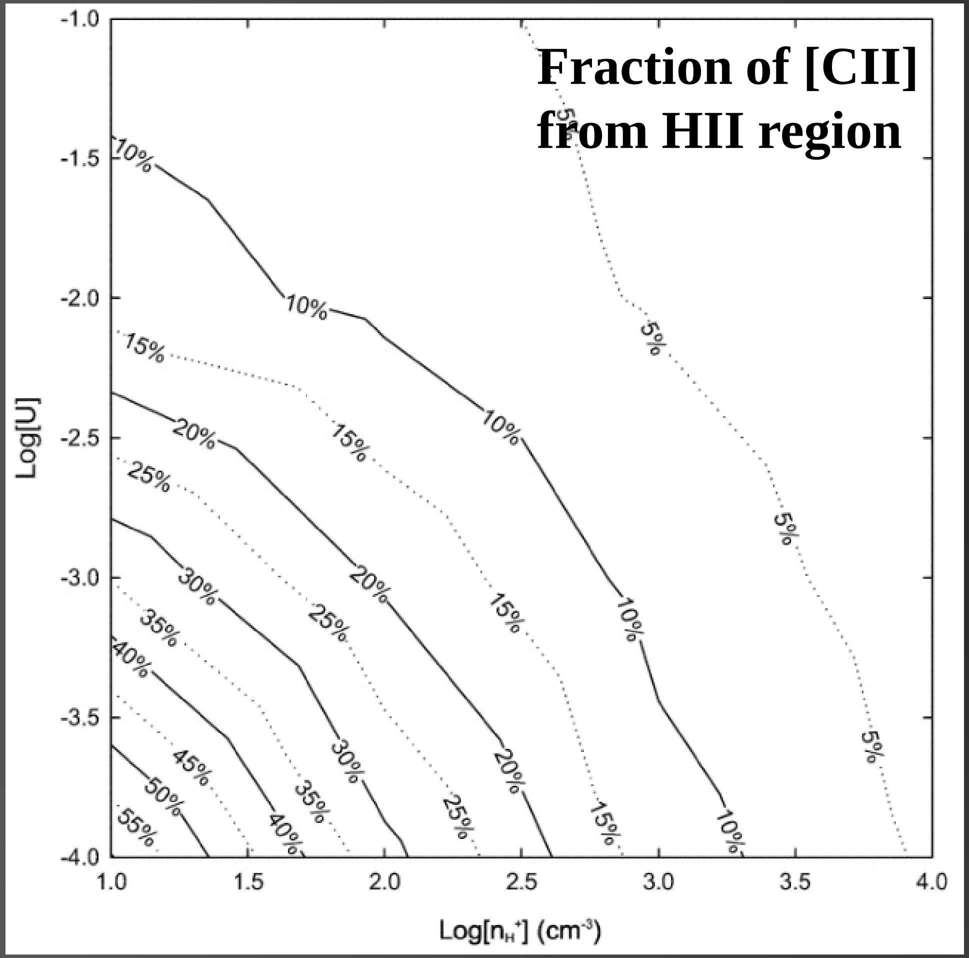

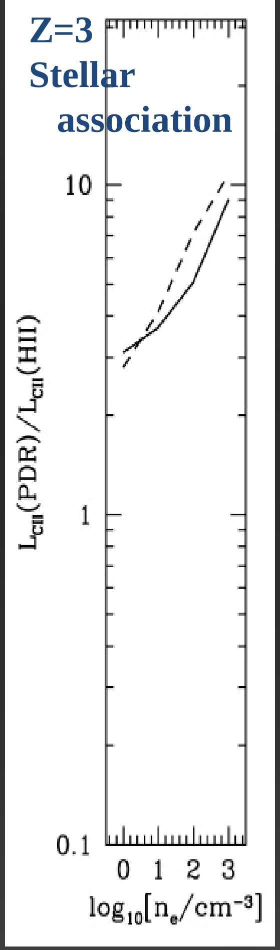

Abel et al 2005 Kaufman et al. 2006

- C^+ is also present in the ionized gas
- When observing a PDR you always observe the neighbouring HII region
- [CII] emission is partly produced in the HII region.

[CII] contribution from HII regions

Teff= 42000 K

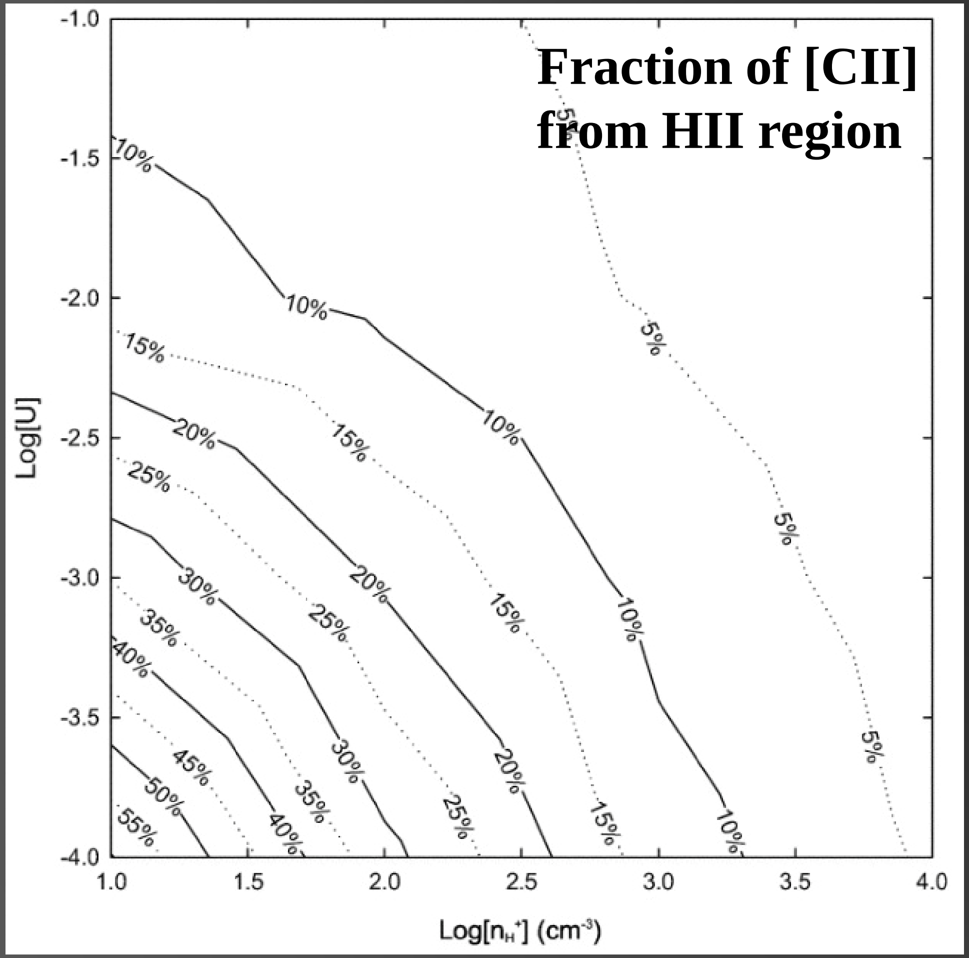

Abel et al 2005

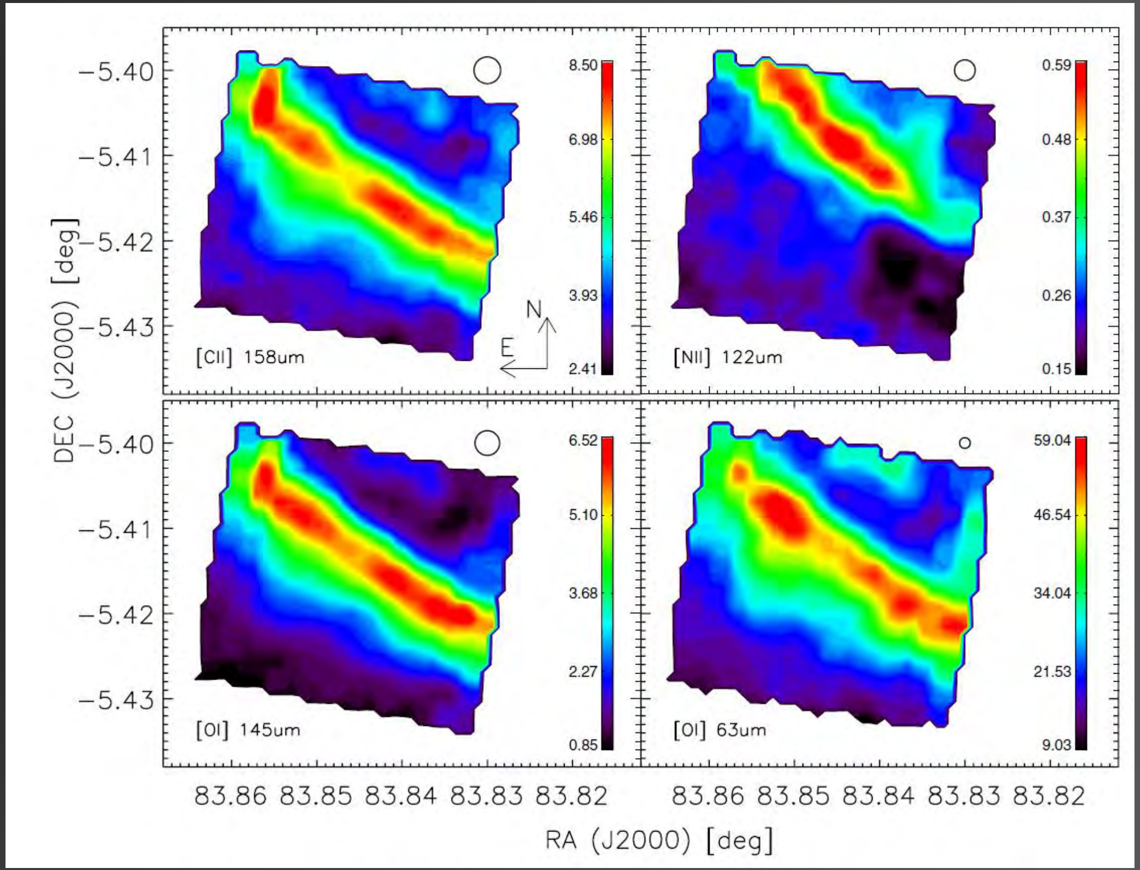

Bernard-Salas et al. 2012

References

- “The Physics and Chemistry of the Interstellar Medium”, A.G.G.M. Tielens, de. Cambridge University Press
- Tielens, A.G.G.M. & Hollenbach, D. J., 1985, ApJ 291, 722
- Hollenbach, D. J., Takahashi, T., Tielens, A.G.G.M. 1985, ApJ 291, 722
- Sternberg & Dalgarno, 1995, ApJSS, 99, 565
- Röllig et al., 2007, A&A, 467, 187
- Kaufmann et al., 1999, ApJ, 527, 795
- Le Petit et al. 2006, ApJSS, 164,506
- van Dishoeck & Black, 1988, 334, 771